



*1st workshop:
Astrophysical winds and disks
Similar phenomena in stars and quasars
Platamonas, Greece, September 3-8, 2009*



*The fruits of collaboration between
Astrophysical Spectroscopy teams
of the University of Athens and
the Observatory of Belgrade*

Platamonas, Greece, September 3-8, 2009

Scientific relations between the Astrophysical Spectroscopy Teams of University of Athens and Belgrade Observatory (2003-2008)

The Astrophysical Spectroscopy Teams of the Faculty of Physics of the University of Athens and of Belgrade Observatory have established their collaboration since 2003.

Scientific grounds of the collaboration

In the optical and UV spectra of hot emission stars some lines have peculiar and complex profiles (see e.g. Danezis 1987, Danezis et al. 1991, Lyratzi & Danezis 2004). Also, in optical and UV spectra of some AGNs the line shapes have complex structure and indicate at least two components that are emitted from Broad Line Region (BLR) and Narrow Line Region (NLR). Moreover, it is hard to conclude about physics and kinematics of the BLR and there are some ideas to apply some methods from laboratory plasma to conclude about physical conditions in this region (see e.g. Popovic 2003, Popovic et al. 2008). On the other hand, there are similarities between line profiles observed in stars and in AGNs (as e.g P-cyg line profile can be observed in stellar as well as in quasar spectra). We suggested that this peculiarity in the spectral line profiles of hot emission stars and AGNs is due to the existence of Discrete or Satellite Absorption Components (DACs-SACs). We were able to explain the origin of DACs and SACs, suggesting that they are created in independent density regions of matter that rotate around their own centers.

Taking into account that DACs and SACs in hot emission stars are created in the region that is between the star and the observer, as well as that we have similar situation in the AGNs, we developed a model (GR model) able to reproduce theoretically the observed complex spectral line profiles (SACs/DACs) from UV to the optical wavelength range in the spectra of both hot emission stars and AGNs (Danezis et al. 2003, 2005, 2007a).

Specifically, in order to explain the very complex profile of spectral lines (e.g. MgII, SiIV, CIV, NV, NIV, FeII, Ly-alpha, H-alpha, H-beta) we have developed the GR model that considers that the regions, where these spectral lines are formed, are not continuous but consist of a number of independent absorbing density regions of matter and a number of emission region. These regions create the absorption or emission components that we observe in the spectra of the studied objects (i.e. Discrete Absorption Components – DACs and Satellite Absorption Components – SACs). In order to construct the GR model, we solved the radiation transfer equations through a complex structure as the one described and we calculated a line function, able to reproduce accurately the observed complex line profiles. We also calculated two new distribution functions (Rotation distribution and Gauss-Rotation distribution).

With GR model we are able to calculate the optical depth, the column density, the absorbed or emitted energy of these regions, as well as some kinematical parameters, such as the apparent rotational (V_{rot}) and radial velocities (V_{rad}) of these density regions and the random velocities (V_{rand}) of the studied ions (see Danezis et al. 2003, 2005, 2007a, Popović et al. 2004).

The GR model has been tested and applied in a great number of spectral lines of hot emission stars and quasars and has given important results in the case of individual objects (study of kinematics and time evolution of stellar atmospheres

of specific hot emission stars and quasars), as well as in statistical studies (kinematic parameters of atmospherical regions that create DACs and SACs in great number of hot emission stars). All these studies have been published in international refereed scientific journals and conference proceedings (see Antoniou et al. 2008a,b, Danezis et al., 2005, 2006, 2007a,b, 2008, Lyratzi et al. 2005, 2007, 2008).

Our research until now and the application of GR model in hot emission stars and quasars have shown that the peculiar and complex profiles that we observe in these objects can be explained by the DACs/SACs, which are created by independent density regions of matter in the environment of the studied objects.

All the above have been published in a series of papers, listed below. The main ideas have been published in the attached papers.

References

Hot Emission Stars and Quasars

1. Popović, L. Č., Danezis, E., Lyratzi, E., Dimitrijević, M. S. & Theodosiou E.: "A model for the Broad Absorption Line Region in BAL-QSOs", The conference of Euro-asian astronomical society, Russian Astronomical conference, July, 2 - 10, 2004, Moscow, Russia.
2. Lyratzi, E., Danezis, E., Popovic, L., Dimitrijević, M., Nikolaidis, D., Theodosiou, E., Soulikias, A. & Antoniou, A.: "The complex structure of the MgII $\lambda\lambda$ 2795.523, 2802.698 A regions of 64 Be stars", 17th International Conference on Spectral Line Shapes (17th ICSLS), June 21-25, 2004, Paris, France.
3. Lyratzi, E., Danezis, E., Popovic, L., Dimitrijević, M., Nikolaidis, D., Theodosiou, E., Soulikias, A. & Antoniou, A.: "The complex structure of the SiIV $\lambda\lambda$ 1393.73, 1402.73 A regions of 42 Be stars", 17th International Conference on Spectral Line Shapes (17th ICSLS), June 21-25, 2004, Paris, France.
4. Lyratzi, E. & Danezis, E.: "SACs and DACs phenomena in the atmospheres of hot emission stars", 22nd Summer School and International Symposium on the Physics of Ionized Gases (SPIG 2004), August, 23 - 27, 2004, at National Park "TARA", Serbia and Montenegro. (Invited Lecture)
5. Popović, L. Č., Dimitrijević, M. S., Mediavilla, E., Danezis, E., Lyratzi, E., Bon, E., Ilić, D., Jovanović, P., Theodosiou E. & Dačić, M.: "Some spectroscopic methods for astrophysical plasma research", 22nd Summer School and International Symposium on the Physics of Ionized Gases (SPIG 2004), August, 23 - 27, 2004, at National Park "TARA", Serbia and Montenegro. (Invited Lecture)
6. Lyratzi, E., Danezis, E., Popovic, L., Dimitrijević, M., Nikolaidis, D., Soulikias, A., Antoniou, A. & Stathopoulou, M.: "The complex structure of the SiIV $\lambda\lambda$ 1393.73, 1402.73 A regions of 57 Be stars", JENAM 2004, Spetember, 13-17, 2004, Granada, Spain.
7. Danezis, E., Antoniou, A., Popovic, L., Dimitrijević, M., Lyratzi, E., Nikolaidis, D., Soulikias, A. & Theodosiou, E.: "Satellite Absorption Components of the UV spectral lines SiIV, CIV, NV, and NIV in the atmosphere of the Oe star HD 175754", JENAM 2004, Spetember, 13-17, 2004, Granada, Spain.

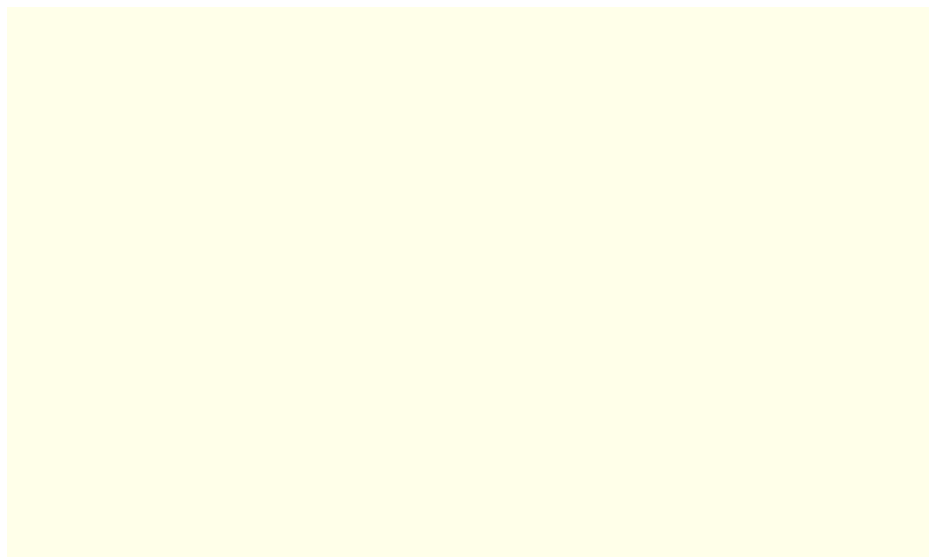
8. Danezis, E., Lyratzi, E., Popovic, L., Dimitrijević, M., Christou, G., Soulikias, A. & Antoniou, A.: "*Satellite Absorption Components of the UV spectral lines SiIV, CIV, NV, and NIV in the atmosphere of the Oe star HD 66811 (ζPup)*", JENAM 2004, Spetember, 13-17, 2004, Granada, Spain.
9. Danezis, E., Nikolaidis, D., Lyratzi, E., Popović, L. Č., Dimitrijević, M. S., Theodossiou, E. & Antoniou, A.: "A new modelling approach for DACs and SACs regions in the atmospheres of hot emission stars", 5th Serbian Conference on Spectral Lines Shapes in Astrophysics (V SCSLSA) June 2005, Vršac, Serbia. (*Invited Lecture*)
10. Lyratzi, E., Danezis, E., Nikolaidis, D., Popović, L. Č., Dimitrijević, M. S., Theodossiou, E. & Antoniou, A.: "A new approach for the structure of H α regions in 120 Be stars", 5th Serbian Conference on Spectral Lines Shapes in Astrophysics (V SCSLSA) June 2005, Vršac, Serbia. (*Invited Lecture*)
11. Danezis, E., Nikolaidis, D., Lyratzi, E., Popović, L. Č., Dimitrijević, M. S., Theodossiou, E. & Antoniou, A.: "A new modeling approach for DACs and SACs regions in the atmospheres of hot emission stars", Proceedings of the 7th Hellenic Astronomical Conference, Kefallinia Island, Greece, September 2005.
12. Lyratzi, E., Danezis, E., Nikolaidis, D., Antoniou, A., Popović, L. Č., Dimitrijević, M. S., Stathopoulou, M. & Theodossiou, E.: "A new approach for the structure of H α regions in 120 Be stars", Proceedings of the 7th Hellenic Astronomical Conference, Kefallinia Island, Greece, September 2005.
13. Antoniou, A., Danezis, E., Nikolaidis, D., Lyratzi, E., Popović, L. Č., Dimitrijević, M. S. & Theodossiou, E.: "Hyperionison phenomena to the coronal and post - coronal regions of the moving atmosphere of the Oe star HD 93521", Proceedings of the 7th Hellenic Astronomical Conference, Kefallinia Island, Greece, September 2005.
14. Antoniou, A., Danezis E., Lyratzi, E., Nikolaidis, D., Popović, L. Č., Dimitrijević, M. S.: "Long Term Variability Of The Coronal and Post - Coronal Regions Of The Oe Star HD 93521", XXVIth IAU General Assembly, Prague, Czech Republic, 2006, August 14-25.
15. Antoniou, A., Danezis, E., Lyratzi, E., Nikolaidis, D., Popović, L. Č., Dimitrijević, M. S.: "Hyper Ionization Phenomena In The C IV Region Of 20 Oe Stars", XXVIth IAU General Assembly, Prague, Czech Republic, 2006, August 14-25.
16. Antoniou, A., Danezis, E., Lyratzi, E., Nikolaidis, D., Popović, L. Č., Dimitrijević, M. S.: "Hyper Ionization Phenomena In The N IV Region Of 20 Oe Stars", XXVIth IAU General Assembly, Prague, Czech Republic, 2006, August 14-25.
17. Antoniou, A., Danezis, E., Lyratzi, E., Nikolaidis, D., Popović, L. Č., Dimitrijević, M. S.: "Hyper Ionization Phenomena In The N V Region Of 20 Oe Stars", XXVIth IAU General Assembly, Prague, Czech Republic, 2006, August 14-25.
18. Nikolaidis, D., Danezis, E., Lyratzi, E., Popović, L. Č., Dimitrijević, M. S., Antoniou, A. & Theodossiou, E.: "A new model for the structure of the DACs and SACs regions in the Oe and Be stellar atmospheres", XXVIth IAU General Assembly, Prague, Czech Republic, 2006, August 14-25.
19. Lyratzi, E., Danezis, E., Antoniou, A., Nikolaidis, D., Popović, L. Č. & Dimitrijević, M. S.: "A new approach for the structure of H α regions in 120 Be-type stars", XXVIth IAU General Assembly, Prague, Czech Republic, 2006, August 14-25.

20. Lyratzi, E., Danezis, E., Antoniou, A., Nikolaidis, D., Popović, L. Č. & Dimitrijević, M. S.: "The complex structure of the Si IV $\lambda\lambda$ 1393.755, 1402.77 E regions of 68 Be-type stars", XXVith IAU General Assembly, Prague, Czech Republic, 2006, August 14-25.
21. Danezis, E., Popović, L. Č., Lyratzi, E. & Dimitrijević, M. S.: "The peculiar absorption and emission phenomena from stars to quasars", [2006, AIPC, 876, 373](#) 23rd Summer School and International Symposium on the Physics of Ionized Gases, (SPIG 2006), August 28 - September 1, 2006, Kopaonik, Serbia (Invited Lecture).
22. Danezis, E., Lyratzi, E., Nikolaidis, D., Antoniou, A., Popović, L. Č. and Dimitrijević, M. S.: "The SACs Broadening", 23rd Summer School and International Symposium on the Physics of Ionized Gases, (SPIG 2006), August 28 - September 1, 2006, Kopaonik, Serbia.
23. Lyratzi, E., Danezis, E., Nikolaidis, D., Antoniou, A., Popović, L. Č., Dimitrijević, M. S. and Theodossiou, E.: "The Photospheric And The Respective Si IV Regions Rotational Velocities In 27 Be Stars", 23rd Summer School and International Symposium on the Physics of Ionized Gases, (SPIG 2006), August 28 - September 1, 2006, Kopaonik, Serbia.
24. Nikolaidis, D., Danezis, E., Lyratzi, E., Popović, L. Č., Antoniou, A. Dimitrijević, M. S., and Theodossiou, E.: "A Study Of DACs And SACs Regions In The Atmospheres Of Hot Emissions Stars", 23rd Summer School and International Symposium on the Physics of Ionized Gases, (SPIG 2006), August 28 - September 1, 2006, Kopaonik, Serbia.
25. Antoniou, A., Danezis, E., Lyratzi, E., Nikolaidis, D., Popović, L. Č., Dimitrijević, M. S. and Theodossiou, E.: "The Photospheric And The Respective C IV Regions Rotational Velocities In 20 Oe Stars", 23rd Summer School and International Symposium on the Physics of Ionized Gases, (SPIG 2006), August 28 - September 1, 2006, Kopaonik, Serbia.
26. Lyratzi, E., Danezis, E., Popović, L. Č., Dimitrijević, M. S. & Nikolaidis D.: "The complex structure of the Mg II $\lambda\lambda$ 2795.523, 2802.698 Å regions of 64 Be stars", [2007, PASJ, 59, 357](#)
27. Danezis, E., Nikolaidis D., Lyratzi, E., Popović, L. Č., Dimitrijević, M. S., Antoniou, A. & Theodosiou, E.: "A new model for the structure of DACs and SACs regions in Oe and Be stellar atmospheres", [2007, PASJ, 59, 827](#)
28. Danezis, E., Antoniou, A., Lyratzi, E., Popović, L. Č., Dimitrijević, M. S., Nikolaidis, D.: "The DACs and SACs Effects From Stars to Quasars. Some First General Notices", VI Serbian Conference on Spectral Line Shapes in Astrophysics (VI SCSLSA), Sremski Karlovci, Serbia, June 2007. (*Invited Lecture*)
29. Lyratzi, E., Danezis, E., Dimitrijević, M. S., Popović, L. Č., Nikolaidis, D., Antoniou, A.: "The Evolution of Some Physical Parameters in the DACs/SACs Regions in Be Stellar Atmospheres", VI Serbian Conference on Spectral Line Shapes in Astrophysics (VI SCSLSA), Sremski Karlovci, Serbia, June 2007.
30. Antoniou, A., Danezis, E., Lyratzi, E., Nikolaidis, D., Popović, L. Č., Dimitrijević, M. S.: "A statistical study of physical parameters of the C IV density regions in 20 Oe stars", VI Serbian Conference on Spectral Line Shapes in Astrophysics (VI SCSLSA), Sremski Karlovci, Serbia, June 2007.
31. Antoniou, A., Danezis, E., Lyratzi, E., Nikolaidis, D., Popović, L. Č., Dimitrijević, M. S.: "The N IV density regions in the spectra of 20 Oe stars", VI

- Serbian Conference on Spectral Line Shapes in Astrophysics (VI SCSLSA), Sremski Karlovci, Serbia, June 2007.
32. Antoniou, A., Danezis, E., Lyratzi, E., Nikolaidis, D., Popović, L. Č., Dimitrijević, M. S.: "Investigation of the post coronal density regions of Oe stars, through the N V UV resonance lines", VI Serbian Conference on Spectral Line Shapes in Astrophysics (VI SCSLSA), Sremski Karlovci, Serbia, June 2007.
 33. Antoniou, A., Danezis, E., Lyratzi, E., Nikolaidis, D., Popović, L. Č., Dimitrijević, M. S.: "Long term variability of the coronal and post-coronal regions of the Oe star HD 149757 (zeta Oph)", VI Serbian Conference on Spectral Line Shapes in Astrophysics (VI SCSLSA), Sremski Karlovci, Serbia, June 2007.
 34. Danezis, E., Nikolaidis D., Lyratzi, E., Popović, L. Č., Dimitrijević, M. S., Antoniou, A. & Theodosiou, E.: «A new model for the structure of DACs and SACs regions in Oe and Be stellar atmospheres», 2007, PASJ, 59, 827
 35. Danezis, E., Lyratzi, E., Popović, L. Č., Dimitrijević, M. S. & Antoniou, A.: «Similarity Between DACs/SACs Phenomena in Hot Emission Stars and Quasars Absorption Lines», 2008, Proceedings of 19th ICSLS, Valladolid, Spain.
 36. Lyratzi, E., Danezis, E., Popović, L. Č., Dimitrijević, M. S. & Antoniou, A.: «Kinematics of Broad Absorption Line Regions of PG 1254+047», 2008, Proceedings of 19th ICSLS, Valladolid, Spain.
 37. Lyratzi, E., Danezis, E., Popović, L. Č., Dimitrijević, M. S. & Antoniou, A.: «DACs and SACs in the UV Spectrum of the Quasar PG 0946+301», 2008, Proceedings of 19th ICSLS, Valladolid, Spain.
 38. Antoniou, A., Danezis, E., Lyratzi, E., Popović, L. Č., Dimitrijević, M. S., Theodosiou, E. & Stathopoulos, D.: «AX Mon (HD 45910) Kinematical Parameters in the Fe II Spectral Lines as a Function of the Excitation Potential», 2008, Proceedings of 19th ICSLS, Valladolid, Spain.
 39. Antoniou, A., Danezis, E., Lyratzi, E., Popović, L. Č., Dimitrijević, M. S., Theodosiou, E. & Katsavrias, G.: «A Study of the Structure of Different Ionization Potential Regions in the Atmosphere of AX Mon (HD 45910)», 2008, Proceedings of 19th ICSLS, Valladolid, Spain.
 40. Antoniou, A., Danezis, E., Lyratzi, E., Popović, L. Č. & Dimitrijević, M. S.: «Kinematical parameters in the coronal and post-coronal regions of the Oe stars», 2008, (*Προσκεκλημένη Ομιλία στο Διεθνές Συνέδριο 24th Summer School and International Symposium on the Physics of Ionized Gases, (SPIG 2008)*, Novi Sad, Serbia.
 41. Danezis, E., Lyratzi, E., Popović, L. Č., Antoniou, A. & Dimitrijević, M. S.: «The very broad lines in the UV spectra of hot emission stars – A possible explanation», 2008, *Publ. Astron. Obs. Belgrade*, 84, 463.
 42. Lyratzi, E., Danezis, E., Popović, L. Č., Dimitrijević, M. S. & Antoniou, A.: «DACs and SACs phenomena in the C IV emitting regions of QSOs», 2008, *Publ. Astron. Obs. Belgrade*, 84, 483.
 43. Antoniou, A., Danezis, E., Lyratzi, E., Popović, L. Č., Dimitrijević, M. S., Theodosiou, E. & Stathopoulos, D.: «A study of AX Mon (HD 45910) kinematical parameters of the Fe II density regions», 2008, *Publ. Astron. Obs. Belgrade*, 84, 455.

44. Danezis, E., Lyratzi, E., Popović, L. Č., Dimitrijević, M. S. & Antoniou, A.: «DACs/SACs phenomena in astrophysical spectra», JENAM 2008, Vienna, Austria.
45. Lyratzi, E., Danezis, E., Popović, L. Č., Dimitrijević, M. S. & Antoniou, A.: «An analysis of C IV and Si IV lines in the spectra of the quasars PG 0946+301 and PG 1254+047», JENAM 2008, Vienna, Austria.
46. Antoniou, A., Danezis, E., Lyratzi, E., Popović, L. Č., Dimitrijević, M. S., Katsavrias, G.: «The structure of atmospherical layers of AX Mon (HD 45910)», JENAM 2008, Vienna, Austria.

Most important papers



A NEW MODEL FOR THE STRUCTURE OF THE DACs REGIONS IN THE Oe AND Be STELLAR ATMOSPHERES

E. DANEZIS, D. NIKOLAIDIS, V. LYRATZI, M. STATHOPOULOU,
E. THEODOSSIOU, A. KOSIONIDIS, C. DRAKOPOULOS, G. CHRISTOU
and P. KOUTSOURIS

*University of Athens, School of Physics Department of Astrophysics, Astronomy and Mechanics,
Panepistimiopolis, Zografos 157 84 Athens – Greece*

(Received 27 March 2001; accepted 5 December 2002)

Abstract. As it is already known, the spectra of many Oe and Be stars present Discrete Absorption Components (DACs) which, because of their profiles' width as well as the values of the expansion / contraction velocities, they create a complicated profile of the main spectral lines. This fact is interpreted by the existence of two or more independent layers of matter, in the region where the main spectral lines are formed. Such a structure is responsible for the formation of a series of satellite components (DACs) for each main spectral line. In this paper we present a first approximation to a mathematical model reproducing the complex profile of the spectral lines of Oe and Be stars that present DACs. This model presupposes that the regions, where these spectral lines are formed, are not continuous but consist of a number of independent absorbing density layers of matter, followed by an emission region and an external general absorption region. When we fit the spectral lines that present DACs, with this model, we can calculate the values of the apparent rotation and expansion / contraction velocities of the regions where the DACs are formed.

1. Introduction

Peton (1974) first pointed out, in the visual spectrum of the double system AX Mon (HD 45910), the existence of a secondary component of the absorption line FeII λ 4233A, which, depending on the phase, appeared in the violet or in the red side of the main spectral line. For this reason the secondary component was named 'satellite component'.

Underhill (1975) observed sharp components of the ions N II, C II and Mg II in the spectrum of HD 58350 and attributed the one of the velocity of 230 km/s to a gas cloud accelerated from the star and moving rapidly out of the star and the other of the velocity of about 25 km/s to a moving circumstellar shell.

Lamers et al. (1982) noted the possibility of the presence of satellite components superimposed on the wide P Cygni profile of the UV resonance lines of the OeII λ star HD 175754 and suggested that they may be the result of ionization gradients in an otherwise spherically symmetric and time-steady wind.

Franco et al. (1983) studied the P Cygni profiles of the above mentioned resonance lines of HD 175754 observed at different epochs and they reported variability at the secondary satellite component. They proposed for this star two different



mechanisms for the explanation of the variability, namely, a thermal mechanism in a hot region at $T_c=2 \times 10^5$ K which produces the principal stationary component and a mechanism which gives rise to the secondary by ionization of cooler high velocity stellar material from X-rays coming from inner coronal region.

Mullan (1984a,b, 1986) suggested that the satellite components may result from 'corotating interaction regions' (CIRs), which may form in stars' winds and depend on asymmetries in the wind velocity or density.

Danezis (1984, 1986) and Danezis et al. (1991) studied the UV spectra of the gaseous envelope of AX Mon taken by the IUE satellite (at phase 0.568) and noted that the absorption lines of many ionization potential ions, not only of those presenting P Cygni profile, are accompanied by two strong absorption components of the same ion and the same wavelength, shifted at different $\Delta\lambda$, in the violet side of each main spectral line. This means that the regions where these spectral lines are created are not continuous, but they are formed by a number of independent density layers of matter. These layers of matter can rotate and move with different apparent velocities.

The existence of satellite components in the UV spectrum of AX Mon has been verified by Sahade et al. (1984) and Sahade and Brandi (1985) at the phase of 0.095. Also, Hutsemekers (1985) in the UV spectrum of another Be star, HD 50138, noticed a number of satellite components that accompanied the main spectral lines.

Bates and Halliwell (1986), naming the satellite components as 'discrete absorption components' (DACs), constructed a model of ejection of gas parcels from above the star's photosphere, accelerated by radiation pressure. In order to describe the DACs, many suggestions about the properties of the winds have been made, which propose that the DACs are due to disturbances in the wind such as material that forms spiral streams as a result of the star's rotation (Mullan, 1984a; Prinja and Howarth, 1988) or to mass ejections constructing 'shells', 'puffs' or gas 'parcels' (Henrichs, 1984; Underhill and Fahey, 1984; Bates and Halliwell, 1986; Grady et al., 1987; Lamers et al., 1988).

Willis et al. (1989) argued against these components being formed in discrete mass conserving density enhancements, such as shells or blobs. They proposed that they result from 'largely chaotic structures in the wind' and that 'they are formed by different material at different times', because of radiative instability (Mulan, 1984; Owocki et al., 1988; Prinja et al., 1988).

Bates and Gilheany (1990) and Gilheany et al. (1990) pointed out that 'it is difficult to identify unambiguously DAC and wind signatures from a single spectrum of a star, as the UV spectrum of late B stars is very crowded with photospheric lines'. So, in their study of twelve B5 – B9 supergiants they employed a code based on spherical symmetry, they fitted 'Gaussian profiles to the spectra and derived values for the observed component velocity widths and equivalent widths'. They concluded to the non-simultaneous appearance of DACs in different ions and they attributed the presence of DACs to mass-loss (Burki et al., 1982).

However, Danezis and Theodossiou (1988, 1990) could not find satellite components (DACs) of the main spectral lines of another Be star, 88 Herculis. Laskarides et al. (1992a) observed one more satellite component in the spectral lines of ions with low ionization potential in the UV spectrum of AX Mon, this in the red side of the main lines. The existence of the spectral lines in the red side of the main lines has been proposed by Doazan in 1983. This fact indicates contraction of the outer layers of the gaseous envelope.

Waldron et al. (1992) studied 'the time-dependent hydrodynamical influence of a spherically symmetric propagating density pulse/shell in the stellar wind' of the O4I(n)f star HD 66811 (ζ Puppis) and suggested that 'the DACs behaviour is associated with these density pulses which are injected into the supersonic wind by some unknown initiating mechanism'. In a later study of ζ Puppis (1994), based on 'the long-term regularity of occurrence (Kaper et al., 1990), the short-term behaviour that appears to be related to the stellar rotation rate (Prinja, 1988, 1992) and the observed photospheric and wind-line variability that appears to be correlated' (Henrichs, 1990), they suggested that 'the mechanism responsible for initiating DACs may be dynamically linked to the photosphere and that they must appear due to the inherently unstable nature of radiatively driven winds'. In this study they tried to give an explanation to the large-scale ejection phenomena by modelling the full time-dependent hydrodynamic response of a stellar wind to a spherically symmetric propagating density shell, which suggests that a substantial amount of material must be present in front of the stellar disk to reproduce the observations. They concluded to DACs' behaviour in UV P Cygni line profiles being the result of the density shells (Lamers et al., 1978; Henrichs et al., 1980, 1983), which are hydrodynamically stable and propagate through the supersonic wind structure as stable solitary waves. They also concluded to the following: 'the shell accelerates in conjunction with the underlying wind structure, the velocity fluctuations are small and the shell dynamics are found to be essentially independent of the adopted energy equation'.

Henrichs et al. (1994) in their study on ξ Per agree with the suggestion that 'the DACs are formed in absorbing layers in the line of sight, projected against the stellar disk' and proposed that 'similar density structures must also be present in the emitting volume around the star'. They suggested that the DACs originate in expanding high-density regions behind fronts due to amplified radiative instabilities in the wind.

Telting et al. (1993, 1994) studied the Be star γ Cas and proposed a model for the description of the envelope, which combines two types of stellar winds: 'a dense equatorial disc in which the Balmer emission lines and the IR excess are formed and a rapidly expanding radiation-driven wind streaming from higher latitudes of the star, which forms the UV resonance lines'. They calculated the same values for the outflow velocity of DACs of different doublets in many spectra, indicating that these DACs must be formed in 'one particular outflowing high-density wind structure'.

Cranmer and Owocki (1996), based on ‘the lack of emission variability in UV P Cygni lines (Prinja and Howarth, 1988) and significant infrared variability (Howarth, 1992)’, as well as to the fact that ‘the observed strong absorption dips can be produced if the structure of the wind is large enough in order to cover a substantial fraction of the stellar disk’, suggested that the DACs originate from ‘moderate size wind structures such as spatially localized clouds, streams or blobs’. They proposed a hydrodynamical model considering an azimuthally inhomogeneous radiation-driven wind for the formation of large-scale CIRs. They suggested that DACs could derive by CIRs resulting from a magnetic field (Mulan, 1984a,b, 1986), with closed and open magnetic loops above the stellar surface (Underhill and Fahey, 1984) and ‘for which the surface mass loss ‘eruption’ lasts long enough to make structure that covers a substantial portion of the stellar disk’.

Rivinius et al. (1997) studied the optical spectra of B hypergiants and suggested a model for the time-dependent wind variations, which accepts ‘spherical steady wind with randomly distributed and outwards moving inhomogeneities (‘blobs’)’. They proposed that when the ‘blobs’ are in front of the stellar disk they give rise to the DACs appearance, otherwise they only contribute to some extra radiation emitted in all directions (Lamers, 1994). Because of the presence of the DACs at very low velocities, they suggested that the ‘blobs’ originate not in the wind but in the photosphere or in even deeper layers.

Prinja et al. (1997) detected an ‘extremely narrow DAC’ (‘Super DAC’) in all the spectral lines of the B supergiant γ Ara, which ‘demonstrates ionization stratification in the wind and is likely due to a very dense region that covers most of the projected surface of the visible hemisphere of the star’. They suggested that the wind of this star may be ‘equatorially enhanced’ probably because of its rapid rotation and that the ‘Super DAC’ is formed in the equatorial region or results from CIRs or ‘arises from time-dependent wind fluctuations, (perhaps enhanced mass loss) which do not invoke latitude-dependence, but simply represents denser gas accelerating more slowly to a lower terminal velocity’.

Fullerton et al. (1997) in their study of the B supergiant HD 64760 suggested that the wind is not spherically symmetric and the wind structures that are responsible for the DACs are not radial, but extend for more than 90° in azimuth and about 30° in longitude and have a spiral shape. These spirals corotate with the stellar surface, implying that they are linked to photospheric phenomena, and form density regions in the stellar wind. They concluded to the interesting fact that ‘the radial expansion of the wind of HD 64760 is not too different from the outflows derived for spherically symmetrical, steady-state models of the winds of early-type stars’. They proposed that this may be due to the possibility that ‘the radial expansion of the wind may not be strongly affected by the presence of the spirals’. They explained the appearance of different ions’ DACs by ‘the presence of an ionization or density gradient across the width of the spirals, such as that the inner edge favors the presence of more highly ionized species’.

Cidale (1998) studied the MgII lines in Be stars considering spherical symmetry for the expanding circumstellar medium to which she attributed the presence of the blueshifted absorption components and proposed that ‘a decelerating wind yields denser outer regions which could enhance the emission’.

Kaper et al. (1996, 1997, 1999) studied a series of 10 bright O stars and described the shape of the individual absorption components by an exponential Gaussian. They calculated the same velocity in resonance lines formed by different ions and proposed that the edge variability is directly related to the DACs (Henrichs et al., 1988, 1994; Prinja, 1991), which actually have an impact on the position of the edge. They suggested that the DACs are related with interacting fast or slow moving wind streams of higher density, corotating with the star (CIRs). The curved streams cause fast wind material to collide with slow wind material in front of it, constructing high density regions, and the star’s rotation results to the interaction region having also spiral shape and corotating with the star. The wind material, though, due to the conservation of its angular momentum, does not corotate with the star, but it moves radially and meets the interaction region at distance from the star. They proposed that ‘the DACs are not formed in the CIRs themselves, but originate in the so-called radiative-acoustic kinks trailing the CIRs’. As the DACs found in different ions’ resonance lines have the same velocity, they should originate from high density regions, which should be geometrically extended in order to be observable by covering a significant fraction of the stellar disk. They also suggested that because of the stable appearance of DACs over long time periods, ‘the physical process responsible for the formation of slow (or fast) streams has to be rather stable’, meaning that the streams may be due to non-radial pulsations or, less likely, a surface magnetic field.

Cranmer et al. (2000) studied the DACs that appear in the spectra of γ Cas in order to determine the nature of the interaction between winds and disks of Be stars (Telting and Kaper, 1994). They pointed out that the outflowing gas responsible for the DACs formation is denser than the mean undisturbed polar wind. They proposed that the density region responsible for the appearance of DACs may be due to ‘the existence of compressible shocks propagating through the polar wind’. They stressed out that ‘the mean DAC structure does not seem to rotate with the star, meaning that it is independent of the more localized spiral-shaped opacity modulations embedded within it’. It is interesting that, as some of the spectral features could not be fitted with a Gaussian function, they decided to fit it by a sum of two or more Gaussians, without implying, though, that ‘the central velocities of these extra terms should be interpreted as independent dynamical wind features’. They confirmed the suggestion that ‘DACs do not represent isolated mass-conserving ‘blobs’, but instead they indicate the presence of a rotating pattern or perturbation through which wind material flows’. They detected slower acceleration or even deceleration of the regions responsible for DACs compared to the mean stellar wind.

Markova (2000) studied the line-profile variability in P Cygni's optical spectrum and concluded to the fact that the recurrence of DACs is hardly related to the stellar rotation and that the DACs are not due to single mass-conserving features, such as outward moving blobs, but that they may originate from outward moving, large-scale, high-density perturbations, which possibly originate from the photosphere, but develop in the outer wind and through which wind material flows. These perturbations may be spherically symmetric density shells or curved structures like kinks.

Danezis et al. (1991, 1995, 1997a,b 1998, 1999, 2000a,b,c, 2001,a,b,c, 2002, a, b, c), Theodossiou et al. (1993, 1997), Laskarides et al. (1992a, 1992b, 1993a, 1993b), Stathopoulou et al. (1995, 1997), Lyratzi et al. (2001, 2002a,b) Kyriakopoulou et al. (2001) and Christou et al. (2001) apart from their study on the UV spectrum of Be stars, where they found satellite components, they have also studied the UV spectrum of several Oe stars and detected satellite components, not only for the spectral lines of low ionization potential, but also for the resonance lines of NV, CIV, SiIV and the spectral line NIV.

2. The Main Idea of Our Research

It is obvious from the above that many suggestions have been made in order to explain the DACs phenomenon. Most researchers have suggested mechanisms that allow the existence of structures which cover all or a significant part of the stellar disk, such as shells, blobs or puffs (Underhill, 1975; Henrichs, 1984; Underhill and Fahey, 1984; Bates and Halliwell, 1986; Grady et al., 1987; Lamers et al., 1988; Waldron et al., 1992; Cranmer and Owocki, 1996; Rivinius et al., 1997; Kaper et al., 1996, 1997, 1999; Markova, 2000), interaction of fast and slow wind components, CIRs, structures due to magnetic fields or spiral streams as a result of the star's rotation (Underhill and Fahey, 1984; Mullan, 1984a,b 1986; Prinja and Howarth, 1988; Cranmer and Owocki, 1996; Fullerton et al., 1997; Kaper et al., 1996, 1997, 1999; Cranmer et al., 2000). Though we do not know yet the mechanism responsible for the formation of such structures, it is positive that DACs result from independent high density regions in the stars' environment.

Specifically, in this paper we test the ideas proposed by Danezis (1984, 1986) and Danezis et al. (1991). In these papers they proposed that probably:

1. DACs are not unknown absorption spectral lines, but spectral lines (satellite absorption components) of the same ion and the same wavelength as a main spectral line, shifted at different $\Delta\lambda$. In addition, DACs are not always discrete absorption spectral lines, but in most cases lines that are blended among themselves as well as with the main spectral line. In such a case they are not observable, but we can detect them through the analysis of our model. This means that when we deal with a significant spectral line, which is accompanied by satellite absorption components, we should not regard them as independent

spectral lines, but as a unified formation which must be dealt with as one spectral line splitted into a series of components. Finally, as Peton (1974) first pointed out, these components appear as ‘satellites’ in the violet or in the red side of the main spectral line as a function of the time or the phase in the case of a binary system. For these reasons we prefer to name them Satellite Absorption Components (SACs) and not Discrete Absorption Components (DACs).

2. This hypothesis may be correct only if the main spectral line and its satellite absorption components (SACs) are born in different, independent density regions, where the prevailing conditions allow the existence of matter, able to form the main spectral line and its satellite absorption components (SACs) in the same time.
3. In the case of absorption spectral lines presenting SACs, as well as a P Cygni profile, the emission spectral line is created in an independent emitting density region.

All the above, are just simple theoretical suppositions. A very important question is whether such a complex structure of the regions, where the spectral lines that present SACs are born, may lead to the formation of a function for the line’s profile able to reproduce, in the best way, the main spectral line and its satellite absorption components (SACs) in the same time. Our main purpose in this paper is to give an answer to this question. By solving the equations of radiation transfer through a complex structure as the one described, we try to conclude to a function for the line’s profile, able to give the best fit for the main spectral line and its satellite absorption components (SACs) in the same time. Such a best fit, through the function of the line’s profile, enables us to calculate parameters of the independent layers of matter which form the main spectral line and its satellite absorption components (SACs), such as the apparent rotation and expansion / contraction velocities.

Applications of this model we have presented at JENAM ’98 in Prague (Danezis et al., 1998), at JENAM 2000 in Moscow (Danezis et al., 2000a,b,c), at the 4th Hellenic Astronomical Society Conf. at Samos, Greece (Danezis et al., 1999), at the 5th Hellenic Astronomical Society Conf. at Crete, Greece (Danezis et al., 2001a,b,c; Lyratzi et al., 2001; Kyriakopoulou et al., 2001; Christou et al., 2001) and at the IAU Symposium 210, Uppsala, Sweden (Danezis et al., 2002a,b,c; Lyratzi et al., 2002a,b).

Finally, we would like to point out once again that our main purpose is to propose a model able to reproduce every spectral line at the specific moment when the spectrum is taken.

3. Description of the Method

3.1. FUNDAMENTAL HYPOTHESES

- i) The stellar envelope is composed of a number of successive independent absorbing density layers of matter, followed by an emission region and an external general absorption region.
- ii) The angular velocity of rotation is constant.
- iii) Thermal and natural broadening of spectral lines is negligible. This means that the whole width of the line is measured as V_{rot} .
- iv) The observer lies on the equatorial plane.
- v) None of the phenomena are relativistic.
- vi) The only effect of a shell's expansion or contraction is a Doppler shift of the center of the lines.

3.2. MATHEMATICAL EXPRESSION

We assume that we have a radiation of intensity I_λ passing through an area of gaseous material of constant density ρ , thickness ds and absorption coefficient k_λ . The effect of the shell on the radiation intensity is given by:

$$dI_\lambda = -k_\lambda I_\lambda \rho ds$$

For a shell of total thickness s and an initial radiation intensity of $I_{\lambda 0}$ the effect will be:

$$I_\lambda = I_{\lambda 0} \exp \{-\tau\} \quad (1)$$

where

$$\tau = \int_0^s k_\lambda \rho ds.$$

Now consider this radiation intensity passing through a second shell, of density ρ_b , thickness s_b and absorption coefficient $k_{\lambda b}$. The radiation intensity exiting this second shell will be:

$$I_{\lambda b} = I_\lambda \exp \{-\tau_b\}$$

where

$$\tau_b = \int_0^{s_b} k_{\lambda b} \rho_b ds.$$

Substituting (1) for I_λ yields:

$$I_{\lambda b} = I_{\lambda 0} \exp \{-\tau\} \exp \{-\tau_b\}$$

Generalising for i absorbing shells, the final exiting radiation will be:

$$I_{\lambda i} = I_{\lambda 0} \prod_i \exp \{-\tau_i\} \tag{2}$$

Consider now a shell that is both absorbing and emitting (henceforth called in this paper a ‘mixed’ shell), with k_λ and j_λ being the respective coefficients. Its effect on the radiation intensity $I_{\lambda i}$ will be:

$$dI_{\lambda i} = -k_\lambda I_{\lambda i} \rho ds + j_\lambda \rho ds$$

And the total effect of such a shell of thickness s_e , and density ρ_e on a radiation flow of intensity $I_{\lambda i}$ will be:

$$I_{\lambda e} = I_{\lambda i} \exp \{-\tau_e\} + \int_0^{\tau_e} \frac{j_{\lambda e}}{k_{\lambda e}} e^{-\tau_e} d\tau$$

where $\frac{j_{\lambda e}}{k_{\lambda e}}$ is the source function $S_{\lambda e}$ and $\tau = \int_0^{s_e} k_{\lambda e} \rho_e ds$.

At the moment when the spectrum is taken, each emission line, with a given wavelength λ , is created in a specific region of the stellar envelope with a given value for $S_{\lambda e}$, that is $S_{\lambda e} = \text{const}$. So:

$$I_{\lambda e} = I_{\lambda i} \exp \{-\tau_e\} + S_{\lambda e} (1 - \exp \{-\tau_e\}). \tag{3}$$

Now consider that an outer shell of general absorption follows the mixed shell. Its effect on the radiation intensity will be:

$$I_{\lambda final} = I_{\lambda e} \exp \{-\tau_g\}$$

in which we replace $I_{\lambda e}$ by the radiation intensity exiting the mixed shell, given by equation (3). Thus:

$$I_{\lambda final} = \left[I_{\lambda 0} \prod_i \exp \{-\tau_i\} \exp \{-\tau_e\} + S_{\lambda e} (1 - \exp \{-\tau_e\}) \right] \exp \{-\tau_g\}$$

If we consider the absorption of the mixed shell as an independent absorption, we can include it to the product $\prod_i \exp \{-\tau_i\}$ and have:

$$I_{\lambda final} = \left[I_{\lambda 0} \prod_i \exp \{-\tau_i\} + S_{\lambda e} (1 - \exp \{-\tau_e\}) \right] \exp \{-\tau_g\}$$

A similar expression will apply to the radiation flux:

$$F(\lambda)_{final} = \left[F_0(\lambda) \prod_i \exp \{-\tau_i\} + S_{\lambda e} (1 - \exp \{-\tau_e\}) \right] \exp \{-\tau_g\}$$

Let us consider the parameters τ_i, τ_e, τ_g . As stated above, each τ is given by:

$$\tau = \int_0^S k_\lambda \rho ds.$$

We substitute for $k_{\lambda i}$, $k_{\lambda e}$, $k_{\lambda g}$ the product of two functions:

1. Omega (Ω) is an expression of k_{λ} and has the same units as k_{λ} .
2. L_i , L_e , L_g are the distribution functions of $k_{\lambda i}$, $k_{\lambda e}$, $k_{\lambda g}$ respectively. Each L depends on the values of the apparent rotational velocity as well as of the radial expansion or contraction velocity of the density shell, which forms the spectral line.

That is:

$$\tau = L \int_0^S \Omega \rho ds$$

We set: $\xi = \int_0^S \Omega \rho ds$, meaning that ξ is an expression of τ .

The resulting, final form of the radiation flux function is:

$$F_{\lambda final} = \left[F_0(\lambda) \prod_i \exp\{-L_i \xi_i\} + S_{\lambda e}(1 - \exp\{-L_e \xi_e\}) \right] \exp\{-L_g \xi_g\} \quad (4)$$

Equation 4 gives the function of the complex profile of a spectral line, which presents SACs. This means that the graphical representation of equation 4 must reproduce not only the main spectral line, but its SACs as well. As we can deduce from the above, the calculation of $F_{\lambda final}$ does not depend on the geometry of the absorbing or emitting independent density layers of matter.

The decision on the geometry is essential for the calculation of the parameters L_i . This means that by deciding on a different geometry we conclude to a different analytical form of L_i , and thus to a different shape of the profile of the spectral line, presenting SACs, that we study.

In order to decide on the appropriate geometry we took into consideration the following important facts:

1. The spectral line's profile was reproduced in the best way when we supposed spherical symmetry for the independent density regions. Such symmetry has been proposed by many researchers (Lamers et al., 1982; Bates and Gilheany, 1990; Gilheany et al., 1990; Waldron et al., 1992; Rivinius et al., 1997; Cidale, 1998, Markova, 2000).
2. However, the independent layers of matter, where a spectral line and its SACs were born, could lie either close to the star, as in the case of the photospheric components of the H α line in Be stars (Andrillat and Fehrenbach, 1982; Andrillat, 1983), in which case spherical symmetry is justified, or at a greater distance from the star, where the spherical symmetry can not be justified.

These thoughts lead us to the conclusions that:

1. In the case of independent density layers of matter that lie close to the star we could suppose the existence of a classical spherical symmetry (Lamers et al., 1982; Bates and Gilheany, 1990; Gilheany et al., 1990; Waldron et al., 1992; Rivinius et al., 1997; Cidale, 1998, Markova, 2000).

2. In the case of independent density layers of matter that lie at a greater distance from the photosphere, we could suppose the existence of independent density regions such as blobs, which should cover a substantial fraction of the stellar disk (Cranmer and Owocki, 1996) and are outwards moving inhomogeneities (Rivinius et al., 1997), spiral streams (Fullerton et al., 1997; Cranmer et al., 2000; Markova, 2000) or CIRs, which may result from non-radial pulsations, magnetic fields or the star's rotation (Mullan, 1984a,b, 1986; Prinja and Howarth, 1988; Kaper et al., 1996, 1997, 1999) and are able to make structures that cover a substantial portion of the stellar disk (Cranmer and Owocki, 1996; Kaper et al., 1996, 1997, 1999). These regions, though they do not present spherical symmetry around the star, they form spectral lines' profiles which are identical with those deriving from a spherically symmetric structure. This means that these line profiles present the same values for V_{rot} , V_{exp} and ξ as the ones deriving from a classical spherical symmetry. In such a case, though the density regions are not spherically symmetric, through their effects on the lines' profiles, they appear as spherically symmetric structures to the observer. This means that in both cases, where either the symmetry is spherical or it appears as spherical through its effects on the lines' profile, the calculation of L_i , is justifiably based on the supposition of spherical symmetry.

The above mentioned thoughts led us to suppose spherical symmetry (or apparent spherical symmetry) for the density regions where the main spectral line as well as its SACs are born, in order to calculate the parameters L_i .

3.3. CALCULATION OF THE DISTRIBUTION FUNCTIONS L

If we consider that the density shell of matter, where the spectral line is produced, lies between angles $-\theta_0$ to $+\theta_0$ from the equatorial plane, then:

$$L = \int_{-\theta_0}^{\theta_0} \cos \theta d\theta = [\sin \theta]_{-\theta_0}^{+\theta_0} = 2 \sin \theta_0, \quad (5)$$

for every

$$\lambda_i : |\lambda_i - \lambda_0| < \frac{\lambda_0 z_0 \cos \theta_0}{1 - z_0^2 \cos \theta_0}$$

and

$$L = 0,$$

for every

$$\lambda_i : |\lambda_i - \lambda_0| < \frac{\lambda_0 z_0 \cos^2 \theta_0}{1 - z_0^2 \cos^2 \theta_0},$$

Normalizing equation (5) we have:

$$L_i = \sin \theta_0 = \sqrt{1 - \cos^2 \theta_0}. \quad (6)$$

As θ_0 lies between the values of $-\frac{\pi}{2}$ and $\frac{\pi}{2}$, equation (5) yields to:

$$\cos \theta_0 = \frac{-\lambda_0 + \sqrt{\lambda_0^2 + 4\Delta\lambda^2}}{2\Delta\lambda z_0} \quad (7)$$

and

$$L = \sqrt{1 - \cos^2 \theta_0}, \text{ if } \cos \theta_0 < 1$$

and

$$L = 0, \text{ if } \cos \theta_0 \geq 1$$

where:

λ_0 is the wavelength of the centre of the spectral line.

If we consider that the density shell, which forms the spectral line, moves radially, then: $\lambda_0 = \lambda_{lab} + \Delta\lambda_{exp}$, where λ_{lab} is the laboratory wavelength of the spectral line produced by a particular ion and $\Delta\lambda_{exp}$ is the radial Doppler shift and $\frac{\Delta\lambda_{exp}}{\lambda_{lab}} = \frac{V_{exp}}{c}$.
 $z_0 = \frac{V_{rot}}{c}$, where V_{rot} is the apparent rotational velocity of the i density shell of matter.

$\Delta\lambda = |\lambda_i - \lambda_0|$, where the values of λ_i are taken in the wavelength range we want to reproduce.

As we can understand from the above, the spectral line's profile, which is formed by the i density shell of matter, must be accurately reproduced by the function $e^{-L_i \xi_i}$ by applying the appropriate values of V_{roti} , V_{expi} and ξ_i .

4. Discussion of the Proposed Model

Introducing the previous final reproduction function of a complex spectral line (equation 4), we would like to note and clarify the following:

1. As we have already mentioned, for each trio of the parameters V_{roti} , V_{expi} and ξ_i , the function $I_{\lambda_i} = e^{-L_i \xi_i}$ reproduces the spectral line's profile formed by the i density shell of matter, meaning that for each trio we have a totally different profile. This results to the existence of only one trio of V_{roti} , V_{expi} and ξ_i giving the best fit of the i component. In order to accept as best fit of the observed spectral line, what is given by the trinities (V_{expi} , V_{roti} , ξ_i) of all the calculated SACs, we must adhere to all the physical criteria and techniques, such as:
 - i) It is necessary to have the superposition of the spectral region we study with the same region of a classical star of the same spectral type and luminosity class, in order to identify the existence of spectral lines that blend with the studied ones, as well as the existence of SACs.

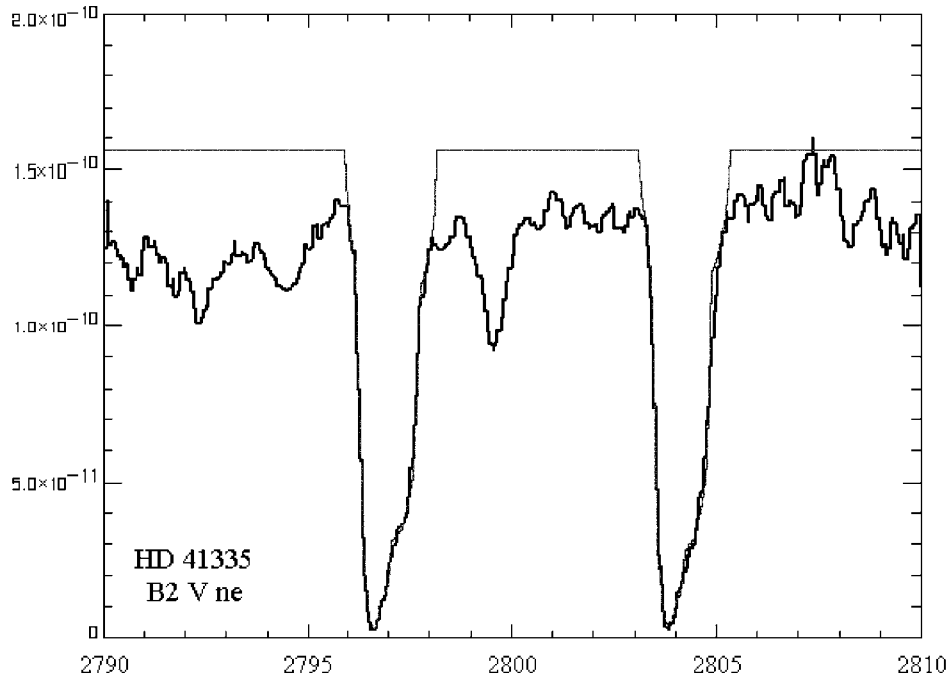


Figure 1. Best fit of Mg II lines $\lambda\lambda$ 2795.523, 2802.698 Å of the Be star HD 41335. The thick line presents the real spectral profile and the thin one the model's fit. The differences between the real spectrum and its fit are hard to see, as we have accomplished the best fit.

- ii) The resonance lines as well as those that form in these regions of the star shells that are close to each other (small difference in ionization potential) must have the same number of SACs.
 - iii) The resonance lines and the spectral lines of ions, which have similar ionization potentials, must have approximately the same values for V_{exp} and V_{rot} , as they form in the same regions. This means that the values of V_{exp} and V_{rot} of the absorption and emission SACs must lay in a range accepted by the statistical error.
2. The profiles of every main spectral line and its SACs are fitted by the function $I_{\lambda i} = e^{-L_i \xi_i}$. This function produces symmetrical line profiles. However, we know that most of the spectral lines we have to reproduce are asymmetric. This fact is interpreted as a systematical variation of the apparent radial velocities of the density regions where the main spectral line and its SACs are created. In order to approximate those asymmetric profiles we have chosen a classical method. This is the separation of the region, which produces the asymmetric profiles of the spectral line, into a small number of sub-regions, every one of which is dealt with as an independent absorptive shell. In this way we can study the variation of the density, the radial shift and the apparent rotation as

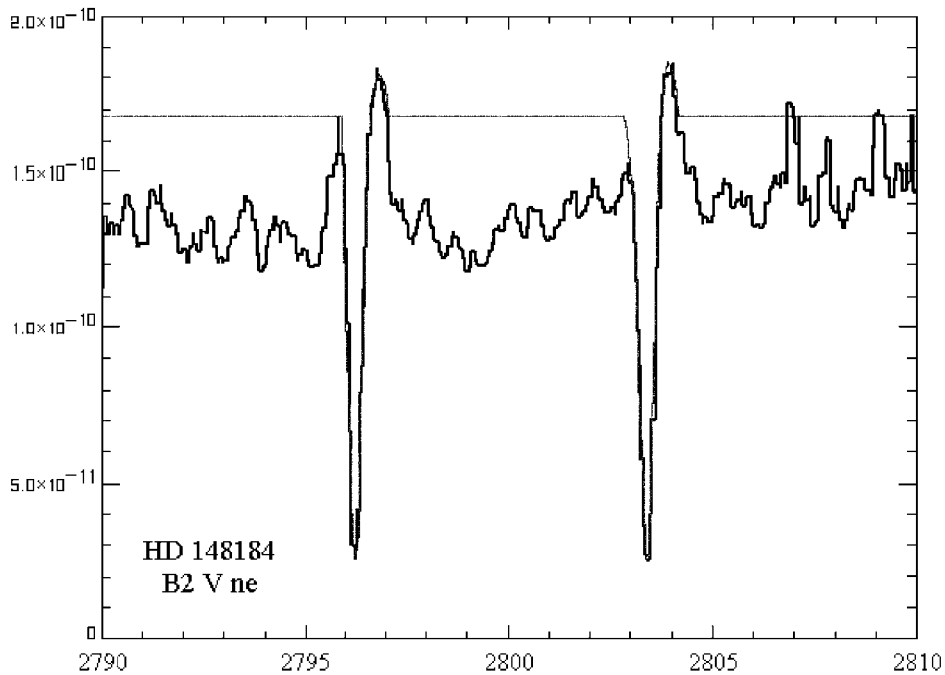


Figure 2. Best fit of Mg II lines $\lambda\lambda$ 2795.523, 2802.698 Å of the Be star HD 148184. The thick line presents the real spectral profile and the thin one the model's fit. The differences between the real spectrum and its fit are hard to see, as we have accomplished the best fit.

a function of the depth in every region which produces a spectral line with an asymmetric profile. All the above must be taken into consideration during the evaluation of our results and one should not consider that the evaluated parameters of those sub-regions correspond to independent matter shells, which form the main spectral line or its SACs.

3. We suggest that the width of the blue wing is the result of the merging of the profiles of the main spectral line and its SACs. Thus, the blue wing of each SAC gives the apparent rotational velocity of the density shell, in which it forms. This means that, in order to have measurements with physical meaning, we should not calculate the width of the blue wing of the final spectral line but the width of the blue wings of each SAC.
4. By the study of the resonance lines of a great number of stars, we measured a statistical error between 10 and 35 km/s.
5. Finally, it is clear that the function $I_{\lambda i} = e^{-L_i \xi_i}$ can produce every spectral line, which is created in a region that presents spherical or apparent spherical symmetry.

We would like to point out that the final criterion to accept or reject a best fit, is the ability of the calculated values of the physical parameters to give us a physical description of the events developing in the regions where the spectral lines presenting

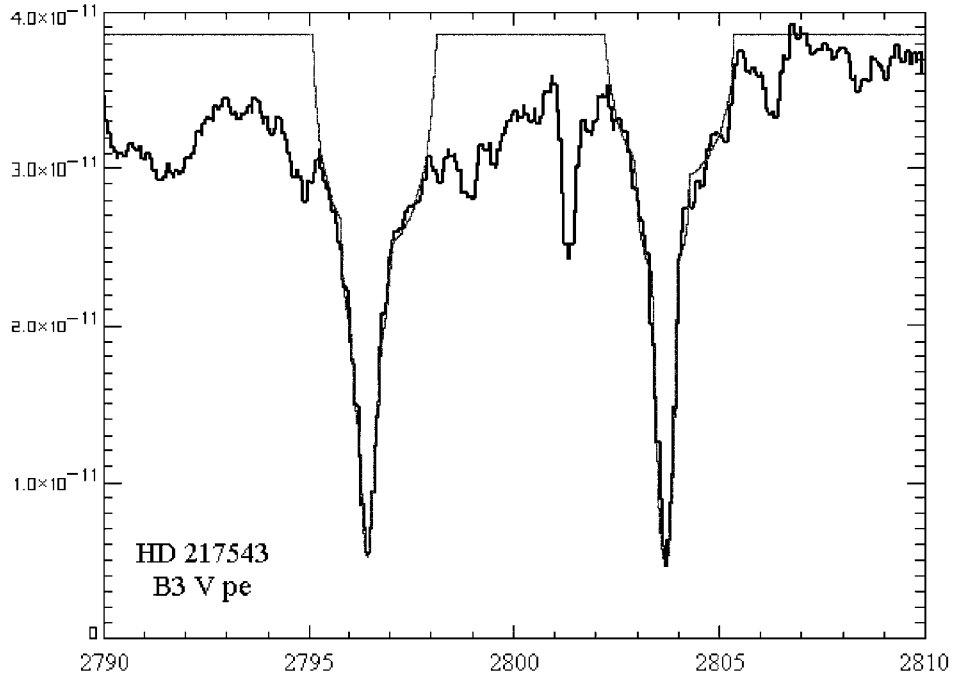


Figure 3. Best fit of Mg II lines $\lambda\lambda$ 2795.523, 2802.698 Å of the Be star HD 217543. The thick line presents the real spectral profile and the thin one the model's fit. The differences between the real spectrum and its fit are hard to see, as we have accomplished the best fit.

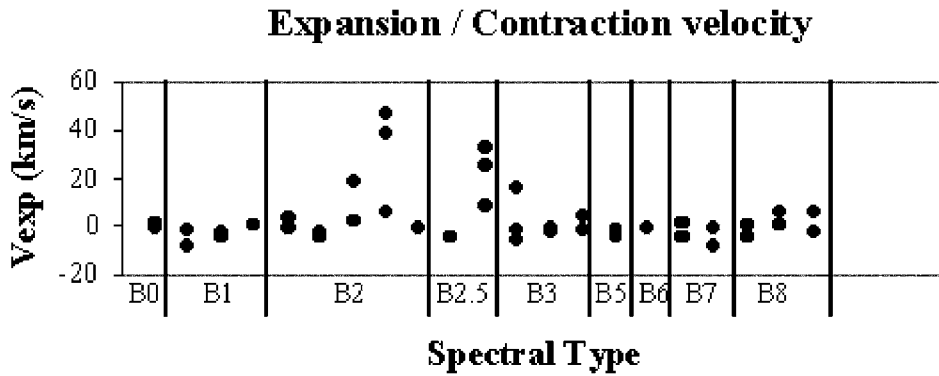


Diagram 1. Expansion / contraction velocities of all the absorption components of Mg II as a function of the spectral type.

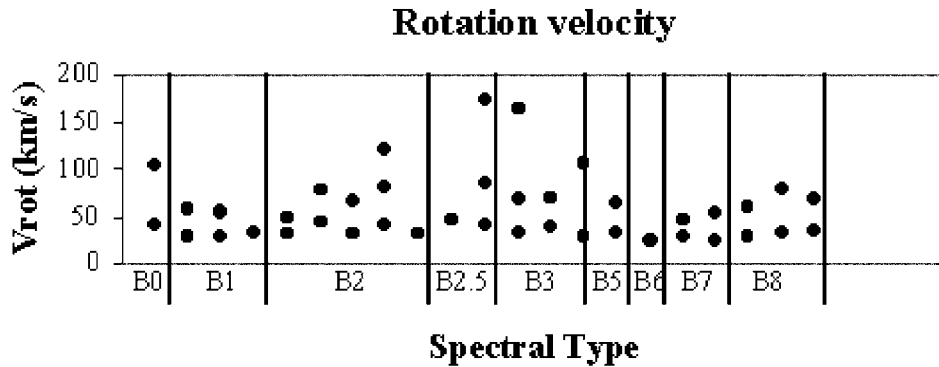


Diagram 2. Rotation velocities of all the absorption components of Mg II as a function of the spectral type.

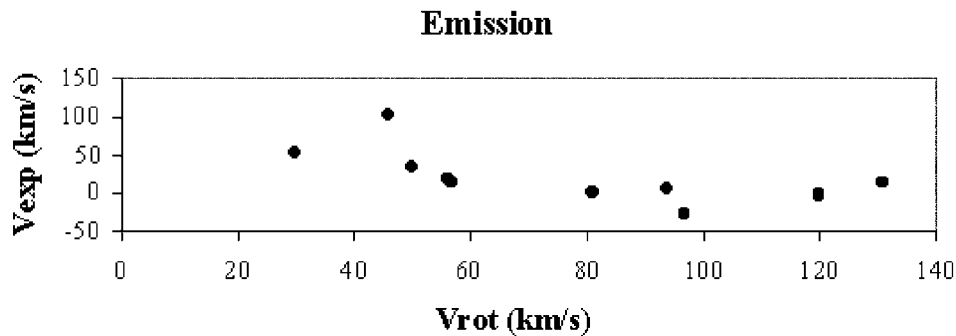


Diagram 3. Expansion / contraction velocities of the emission component of Mg II as a function of the respective rotation velocities.

SACs are created. This means that the calculated values of the physical parameters should not go against the classical physical theory.

In order to test the accuracy of the spectral lines' fits deriving from equation 4, we presented a series of poster papers at the JENAM 1998 in Prague and its applications were presented at the JENAM 2000 in Moscow. A new series of applications was also presented at the IAU Symposium 210 (Uppsala, Sweden, 2002). A summary of two of these papers is presented as an application in this paper.

5. Application to the Spectral Lines of Selected Oe and Be Stars

5.1. MG II REGIONS IN THE GASEOUS ENVELOPE OF BE V STARS

Danezis et al. (2002a) by applying the above presented model, studied the variation of the calculated parameters V_{rot} and V_{exp} of the density regions where the Mg II

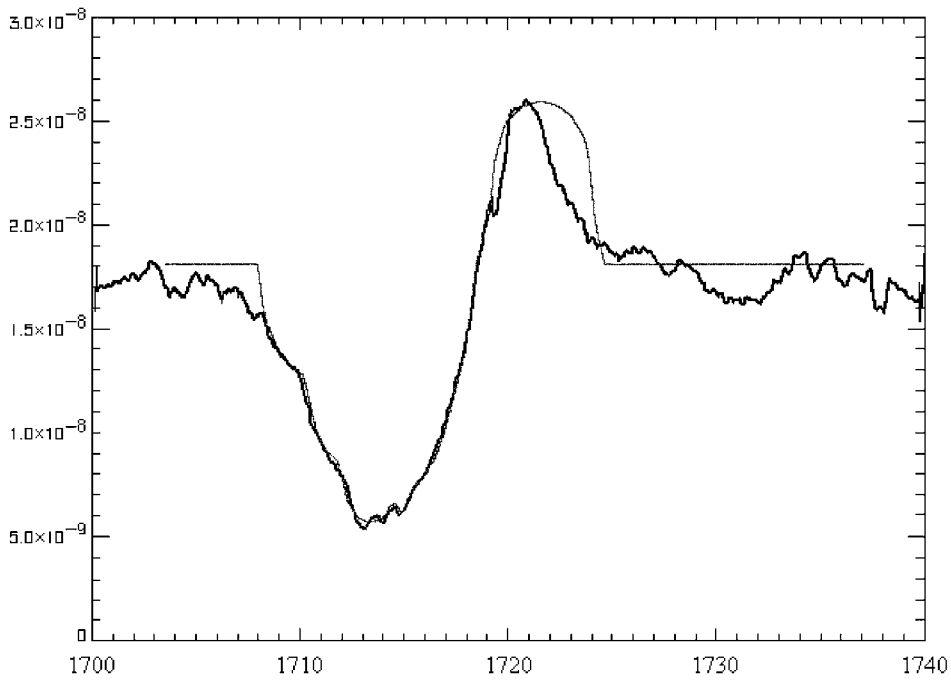


Figure 4. Best fit of NIV λ 1718.8Å line of the Oe star HD66811. The thick line presents the real spectral profile and the thin one the model's fit. The differences between the real spectrum and its fit are some times hard to see, as we have accomplished the best fit.

Expansion / contraction velocities of the SiIV region

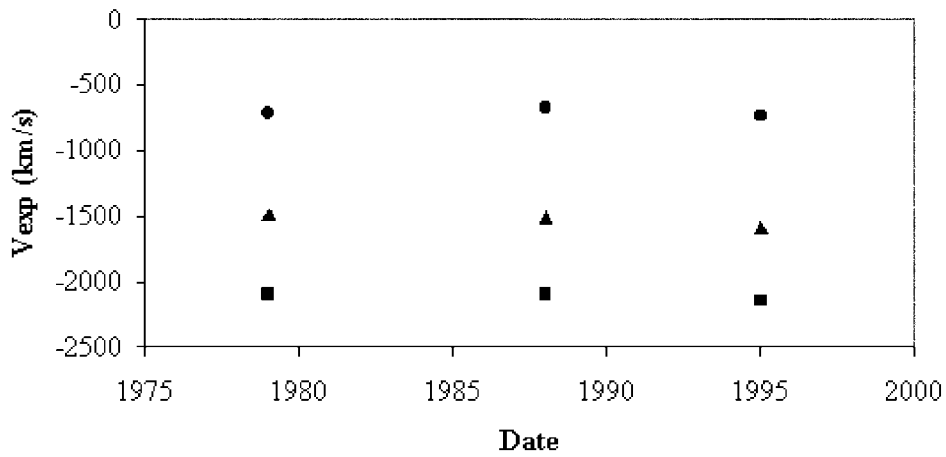


Diagram 4. Apparent radial velocities of expansion / contraction of the density regions where the Si IV lines of the star HD66811 are created, as a function of time.

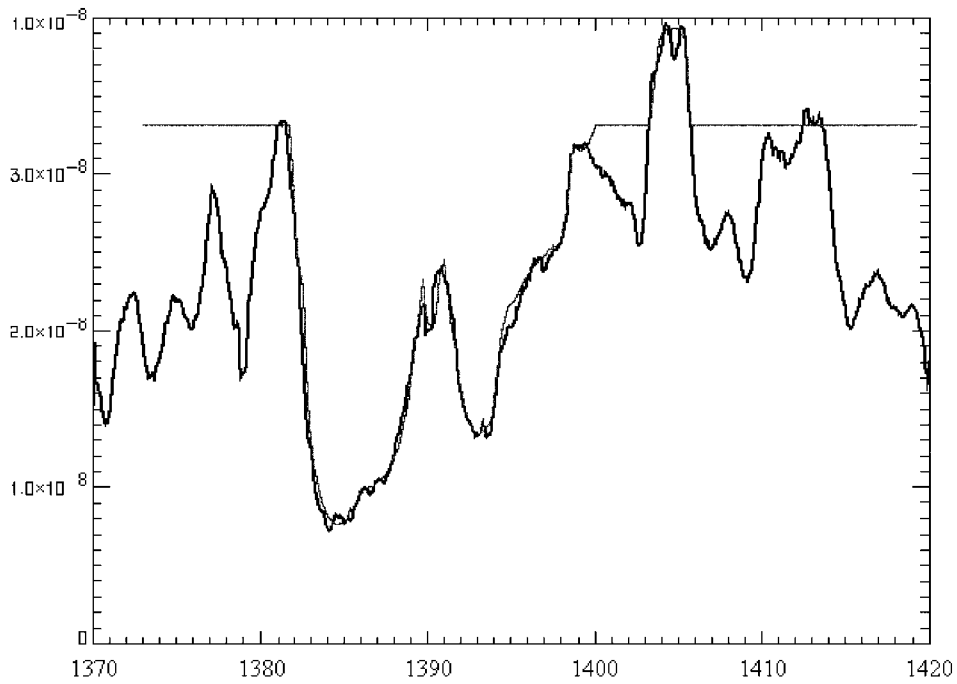


Figure 5. Best fit of SiIV $\lambda\lambda$ 1393.75, 1402.73Å line of the Oe star HD66811. The thick line presents the real spectral profile and the thin one the model's fit. The differences between the real spectrum and its fit are some times hard to see, as we have accomplished the best fit.

Rotation velocities of the SiIV region

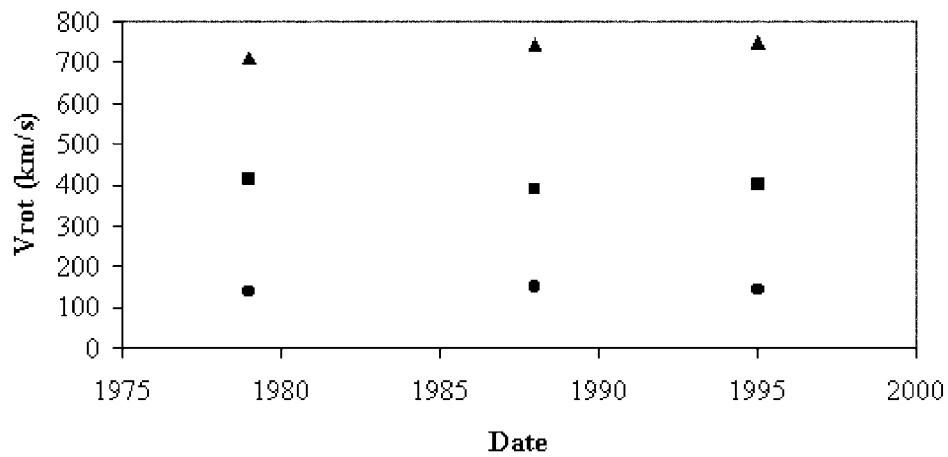


Diagram 5. Apparent rotation velocities of the density regions where the Si IV lines of the star HD66811 are created, as a function of time.

Apparent rotation velocities (mean values derived from the three spectra) as a function of expansion / contraction velocities (mean absolute values), of all layers of matter.

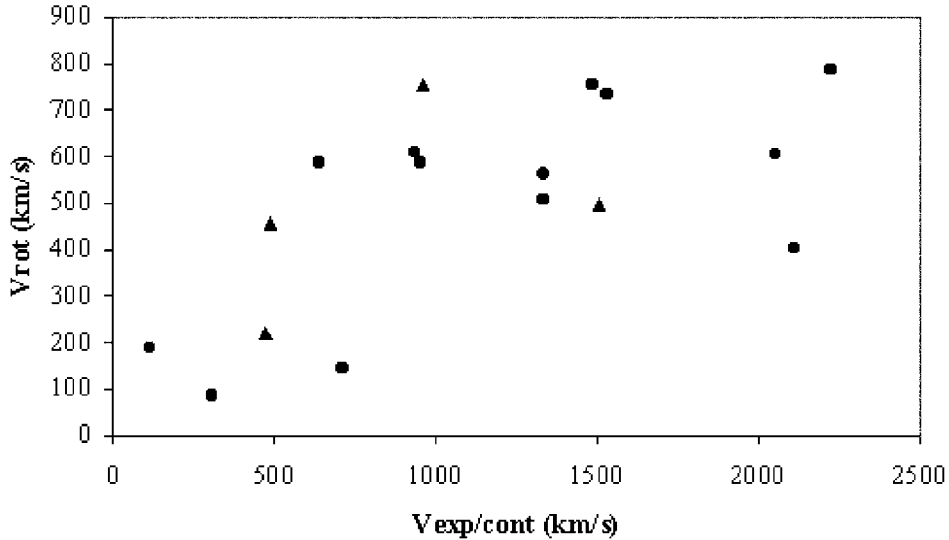


Diagram 6. Mean apparent rotation velocities as a function of the absolute mean velocities of expansion / contraction, for the density regions (absorbing and emitting) of the star HD66811. Velocities related to absorbing layers of matter are shown with circles. Velocities related to emitting layers of matter are shown with triangles.

resonance lines ($\lambda\lambda$ 2795.523, 2802.698 Å) are formed of a series of 21 Be V stars of all the spectral subtypes. In Figures 1–3 we present three best fits of the Mg II resonance lines of the stars HD 41335, HD 148184 and HD 217543. The thick line presents the observed spectral line's profile and the thin one the model's fit. The differences between the observed spectrum and its fit are some times hard to see, as we have accomplished the best fit. Some of our conclusions are presented in diagrams 1–3. In Diagram 1 we present the expansion / contraction velocities of all the absorption components as a function of the spectral subtype. In Diagram 2 we present the rotation velocities of all the absorption components as a function of the spectral subtype. In Diagram 3 we present the expansion / contraction velocities of the emission component as a function of the respective rotation velocities. In these three diagrams one can see that all the studied stars present discernible or indiscernible SACs of the Mg II resonance lines. The indiscernible SACs appear in the spectra of the stars with spectral subtypes B0–B1 and B4–B8. This is due to the fact that the SACs of the Mg II resonance lines in the spectra of the stars of these spectral subtypes present similar radial velocities. In this case, we can separate

**Mean apparent rotation velocities and
mean velocities of expansion as a function of ξ
of the absorbing layers of matter.**

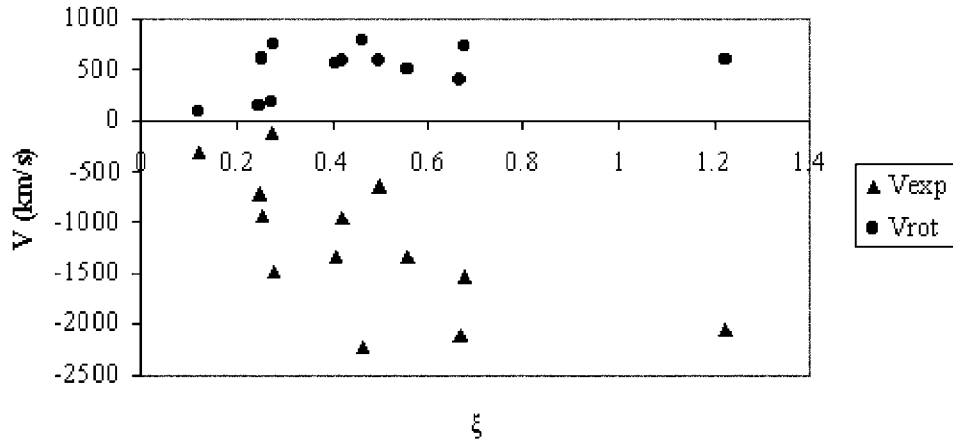


Diagram 7. Mean apparent rotation velocities and mean expansion velocities of the absorbing layers of matter of the star HD66811, as a function of ξ .

these lines by the systematic differentiations of the apparent rotation velocities and the values of ξ_i . The SACs of the Mg II resonance lines are discernible in the spectra of the stars with spectral subtypes B2-B3, as they present different radial shifts. We would also like to point out that in this case the density regions present much greater values of the apparent rotation velocities.

5.2. THE CORONAL AND POST-CORONAL REGIONS OF THE MOVING ATMOSPHERE OF THE O_E STAR HD66811 (ζ PUPPIS)

Danezis et al. (2002b) by applying the above presented model, studied the variation of the calculated parameters V_{rot} and V_{exp} and ξ of the density regions where the spectral lines CIV, NIV, NV and SiIV are formed of the star HD 66811 (ζ Puppis) at three different moments (1979, 1988, 1995). Our purpose was to study the variations of the parameters V_{rot} and V_{exp} and ξ of the SACs that present the complex profiles of these spectral lines. In figures 4 and 5 we present two best fits of the NV and SiIV resonance lines of the stars HD 41335, HD 148184 and HD 217543. The thick line presents the observed spectral line's profile and the thin one the model's fit. The differences between the observed spectrum and its fit are some times hard to see, as we have accomplished the best fit. Some of our conclusions are presented in diagrams 4–7.

Acknowledgements

Dr Danezis E. and Dr Theodossiou E. would like to express their gratitude to Dr V. Doazan and Dr R. Stalio for their constant encouragement and stimulated discussions in the first steps of the construction of this model.

Also Dr Danezis E. and Dr Theodossiou E. would like to thank Dr M. Dimitrijevic, Director of the Astronomical Observatory of Belgrade for his help and comments. We would like to thank Prof. S. Svolopoulos, Dr M. Kontizas, Prof. X. Moussas and Dr A. Kakouris, of the University of Athens (School of Physics), as well as Dr E. Kontizas of the National Observatory of Athens for their helpful comments.

Finally we would like to express our thanks to Mr. G. Danezis Ph.D. student at Queen's College of the University of Cambridge (Computer Laboratory) for his help on software development of the model.

This research project is progressing at the University of Athens, Department of Astrophysics – Astronomy and Mechanics, under the financial support of the Special Account for Research Grants, which we thank very much.

References

- Andrillat, Y. and Fehrenbach, Ch.: 1982, *A&ASS* **48**, 93–136.
 Andrillat, Y.: 1983, *A&ASS* **53**, 319–338.
 Bates, B. and Halliwell, D.R.: 1986, *MNRAS* **223**, 673.
 Bates, B. and Gilheany, S.: 1990, *MNRAS* **243**, 320B.
 Burki, G., Heck A., Bianchi, L. and Cassatella, A.: 1982, *A&A* **107**, 112.
 Cidale, L.S.: 1998, *ApJ* **502**, 824.
 Cranmer, S.R. and Owocki, S.P.: 1996, *ApJ* **462**, 469C.
 Cranmer, S.R., Smith, M.A. and Robinson, R.D.: 2000, *ApJ* **537**, 433.
 Christou, G., Danezis, E., Theodossiou, E., Stathopoulou, M., Nikolaidis, D., Lyratzi, E., Drakopoulos, C., Koutsouris, P. and Soulikias, A.: 2001, *Application of a New Model of Density Layers of Matter to the Expanding Gaseous Envelope of the star HD 66811*, Proc. 5th Hellenic Astronomical Society Conf. September 2001, Crete, Greece.
 Danezis, E.: 1984, *The Nature of Be Stars*, PhD Thesis, University of Athens.
 Danezis, E.: 1986, *IAU*, Colloq. No 92, Physics of Be Stars, Cambridge University Press.
 Danezis, E. and Theodossiou, E.: 1988, *A&ASS* **72**, 497–504.
 Danezis, E. and Theodossiou, E.: 1990, *SS* **174**, 49–90.
 Danezis, E., Theodossiou, E. and Laskarides, P.G.: 1991, *Astrophysics and Space Science* **179**, 111–139.
 Danezis, E., Theodossiou, E. and Laskarides, P.G.: 1995, *A First Approach to the Shell Structure of Be Binary Stars*, 2nd Hellenic Astronomical Conf., 29 July, Thessaloniki Greece.
 Danezis, E., Stathopoulou, M., Theodossiou, E., Grammenos, Th. and Soulikias, A.: 1997a, *A Study of the Superionized Spectral Lines of the Star HD 164794*, in 6th European and 3rd Hellenic Astronomical Society Conf., 2–5 July, Thessaloniki, Greece.
 Danezis, E., Stathopoulou, M., Theodossiou, E., Grammenos, Th. and Kosionidis, A.: 1997b, *A Study of the Superionized Spectral Lines of the Star HD 66811*, in 6th European and 3rd Hellenic Astronomical Society Conf., 2–5 July, Thessaloniki, Greece.

- Danezis, E., Nikolaidis, D., Theodossiou, E., Stathopoulou, M. and Kosionidis, A.: 1998, *Satellite Spectral Components and Moving Shells in the Atmospheres of Early Type Stars – The example of HD 175754*, Proc. 65th Czech and the 7th European Joint Conf., JENAM' 98, Prague, Czech Republic, September.
- Danezis, E., Nikolaidis, D., Theodossiou, E., Grammenos, Th., Stathopoulou, M. and Kosionidis, A.: 1999, *A Simple Model for the Complex Structure of Moving Atmospheric Shells in Oe and Be Stars*, Proc. 4th Hellenic Astronomical Soc. Conf., September 1999, Samos, Greece.
- Danezis, E., Nikolaidis, D., Theodossiou, E., Kosionidis, A., Stathopoulou, M., Lyratzi, E., Drakopoulos C. and Bourma, P.: 2000a, *A Simple Model for the Complex Structure of Moving Atmospheric Shells in Oe and Be Stars. The Example of HD 36861, some First Conclusions*, JENAM 2000, May 29–June 3, Moscow, Russia.
- Danezis, E., Nikolaidis, D., Theodossiou, E., Kosionidis, A., Stathopoulou, M., Lyratzi, E., Drakopoulos C. and Bourma, P.: 2000b, *A Simple Model for the Complex Structure of Moving Atmospheric Shells in Oe and Be Stars. The Example of HD 36861, some First Conclusions*, JENAM 2000, May 29–June 3, Moscow, Russia.
- Danezis, E., Nikolaidis, D., Theodossiou, E., Kosionidis, A., Stathopoulou, M., Lyratzi, E., Drakopoulos C. and Bourma, P.: 2000c, *A Simple Model for the Complex Structure of Moving Atmospheric Shells in Oe and Be Stars. The Example of HD 36861, some First Conclusions*, JENAM 2000, May 29–June 3, Moscow, Russia.
- Danezis, E., Lyratzi, E., Theodossiou, E., Nikolaidis, D., Stathopoulou, M., Kyriakopoulou, A., Christou, G. and Drakopoulos C.: 2001a, *Application of a New Model of Density Layers of Matter to the Expanding Gaseous Envelope of the Star HD 175754*, Proc. 5th Hellenic Astronomical Soc. Conf., September 2001, Crete, Greece.
- Danezis, E., Nikolaidis, D., Lyratzi, E., Stathopoulou, M., Theodossiou, E., Kyriakopoulou, A., Christou, G., Kosionidis, A. and Drakopoulos C.: 2001b, *Hyperionization and Emission Phenomena in the Gaseous Envelope of the Star 9Sgr*, Proc. 5th Hellenic Astronomical Soc. Conf. September 2001, Crete, Greece.
- Danezis, E., Nikolaidis, D., Lyratzi, E., Theodossiou, E., Stathopoulou, M., Kyriakopoulou A., Christou, G. and Drakopoulos C.: 2001c, *Hyperionization and Emission Phenomena in the Gaseous Envelope of the Star λ Orionis*, Proc. 5th Hellenic Astronomical Soc. Conf., September 2001, Crete, Greece.
- Danezis, E., Nikolaidis, D., Lyratzi, E., Stathopoulou, M., Theodossiou, E., Kosionidis, A., Drakopoulos, C., Christou, G. and Koutsouris, P.: 2002a, *A New Model of Density Layers of Matter in the Expanding Gaseous Envelope of Oe and Be Stars*, Proc. IAU Symp. 210: Modeling of Stellar Atmospheres, June 17–21, 2002, Uppsala, Sweden.
- Danezis, E., Lyratzi, E., Nikolaidis, D., Theodossiou, E., Stathopoulou, M., Christou, G. and Soulikias, A.: 2002b, *The Complex Structure of Mg II Regions in the Gaseous Envelope of Be V Stars*, Proc. IAU Symp. 210: Modeling of Stellar Atmospheres, June 17–21, 2002, Uppsala, Sweden.
- Danezis, E., Lyratzi, E., Christou, G., Theodossiou, E., Stathopoulou, M., Nikolaidis, D. and Kyriakopoulou, A.: 2002c, *Hyperionisation Phenomena in the Coronal and Post-Coronal Regions of the Moving Atmosphere of the Oe Star HD 66811 (ζ Puppis)*, Proc. IAU Symp. 210: Modeling of Stellar Atmospheres, June 17–21, 2002, Uppsala, Sweden.
- Doazan, V.: 1982, *B Stars with and without Emission Lines*, NASA SP-456.
- Franco, M.L., Kontizas, E., Kontizas, M. and Stalio, R.: 1983, *A&A* **122**, 9.
- Fullerton, A.W., Massa, D.L., Prinja R.K., Owocki, S.P. and Cranmer, S.R.: 1997, *A&A* **327**, 699.
- Gilheany, S., Bates, B., Catney, M.G. and Dufton, P.L.: 1990, *Ap&SS* **169**, 85G.
- Grady, C.A., Sonneborn, G., Chi-chao Wu and Henrichs, H.F.: 1987, *ApJ Supl.* **65**, 673.
- Henrichs, H.F., Hammerschlag-Hensberge, G. and Lamers, H.J.G.L.M.: 1980, in B. Battrick and J. Mort (eds.), Proc. 2nd European IUE Conf. Tübingen, (ESA SP-157), Noordwijk: ESO, **4**, 147.
- Henrichs, H.F., Hammerschlag-Hensberge, G., Howarth, I.D. and Barr P.: 1983, *ApJ* **268**, 807.

- Henrichs, H.F.: 1984, in E. Rolfe and B. Battrick (eds.), Proc. 4th European IUE Conf., ESA SSSP-218, p. 43, Rome.
- Henrichs, H.F., Kaper, L. and Zwarthoed, G.A.A.: 1988, *Proc Celebratory Symp.: A Decade of UV Astronomy with IUE*, ESA SP-281, **2**, 145.
- Henrichs, H.F., Kaper, L. and Nichols, J.S.: 1994 *A&A* **285**, 565H.
- Henrichs, H.F.: 1990, in D. Baade (ed.), *Rapid Variability of OB-Stars: Nature and Diagnostic Value* (ESO Workshop 36), Garching bei Munchen: ESO, 199.
- Hutsemekers, D.: 1985, *A&ASS* **60**, 373–388.
- Kaper, L., Henrichs, H.F., Zwarthoed, G.A.A. and Nichols-Bohlin, J.: 1990, in L.A. Willson and R. Stalio (eds.), *Angular Momentum and Mass Loss for Hot Stars*, Kluwer, Dordrecht, p. 213.
- Kaper, L., Henrichs, H.F., Nichols, J.S., Snoek, L.C., Volten, H. and Zwarthoed, G.A.A.: 1996, *Astron. Astrophys. Suppl.* **116**, 257.
- Kaper, L., Henrichs, H.G., Fullerton, A.W., Ando, H., Bjorkman, K.S., Gies, D.R., Hirata, R., Dambe, E., McDavid, D. and Nichols, J.S.: 1997, *A&A* **327**, 281.
- Kaper, L., Henrichs, H.F., Nichols, J.S. and Telting, J.H.: 1999, *A&A* **344**, 231.
- Kyriakopoulou, A., Danezis, E., Nikolaidis, D., Theodossiou, E., Stathopoulou, M., Lyratzi, E., Christou, G. and Koutsouris, P.: 2001, *The Complex Structure of the Expanding Gaseous Envelope of the Star HD 50138*, Proc. 5th Hellenic Astronomical Society Conf. September 2001, Crete, Greece.
- Lamers, H.J.G.L.M. and Snow, T.P.: 1978, *ApJ* **219**, 504L.
- Lamers, H.J.G.L.M., Gathier, R. and Snow, T.P.: 1982, *ApJ* **258**, 186.
- Lamers, H.J.G.L.M., Snow, T.P., de Jager, C. and Langerwerf, A.: 1988, *ApJ* **325**, 342.
- Lamers, H.J.G.L.M.: 1994, in A.F.J. Moffat, S.P. Owocki and A.W. Fullerton (eds.), *Observational Aspects of Wind Variability, Instability and Variability of Hot-Star Winds*, Kluwer, St.-Louis N, p. 41.
- Laskarides, P.G., Danezis, E. and Theodossiou, E.: 1992a, *Sp. Sc.* **179**, 13.
- Laskarides, P.G., Danezis, E. and Theodossiou, E.: 1992b, *Sp. Sc.* **183**, 67.
- Laskarides, P.G., Danezis, E. and Theodossiou, E.: 1993a, *A Structure Proposal of the Gas Shell of the Double System AX Mon*, Proc. 6th Panhellenic Conf., Komotini, Greece.
- Laskarides, P.G., Danezis, E. and Theodossiou, E.: 1993b, in P.G. Laskarides (ed.), *The far UV Spectrum of AX Monocerotis*, Proc. 1st Panhellenic Astronomical Meeting, Athens.
- Lyrtzi, E., Danezis, E., Nikolaidis, D., Theodossiou, E., Stathopoulou, M. and Drakopoulos, C.: 2001, *Application of a New Model of Density Shells of Matter to the Expanding Gaseous Envelope of the Star HD 45910 (AXMon)*, Proc. 5th Hellenic Astronomical Soc. Conf., September 2001, Crete, Greece.
- Lyrtzi, E., Danezis, E., Nikolaidis, D., Theodossiou, E., Stathopoulou, M. and Soulikias, A.: 2002a, *The Complex Structure of the Expanding Gaseous Envelope of the Be Star HD 45910 (AX Mon)*, Proc. IAU Symp. 210: Modeling of Stellar Atmospheres, June 17–21, 2002, Uppsala, Sweden.
- Lyrtzi, E., Danezis, E., Nikolaidis, D., Theodossiou, E., Stathopoulou, M., Kyriakopoulou, A. and Soulikias, A.: 2002b, *The Complex Structure of H α Regions in the Gaseous Envelope of Be V Stars*, Proc. IAU Symp. 210: Modeling of Stellar Atmospheres, June 17–21, 2002, Uppsala, Sweden.
- Markova, N.: 2000 *A&AS* **144**, 391.
- Mulan, D.J.: 1984a, *ApJ* **283**, 303.
- Mulan, D.J.: 1984b, *ApJ* **284**, 769.
- Mulan, D.J.: 1986, *A&A* **165**, 157.
- Owocki, S.P., Castor, J.I. and Rybicki, G.B.: 1988, *ApJ* **335**, 914.
- Peton, A.: 1974, *Sp. Sc.* **30**, 481.
- Prinja, R.K. and Howarth, I.D.: 1984, *Astr. Astrophys. J.* **133**, 110.
- Prinja, R.K. and Howarth, I.D.: 1986, *Astrophys. J. Suppl.* **61**, 357.
- Prinja, R.K. and Howarth, I.D.: 1988, *MNRAS* **233**, 123.

- Prinja, R.K.: 1988, *MNRAS* **231**, 21P.
- Prinja, R.K.: 1991, in D. Baade (ed.), *ESO Workshop on Rapid Variability of OB Stars: Nature and Diagnostic Value*, p. 221.
- Prinja, R.K.: 1992, in L. Drissen, C. Leitherer and A. Nota (eds.), *Nonisotropic and Variable Outflows from Stars*, ASP Conf. Ser. **22**, 167.
- Rivinius, Th., Stahl, O., Wolf, B., Kaufer, A., Gäng Th., Gummersbach, C.A., Jankovics, I., Kovács, J., Mandel, H., Peitz, J., Szeifert, Th. and Lamers, H.J.G.L.M.: 1997, *A&A* **318**, 819.
- Sahade, J. Brandi, E. and Fontela, J.M.: 1984, *Astron. Astrophys. Supplement* **56**, 17.
- Sahade, J. and Brandi, E.: 1985, *Rev. Mex.* **10**, 229.
- Stathopoulou, M., Danezis, E., Laskarides, P.G. and Theodossiou, E.: 1995, *The UV The spectrum of HD 175754*, 2nd Hellenic Astronomical Conf., 29 July, Thessaloniki, Greece.
- Stathopoulou, M., Danezis, E., Theodossiou, E., Grammenos, Th. and Soulikias, A.: 1997, *A Study of the Superionized Spectral Lines of the Star HD 152408*, 6th European and 3rd Hellenic Astronomical Society Conf., 2–5 July, Thessaloniki, Greece.
- Telting, J.H., Waters, L.B.F.M., Persi, P. and Dunlop, S.: 1993, *A&A* **270**, 355.
- Telting, J.H. and Kaper, L.: 1994, *A&A* **284**, 515T.
- Theodossiou, E., Laskarides, P.G., Danezis, E., Stathopoulou, M. and Grammenos, Th.: 1993, *The UV Spectrum of the Star λ Orionis*, Proc. 6th Panhellenic Physics Conf., Komotini, Greece.
- Theodossiou, E., Laskarides, P.G. and Danezis, E.: 1997, *A Study of the Superionized Spectral Lines of the Star HD 36861*, 6th European and 3rd Hellenic Astronomical Society Conf., 2–5 July, Thessaloniki, Greece.
- Underhill, A.B.: 1975, *ApJ* **199**, 693.
- Underhill, A. and Doazan, V.: 1982, *B Stars with and without Emission Lines*, NASA SP-456, Centre National de la Recherche Scientifique Paris, France.
- Underlill, A.B. and Fahey, R.P.: 1984, *ApJ* **280**, 712.
- Waldron, W.L., Klein, L. and Altner, B.: 1992, *nvos.work*, 181W.
- Waldron, W.L., Klein, L. and Altner, B.: 1994, *ApJ* **426**, 725W.
- Willis, A.J., Howarth, I.D., Stickland, D.J. and Heap, S.R.: 1989, *ApJ* **347**, 413W.

A New Model for the Structure of the DACs and SACs Regions in the Oe and Be Stellar Atmospheres

Emmanouel DANEZIS,¹ Dimitris NIKOLAIDIS,¹ Evaggelia LYRATZI,¹ Luka Č. POPOVIĆ,²

Milan S. DIMITRIJEVIĆ,² Antonis ANTONIOU,¹ and Efstratios THEODOSIOU¹

¹*University of Athens, Faculty of Physics, Department of Astrophysics, Astronomy and Mechanics,
Panepistimioupoli, Zographou 157 84, Athens, Greece*

²*Astronomical Observatory of Belgrade, Volgina 7, 11160 Belgrade, Serbia,*

Isaac Newton Institute of Chile, Yugoslavia Branch

edanezis@phys.uoa.gr, dlrrrr@tellas.gr, elyratzi@phys.uoa.gr, lpopovic@aob.bg.ac.yu,

mdimitrijevic@aob.bg.ac.yu, ananton@phys.uoa.gr, etheodos@phys.uoa.gr

(Received 2007 March 14; accepted 2007 May 1)

Abstract

We present a new mathematical model for the density regions where a specific spectral line and its SACs/DACs are created in the Oe and Be stellar atmospheres. In calculations of final spectral line function we consider that the main processes for the line broadening are the rotation of the density regions creating the spectral line and its DACs/SACs, as well as the random motions of the ions. This line function is able to reproduce the spectral feature, which enables us to calculate some important physical parameters, such as the rotational, radial, and random velocities, the full width at half maximum, the Gaussian deviation, the optical depth, the column density, and the absorbed or emitted energy. Additionally, we can calculate the percentage of the contribution of the rotational velocity and the ions' random motions of the DACs/SACs regions to the line broadening. Finally, we present two tests and three short applications of the proposed model.

Key words: stars: early type, emission-line — ultraviolet: stars

1. Introduction

When we study the UV lines of hot emission stars we have to deal with two problems: (i) The presence of a very complex structure of many spectral lines in the UV region, such as the resonance lines of Si IV, C IV, N V, Mg II, and the N IV spectral line. (ii) The presence of Discrete Absorption Components (DACs, Bates & Halliwell 1986).

DACs are discrete, but not unknown, absorption spectral lines. They are spectral lines of the same ion and the same wavelength as a main spectral line, shifted at different $\Delta\lambda$, since they are created in different density regions, which rotate and move radially with different velocities (Danezis 1983, 1987; Danezis et al. 2003; Lyratzi et al. 2007). DACs are lines, easily observed in the case that the regions that give rise to them rotate with low velocities and move radially with high velocities.

Many suggestions have been made to explain the DACs phenomenon. Most researchers have suggested mechanisms that allow the existence of structures which cover all or a significant part of the stellar disk, such as shells, blobs, or puffs (Underhill 1975; Henrichs 1984; Underhill & Fahey 1984; Bates & Halliwell 1986; Grady et al. 1987; Lamers et al. 1988; Waldron et al. 1992, 1994; Cranmer & Owocki 1996; Rivinius et al. 1997; Kaper et al. 1996, 1997, 1999; Markova 2000). Some researchers have also suggested interaction of fast and slow wind components, Corotation Interaction Regions (CIRs), and structures due to magnetic fields or spiral streams as a result of the stellar rotation (Underhill & Fahey 1984;

Mullan 1984a, 1984b, 1986; Prinja & Howarth 1988; Cranmer & Owocki 1996; Fullerton et al. 1997; Kaper et al. 1996, 1997, 1999; Cranmer et al. 2000). Though we do not yet know the mechanism responsible for the formation of such structures, it is positive that DACs result from independent high-density regions in the stellar environment.

An important question is whether there is a connection between the observed complex structure of the above-mentioned spectral lines and the presence of DACs. A possible answer is that if the regions that create the DACs rotate with large velocities and move radially with small velocities, the produced lines would have large widths and small shifts. As a result, they are blended among themselves as well as with the main spectral line, and thus they are not discrete. In such a case the name Discrete Absorption Components is inappropriate, and we use only the name Satellite Absorption Components (SACs) (Lyratzi & Danezis 2004; Danezis et al. 2005, 2006; Nikolaidis et al. 2006; D. Nikolaidis et al. 2006, presentation in 26th IAU General Assembly). A very important question is whether it is possible that the existence of SACs may be responsible for the complex structure of the observed spectral feature.

As is clear, for a future study of the mechanisms responsible for the creation of density regions that produce the complex profiles of the above-mentioned spectral lines, as well as for a study of their structure and evolution, we need to calculate the values of some physical parameters of these regions.

In order to calculate these parameters, it is necessary to construct a line function, based on the idea of DACs

and SACs phenomena able to reproduce, in the best way, the observed spectral feature.

Danezis et al. (2003) presented such a line function in the case that the process of the line broadening is only the rotation of the regions that create the observed spectral lines and their components and when these regions present spherical symmetry around their own center or the center of the star (see also Lyratzi et al. 2007). With this line function we can calculate some important physical parameters, such as the rotational and the radial velocities, the optical depth, the column density (Danezis et al. 2005) and the absorbed/emitted energy. However, in some cases the chaotic motion of emitters/absorbers inside the dense layers can be significant (see e.g., Danezis et al. 2006) and the estimated rotation might be overestimated. Therefore, a modification of the previously given model (Danezis et al. 2003) is needed, in sense that the possible contribution of random velocities to the line broadening can be taken into account.

Here, we present a new model that also includes the random motions of the ions, since in the case of hot emission stars one can expect a significant contribution of random motion of the emitters/absorbers to the line profile. Based on this idea, besides the above-mentioned physical parameters of the regions that create the complex spectral lines, we can calculate the mean random velocity of the ions, but also the percentage of the contribution of the rotational velocity and emitter/absorber random motions of the DACs/SACs regions to the line broadening, as well as the Gaussian deviation for each DAC/SAC profile.

This paper is organized as follows: In section 2 we give a description of the model. In section 3 we discuss it, in section 4 we give two tests, and in section 5 we present applications. Finally, in section 6 we outline our conclusions.

2. Description of the Model — the Line Function

As was already mentioned above, Danezis et al. (2003) presented a line function that is able to accurately reproduce the observed spectral lines and their SACs/DACs at the same time. The proposed line function is

$$F_{\lambda_{\text{final}}} = \left[F_0(\lambda) \prod_i e^{-L_i \xi_i} + \sum_j S_{\lambda_{ej}} (1 - e^{-L_{ej} \xi_{ej}}) \right] e^{-L_g \xi_g}, \quad (1)$$

where: $F_0(\lambda)$ is the initial radiation flux; L_i , L_{ej} , and L_g are the distribution functions of the absorption coefficients (k_{λ_i} , $k_{\lambda_{ej}}$, and k_{λ_g} , respectively). Each L depends on the values of the apparent rotational velocity as well as of the radial velocity of the density shell, which forms the spectral line (V_{rot} , V_{rad}); ξ_i is the optical depth in the center of the line; $S_{\lambda_{ej}}$ is the source function, which, at the moment when the spectrum is taken, is constant.

In equation (1), the functions $e^{-L_i \xi_i}$, $S_{\lambda_{ej}} (1 - e^{-L_{ej} \xi_{ej}})$, $e^{-L_g \xi_g}$ are the distribution functions of each satellite component; we can replace them with a known distribution function (Gauss, Lorentz, Voigt, or disk model). An important fact is that in the calculation of $F(\lambda)$ we can include different

geometries (in the calculation of L) of the absorbing or emitting independent density layers of matter.

A decision concerning the geometry is essential to calculate the distribution function that we use for each component; i.e. for different geometries we have different line shapes, representing the considered SACs.

Equation (1) gives a function of the complex profile of a spectral line, which presents SACs or DACs. This means that equation (1) is able to reproduce not only the main spectral line, but its SACs as well.

The main hypotheses when we constructed the rotation distribution function were that the line width, $\Delta\lambda$, is only due to rotation of the regions that create the observed spectral lines and their components, and that these regions present spherical symmetry around their own center, or the center of the star (see also Lyratzi et al. 2007). Consequently, the random velocities of the emitters/absorbers in the density region are assumed to be negligible, i.e., they do not significantly contribute to the line profile. Here, we consider that the random velocities may have a significant contribution to the distribution function, L (see Appendix). In this case the final form of L is given as

$$L(\lambda) = \frac{\sqrt{\pi}}{2\lambda_0 z} \int_{-\frac{\pi}{2}}^{\frac{\pi}{2}} \left[\operatorname{erf} \left(\frac{\lambda - \lambda_0}{\sigma\sqrt{2}} + \frac{\lambda_0 z}{\sigma\sqrt{2}} \cos\theta \right) - \operatorname{erf} \left(\frac{\lambda - \lambda_0}{\sigma\sqrt{2}} - \frac{\lambda_0 z}{\sigma\sqrt{2}} \cos\theta \right) \right] \cos\theta d\theta, \quad (2)$$

where λ_0 is the transition wavelength of a spectral line that arises from a specific point of the equator of a spherical density region that produces one satellite component, $z = \frac{V_{\text{rot}}}{c}$ (V_{rot} is the rotational velocity of the specific point) and $\operatorname{erf}(x) = \frac{2}{\pi} \int_0^x e^{-u^2} du$ is the function that describes the Gaussian error distribution.

3. Discussion and Way of Application of the Proposed Model

Introducing the previous final function of a complex spectral line [equation (1)], in combination with the distribution function, L , given in equation (2), we note the following:

1. The proposed line function [equation (1)] can be used for any number of absorbing or emitting regions. This means that it can also be used in the simple case that $i = 1$ and $j = 0$ or $i = 0$ and $j = 1$, meaning when we deal with simple, classical absorption or emission spectral lines, respectively. This allows us to calculate all of the important physical parameters, such as the rotational, radial, and random velocities, the full width at half maximum, the Gaussian deviation, the optical depth, the column density (Danezis et al. 2005), and the absorbed or emitted energy, for all simple and classical spectral lines in all spectral ranges.

2. For each group of parameters ($V_{\text{rot}i}$, $V_{\text{rad}i}$, $V_{\text{rand}i}$, and ξ_i), the function $I_{\lambda i} = e^{-L_i \xi_i}$ reproduces the spectral line profile formed by the i density region of matter, meaning that for each group we have a totally different profile. This results

in the existence of only one group of V_{rot_i} , V_{rad_i} , V_{rand_i} , and ξ_i giving the best fit of the i component. In order to accept that as the best fit of the observed spectral line, given by the groups (V_{rot_i} , V_{rad_i} , V_{rand_i} , ξ_i) of all calculated SACs, one has to adhere to all physical criteria and techniques, such as:

i) To make a complete identification of spectral lines in the region around the studied spectral line and to have the superposition of the spectral region that we study with the same region of a classical star of the same spectral type and luminosity class, in order to identify the existence of spectral lines that blend with the studied ones, as well as the existence of SACs.

ii) The resonance lines as well as all lines originating in a particular region should have the same number of SACs, depending on the structure of this region, without any influence of the ionization stage or ionization potential of the emitters/absorbers. As a consequence, the respective SACs should have similar values of the radial and rotational velocities.

iii) The ratio of the optical depths of two resonance lines must be the same as the ratio of the respective relative intensities.

3. In order to decide which group of parameters gives the best fit, we propose a model according to the following two steps:

(i) In the first step we consider that the main process for line broadening of the main line and satellite components is rotation of the region that creates the components of the observed feature; a secondary cause is thermal Doppler broadening. This means that we start fitting the line using the maximum V_{rot} . We then include Doppler broadening, in order to accomplish the best fit (rotation case). (ii) In the second step, we consider the opposite. In this case the main process of line broadening of the main line and satellite components is supposed to be Doppler broadening; a secondary process is rotation of the regions that create the components of the observed feature. This means that we start fitting the line using the maximal Doppler broadening. We then include V_{rot} , in order to accomplish the best fit (Doppler case).

In both cases (rotation case and Doppler case) we check the correct number of satellite components that construct the whole line profile. At first we fit using the number of components that give the best difference graph between the fit and the real spectral line. We then make a fit using one component less than in the previous fit. The F -test between them allows us to take the correct number of satellite components that construct in the best way the whole line profile. The F -test between these two cases indicates the best way to fit spectral lines. When the F -test cannot give a definite conclusion on which case we should use, we can still obtain information about the limits of V_{rot} and σ . If the F -test gives similar values, then the rotation case defines the maximal V_{rot} and the minimal σ and the Doppler case defines the minimal V_{rot} and the maximal σ .

4. The profiles of each main spectral line and its SACs are fitted by the function $e^{-L_i\xi_i}$ in the case of an absorption component, or $S_{\lambda e_j} (1 - e^{-L_{e_j}\xi_{e_j}})$ in the case of an emission component. These functions produce symmetrical line profiles. However, most of the spectral lines are asymmetric. This fact is interpreted as being a systematical variation of the apparent

radial velocities of the density regions where the main spectral line and its SACs are created. In order to approximate those asymmetric profiles we have chosen a classical method. This is the separation of the region that produces asymmetric profiles of the spectral line, into a small number of sub-regions, and each of them is treated as an independent absorbing shell. In this way we can study the variation of the density, the radial shift and the apparent rotation as a function of the depth in every region that produces a spectral line with an asymmetric profile. Everything mentioned above must be taken into account during an evaluation of our results; also, one should not consider that the evaluated parameters of those sub-regions correspond to independent regions of matter, which form the main spectral line or its SACs.

5. We suggest that the width of the blue wing is the result of the composition of profiles of the main spectral line and its SACs. Thus, the blue wing of each SAC gives the apparent rotational velocity of the density shell, in which it forms. In order to conduct measurements with physical meaning, we should not calculate the width of the blue wing of the observed spectral feature, but the width of the blue wing of each SAC.

6. We would like to point out that the final criterion to accept or reject a best fit is the ability of the calculated values of the physical parameters to give us a physical description of the events developing in the regions where the spectral lines presenting SACs are created.

7. In the proposed distribution function an important factor is $m = \frac{\lambda_0 z}{\sqrt{2}\sigma}$. This factor indicates the kind of the distribution function that is able to fit in the best way each component's profile.

i) If $m \simeq 3$, we have equivalent contributions of the rotational and random motions to the line widths.

ii) If $m \simeq 500$, the line broadening is only an effect of the rotational velocity, and the random velocity is negligible. In this case, the profile of the line is the same as the theoretical profile derived from the rotation distribution function.

iii) Finally, if $m < 1$, the line broadening is only an effect of random velocities and the line distribution is Gaussian.

4. Testing the Model

In order to check the validity of our model we perform two tests:

I) In order to check the above spectral line function, we calculated the rotational velocity of He I λ 4387.928 Å absorption line for five Be stars, using two methods, the classical Fourier analysis and our model. In figure 1 we present five He I λ 4387.928 Å fittings for the studied Be stars and the measured rotational velocities with both methods. The obtained rotational velocities from our model are in good agreement with ones obtained with Fourier analysis.

The values of the rotational velocities, calculated with Fourier analysis, some times, may present small differences compared to those calculated with our method, because in Fourier analysis the total broadening of the spectral lines is assumed to represent the rotational velocity. On the contrary, our model accepts that a part of this broadening arises from the random motion of the ions.

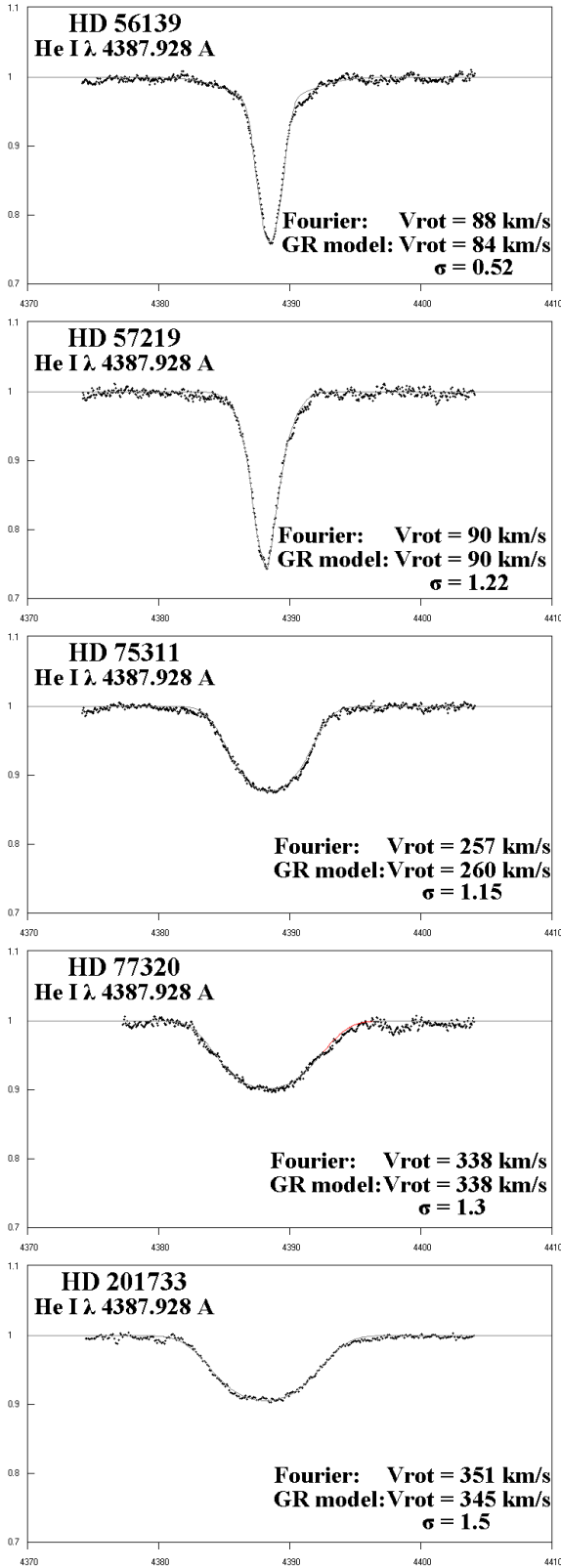


Fig. 1. Five He I λ 4387.928 Å fittings for the studied Be stars with the GR model and the measured rotational velocities with Fourier analysis and the GR model. The differences between the observed and reproduced spectral lines are hard to see, as we have accomplished the best fit.

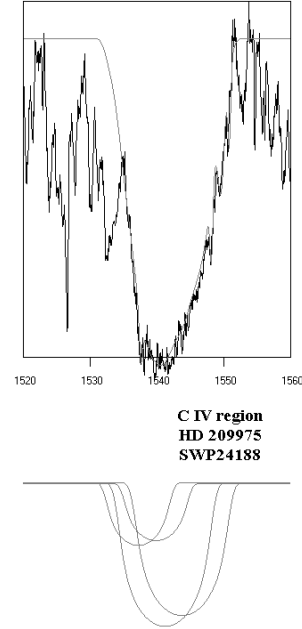


Fig. 2. C IV resonance lines ($\lambda\lambda$ 1548.155, 1550.774 Å) best fit with the GR model for the star HD 209975. The components obtained from the best fit are shown at the bottom.

We point out that with our model, apart from the rotational velocities, we can also calculate some other parameters, such as the standard Gaussian deviation, σ , the velocity of random motions of emitters/absorbers, the radial velocities of the regions producing studied spectral lines, the full width at half maximum (FWHM), the optical depth, the column density, and the absorbed or emitted energy.

II) An additional test of our model is to calculate the random velocities of layers that produce the C IV satellite components of 20 Oe stars with different rotational velocities.

We analyzed the C IV line profiles of 20 Oe stars, the spectra of which were observed with the IUE - satellite (IUE Archive Search database¹). We examined the complex structure of the C IV resonance lines ($\lambda\lambda$ 1548.155, 1550.774 Å). Our sample included the subtypes O4 (one star), O6 (four stars), O7 (five stars), O8 (three stars), and O9 (seven stars). The values of the photospheric rotational velocities were taken from the catalogue of Wilson (1963) (see also Antoniou et al. 2006).

In the composite C IV line profiles we detect two components in 9 stars, three in 7 stars, four in 3 stars, and five in one star.

In figure 2 we present the C IV resonance lines best fit for the star HD 209975.

In figure 3 we present random velocities (V_{rand}) of each SAC as a function of the photospheric rotational velocity (V_{phot}) for all of the studied stars.

As one can see in figure 3, the obtained values for random velocities are in accordance with classical theory; the values of the random velocities do not depend on the inclination angle

¹ (<http://archive.stsci.edu/iue/search.php>).

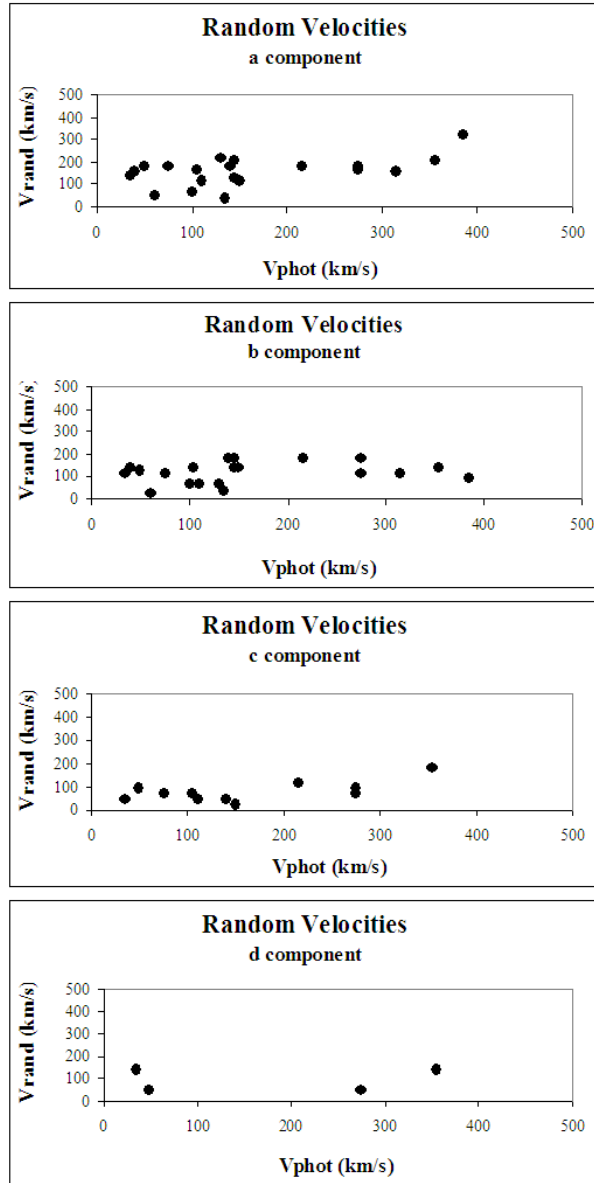


Fig. 3. Random velocities (V_{rand}) of the four SACs as a function of the photospheric rotational velocity (V_{phot}) for all of the studied Oe stars.

of the rotational axis. Because the ionization potential of the regions where satellite components are created is the same for all studied stars, one can expect similar average values of the random velocities for each absorbing region (here denoted as the a–d components; see figure 3) for all studied stars, as we obtained by using the model.

Both of the tests, described above, support our new approach to investigating the regions around hot stars, implying that besides rotation of the regions, one should also consider the random motion of emitters/absorbers.

5. Applications of the Model: Rotation – Density Regions vs. Photosphere

Here, we give some examples of applications of the model. We apply the model to study the complex structure of C IV and Si IV spectral lines in Oe and Be stars, as well as the rotational velocities of different components, in order to find a more precise rotational component.

5.1. C IV Density Regions of 20 Oe Stars

In this application we use the previously mentioned C IV IUE spectra of the second test. We study the relation between the ratio $V_{\text{rot}}/V_{\text{phot}}$ of the first, second, third, and fourth detected components with the photospheric rotational velocity (V_{phot}). This ratio indicates how much the rotational velocity of the specific C IV layer is higher than the apparent rotational velocity of a star (see also Antoniou et al. 2006). In figure 4 we present our results.

In each region and for each component we can conclude that there exists an exponential relation between the ratio $V_{\text{rot}}/V_{\text{phot}}$ and the photospheric rotational velocity, V_{phot} . The maximum ratio, $V_{\text{rot}}/V_{\text{phot}}$, varies from 40 for the first to 5 for the fourth component (figure 4). A possible explanation of this situation is the inclination of the stellar axis.

5.2. Si IV Density Regions of 27 Be Stars

This study was based on an analysis of 27 Be stellar spectra taken with the IUE-satellite. We examined the complex structure of the Si IV resonance lines ($\lambda\lambda$ 1393.755, 1402.77 Å). Our sample included all subtypes from B0 to B8. The values of the photospheric rotational velocities were taken from the catalogue of Chauville et al. (2001).

We found that the Si IV spectral lines consist of three components in 7 stars, four in 15 stars, and five in 5 stars. We studied the relation between the ratio $V_{\text{rot}}/V_{\text{phot}}$ of the first, second, third, fourth, and fifth detected components with the photospheric rotational velocity (V_{phot}). This ratio indicates how much the rotational velocity of the specific Si IV layer is higher than the apparent rotational velocity of the star (see also Lyrtzi et al. 2006). In figure 5 we present our results.

The Si IV resonance lines are composed of three, four, or five components. The difference from the case of the C IV resonance lines in the spectra of 20 Oe stars is that they are composed of two, three, or four components. However, in both cases, in each region and for each component there exists an exponential relation between the ratio $V_{\text{rot}}/V_{\text{phot}}$ and the photospheric rotational velocity, V_{phot} . For the satellite components of the Si IV resonance lines, the maximum ratio, $V_{\text{rot}}/V_{\text{phot}}$, varies from 19 for the first, to 1 for the fifth component (figure 5).

5.3. Rotation in Photosphere vs. Rotation of Density Regions

As one can see in figures 4 and 5, there is a good correlation between the rotational velocities of the density regions and the photosphere. In both cases (Be and Oe stars) for rotational velocity of the photosphere, $V_{\text{phot}} > 200 \text{ km s}^{-1}$, the rotation of the photosphere correlates with the rotation of the density regions ($V_{\text{rot}} \approx \text{const.} \times V_{\text{phot}}$). On the other hand, for $V_{\text{phot}} < 200 \text{ km s}^{-1}$, the ratio $V_{\text{rot}}/V_{\text{phot}}$ decreases with the

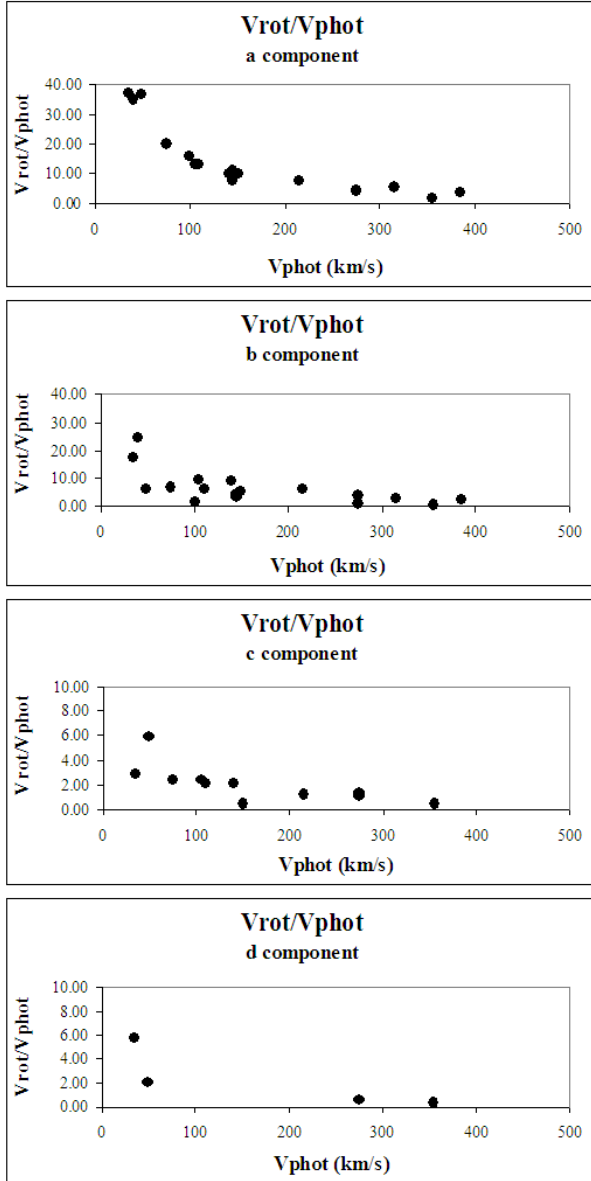


Fig. 4. Ratio V_{rot}/V_{phot} of the four SACs as a function of the photospheric rotational velocity (V_{phot}) for all of the studied Oe stars.

rotation in the photosphere. This can be explained by the inclination effect and the fact that the density regions are extensive around the star, i.e., for a high inclination angle the projected photospheric rotational velocity is small, but in a density region (that lies extensively around the star), one can detect faster rotation.

6. Conclusions

Here we present a new model for fitting the complex UV lines of Be and Oe stars, where we take into account the possibility that the random motion of ions can significantly contribute to the line widths. The proposed model can be applied to the spectral photospherical lines as well as the UV lines originating in the post-coronal regions. Concerning our work, we can make the following conclusions:

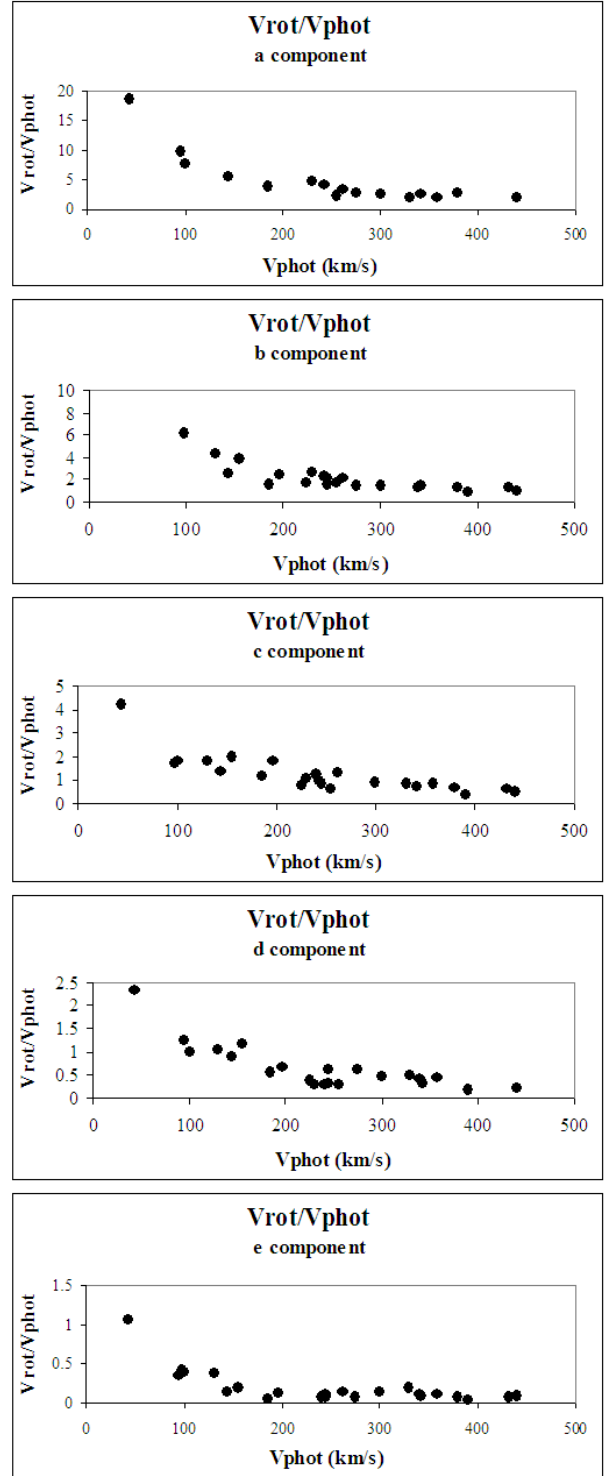


Fig. 5. Ratio V_{rot}/V_{phot} of the five SACs as a function of the photospheric rotational velocity (V_{phot}) for all of the studied Be stars.

- (i) The proposed model can accurately reproduce the complex UV lines of Be and Oe stars.
- (ii) Using the proposed model one can very well separate the contribution of the rotational and radial velocities in the density region by fitting the complex line profiles.

(iii) The proposed model provides an opportunity to investigate the physical parameters of the regions creating the UV complex line profiles.

(iv) The proposed model allows us to use the photospheric lines, in order to determine the photospheric rotation.

At the end, let us point out that in spite of the fact that today there exists a number of models that are able to reproduce the spectra from stellar atmospheres, there is a problem to find an appropriate model that can fit the complex UV line profiles that are created not only in the photosphere, but also in the density regions. On the other hand, the proposed model is able to provide information about the physical parameters of density regions as well as the rotation of the photosphere. We hope that the proposed model will be useful first of all to allow a first impression about the physics of density layers.

We would like to thank Professor Ryuko Hirata for his very useful suggestions. This research project is progressing at the University of Athens, Department of Astrophysics - Astronomy and Mechanics, under the financial support of the Special Account for Research Grants, which we thank very much. The project is co-financed within Op. Education by the ESF (European Social Fund) and National Resources, under the “Herakleitos” project. This work also was supported by Ministry of Science of Serbia, through the following projects: *Influence of collisional processes on astrophysical plasma line shapes* - P146001 and *Astrophysical spectroscopy of extragalactic objects* - P146002.

Appendix. Including the Random Motion in the Calculation of L — The Gauss-Rotation model (GR model)

We consider a spherical shell and a point A_i in its equator. If the laboratory wavelength of a spectral line that arises from A_i is λ_{lab} , the observed wavelength is: $\lambda_0 = \lambda_{\text{lab}} \pm \Delta\lambda_{\text{rad}}$. If the spherical density region rotates, we observe a displacement $\Delta\lambda_{\text{rot}}$ and the new wavelength of the center of the line is $\lambda_i = \lambda_0 \pm \Delta\lambda_{\text{rot}}$, where $\Delta\lambda_{\text{rot}} = \lambda_0 z \sin \varphi$, $z = \frac{V_{\text{rot}}}{c}$, V_{rot} is the rotational velocity of point A_i .

This means that $\lambda_i = \lambda_0 \pm \lambda_0 z \sin \varphi = \lambda_0 (1 \pm z \sin \varphi)$ and if $-\frac{\pi}{2} < \varphi < \frac{\pi}{2}$, then $\lambda_i = \lambda_0 (1 - z \sin \varphi)$.

If we consider that the spectral line profile is a Gaussian distribution, $I(\lambda) = \frac{1}{\sqrt{2\pi}\sigma} e^{-\left[\frac{\lambda-\kappa}{\sigma\sqrt{2}}\right]^2}$, where κ is the mean value of the distribution and in the case of the line profile it indicates the center of the spectral line that arises from A_i . This means that

$$I(\lambda) = \frac{1}{\sigma\sqrt{2\pi}} e^{-\left[\frac{\lambda-\lambda_0(1-z\sin\varphi)}{\sigma\sqrt{2}}\right]^2} = \frac{1}{\sigma\sqrt{2\pi}} e^{-\frac{[\lambda-\lambda_0(1-z\sin\varphi)]^2}{2\sigma^2}}. \quad (\text{A1})$$

The distribution function for all of the semi-equator is

$$I_1(\lambda) = \int_{-\frac{\pi}{2}}^{\frac{\pi}{2}} \frac{1}{\sqrt{2\pi}\sigma} e^{-\frac{[\lambda-\lambda_0(1-z\sin\varphi)]^2}{2\sigma^2}} \cos \varphi d\varphi. \quad (\text{A2})$$

If $\sin \varphi = x$, then $dx = \cos \varphi d\varphi$, $-1 \leq x \leq 1$, and equation (A2) takes the form

$$I_1(\lambda) = \int_{-1}^1 \frac{1}{\sigma\sqrt{2\pi}} e^{-\frac{[\lambda-\lambda_0(1-zx)]^2}{2\sigma^2}} dx. \quad (\text{A3})$$

If we set $u = \frac{\lambda - \lambda_0(1-zx)}{\sqrt{2}\sigma}$, we have

$$I_1(\lambda) = \frac{1}{\lambda_0 z \sqrt{\pi}} \int_{\frac{\lambda-\lambda_0(1+z)}{\sigma\sqrt{2}}}^{\frac{\lambda-\lambda_0(1-z)}{\sigma\sqrt{2}}} e^{-u^2} du. \quad (\text{A4})$$

We consider the function $\text{erf}(x) = \frac{2}{\pi} \int_0^x e^{-u^2} du$. It is a

known function that describes the Gaussian error distribution.

If we take into account this function, $I_1(\lambda)$ takes the form

$$I_1(\lambda) = \frac{1}{\lambda_0 z \sqrt{\pi}} \left[\int_0^{\frac{\lambda-\lambda_0(1-z)}{\sigma\sqrt{2}}} e^{-u^2} du - \int_0^{\frac{\lambda-\lambda_0(1+z)}{\sigma\sqrt{2}}} e^{-u^2} du \right], \quad (\text{A5})$$

$$I_1(\lambda) = \frac{1}{\lambda_0 z \sqrt{\pi}} \left\{ \frac{\pi}{2} \text{erf} \left[\frac{\lambda - \lambda_0(1-z)}{\sigma\sqrt{2}} \right] - \frac{\pi}{2} \text{erf} \left[\frac{\lambda - \lambda_0(1+z)}{\sigma\sqrt{2}} \right] \right\}. \quad (\text{A6})$$

Thus, we finally have

$$I_1(\lambda) = \frac{\sqrt{\pi}}{2\lambda_0 z} \left[\text{erf} \left(\frac{\lambda - \lambda_0(1-z)}{\sigma\sqrt{2}} \right) - \text{erf} \left(\frac{\lambda - \lambda_0(1+z)}{\sigma\sqrt{2}} \right) \right], \quad (\text{A7})$$

and the distribution function from the semi-spherical region is

$$I_{\text{final}}(\lambda) = \frac{\sqrt{\pi}}{2\lambda_0 z} \int_{-\frac{\pi}{2}}^{\frac{\pi}{2}} \left[\text{erf} \left(\frac{\lambda - \lambda_0}{\sigma\sqrt{2}} + \frac{\lambda_0 z}{\sigma\sqrt{2}} \cos \theta \right) - \text{erf} \left(\frac{\lambda - \lambda_0}{\sigma\sqrt{2}} - \frac{\lambda_0 z}{\sigma\sqrt{2}} \cos \theta \right) \right] \cos \theta d\theta, \quad (\text{A8})$$

(Method Simpson).

In equation (A8), from λ_0 we can calculate the value of the radial velocity (V_{rad}); from z we calculate the rotational velocity (V_{rot}), and from σ we calculate the random velocity (V_{rand}).

This distribution function, $I_{\text{final}}(\lambda)$, has the same form as the distribution function of the absorption coefficient, L , and may replace it in the line functions $e^{-L\xi}$ or $S_{\lambda_e}(1 - e^{-L_e \xi_e})$, in the case when the line broadening is an effect of both the rotational velocity of the density region as well as the random velocities of the ions. This means that we now have a new distribution function to fit each satellite component of a complex line profile that represents DACs or SACs. We name this function the Gauss-Rotation distribution function (GR distribution function).

References

- Antoniou, A., Danezis, E., Lyratzi, E., Nikolaidis, D., Popović, L. Č., Dimitrijević, M. S., & Theodossiou, E. 2006, in Proc. 23rd Summer School and International Symposium on the Physics of Ionized Gases, ed N. S. Simonović, B. P. Marinković, & L. Hadžievski (Melville, NY: AIP)
- Bates, B., & Halliwell, D. R. 1986, MNRAS, 223, 673
- Chauville, J., Zorec, J., Ballereau, D., Morrell, N., Cidale, L., & Garcia, A. 2001, A&A, 378, 861
- Cranmer, S. R., & Owocki, S. P. 1996, ApJ, 462, 469
- Cranmer, S. R., Smith, M. A., & Robinson, R. D. 2000, ApJ, 537, 433
- Danezis, E. 1983, PhD Thesis, University of Athens
- Danezis, E. 1987, in IAU Colloq. 92, Physics of Be Stars, ed A. Slettebak & T. P. Snow (Cambridge, UK: Cambridge University Press), 445
- Danezis, E., et al. 2003, Ap&SS, 284, 1119
- Danezis, E., Lyratzi, E., Nikolaidis, D., Antoniou, A., Popović, L. Č., & Dimitrijević, M. S. 2006, in Proc. 23rd Summer School and International Symposium on the Physics of Ionized Gases, ed N. S. Simonović, B. P. Marinković, & L. Hadžievski (Melville, NY: AIP)
- Danezis, E., Nikolaidis, D., Lyratzi, E., Popović, L. Č., Dimitrijević, M. S., Theodossiou, E., & Antoniou, A. 2005, Mem. Soc. Astron. Ital., 7, 107
- Fullerton, A. W., Massa, D. L., Prinja, R. K., Owocki, S. P., & Cranmer, S. R. 1997, A&A, 327, 699
- Grady, C. A., Sonneborn, G., Wu, C.-C., & Henrichs, H. F. 1987, ApJS, 65, 673
- Henrichs, H. F. 1984, in ESA SSSP-218, Proc. 4th European IUE Conf., ed E. Rolfe & B. Battrick (Noordwijk: ESA), 43
- Kaper, L., et al. 1997, A&A, 327, 281
- Kaper, L., Henrichs, H. F., Nichols, J. S., Snoek L. C., Volten, H., & Zwarthoed G. A. A. 1996, A&AS, 116, 257
- Kaper, L., Henrichs, H. F., Nichols, J. S., & Telting, J. H. 1999, A&A, 344, 231
- Lamers, H. J. G. L. M., Snow, T. P., de Jager, C., & Langerwerf, A. 1988, ApJ, 325, 342
- Lyratzi, E. & Danezis, E. 2004, in AIP Conf. Proc., 740, 458
- Lyratzi, E., Danezis, E., Nikolaidis, D., Antoniou, A., Popović, L. Č., & Dimitrijević, M. S., & Theodossiou, E. 2006, in Proc. 23rd Summer School and International Symposium on the Physics of Ionized Gases, ed N. S. Simonović, B. P. Marinković, & L. Hadžievski (Melville, NY: AIP)
- Lyratzi, E., Danezis, E., Popović, L. Č., & Dimitrijević, M. S., Nikolaidis, D., & Antoniou, A. 2007, PASJ, 59, 357
- Markova, N. 2000, A&AS, 144, 391
- Mullan, D. J. 1984a, ApJ, 283, 303
- Mullan, D. J. 1984b, ApJ, 284, 769
- Mullan, D. J. 1986, A&A, 165, 157
- Nikolaidis, D., Danezis, E., Lyratzi, E., Popović, L. Č., Antoniou, A., Dimitrijević, M. S., & Theodossiou, E. 2006, in Proc. 23rd Summer School and International Symposium on the Physics of Ionized Gases, ed N. S. Simonović, B. P. Marinković, & L. Hadžievski (Melville, NY: AIP)
- Prinja, R. K., & Howarth, I. D. 1988, MNRAS, 233, 123
- Rivinius, Th. et al. 1997, A&A, 318, 819
- Underhill, A. B. 1975, ApJ, 199, 691
- Underhill, A. B., & Fahey, R. P. 1984, ApJ, 280, 712
- Waldron, W. L., Klein, L., & Altner B. 1992, ASP Conf. Series, 22, 181
- Waldron, W. L., Klein, L., & Altner B. 1994, ApJ, 426, 725
- Wilson, R. E. 1963, General Catalogue of Stellar Radial Velocities (Washington: Carnegie Institution of Washington), 601

The Complex Structure of the Mg II $\lambda\lambda$ 2795.523, 2802.698 Å Regions of 64 Be Stars

Evaggelia LYRATZI,¹ Emmanouel DANEZIS,¹ Luka Č. POPOVIĆ,²
Milan S. DIMITRIJEVIĆ,² Dimitris NIKOLAIDIS,¹ and Antonis ANTONIOU¹

¹*University of Athens, Faculty of Physics, Department of Astrophysics, Astronomy and Mechanics,
Panepistimioupoli, Zographou 157 84, Athens, Greece*

²*Astronomical Observatory of Belgrade, Volgina 7, 11160 Belgrade, Serbia
Isaac Newton Institute of Chile, Yugoslavia Branch*

elyratzi@phys.uoa.gr, edanezis@phys.uoa.gr, lpopovic@aob.bg.ac.yu, mdimitrijevic@aob.bg.ac.yu, ananton@phys.uoa.gr

(Received 2006 February 3; accepted 2007 January 29)

Abstract

Here we consider the presence of absorption components shifted to the violet or red side of the main spectral line (satellite or discrete absorption components, i.e., SACs or DACs) in the regions of the Mg II resonance lines in Be stars as well as their kinematical characteristics. Namely, our objective is to check whether there exists a common physical structure for the atmospheric regions creating SACs or DACs of the Mg II resonance lines. In order to do this, a statistical study of the Mg II $\lambda\lambda$ 2795.523, 2802.698 Å lines in the spectra of 64 Be stars of all spectral subtypes and luminosity classes was performed. We found that the atmospheric absorption regions where the Mg II resonance lines originated may be formed of several independent density layers of matter that rotate with different velocities. It was also attempted to separate SACs and DACs according to low or high radial velocity. The emission lines were detected only in the earliest and latest spectral subtypes.

Key words: stars: atmospheres — stars: early type — stars: emission-line, Be — stars: kinematics

1. Introduction

The Mg II resonance lines have a peculiar profile in the Be stellar spectra, which indicates a multicomponent nature of their origin region. Many researchers have observed the existence of absorption components shifted to the violet or red side of the main spectral line (Underhill 1970; Marlborough et al. 1978; Dachs 1980; Doazan 1982; Danezis 1983, 1987; Sahade et al. 1984; Sahade & Brandi 1985; Hutsemékers 1985; Danezis et al. 1991; Doazan et al. 1991; Laskarides et al. 1992; Cidale 1998; Lyratzi et al. 2003). These components — Discrete Absorption Components (DACs: Bates & Halliwell 1986) or Satellite Absorption Components (SACs: Danezis et al. 2003; Lyratzi & Danezis 2004) — probably originate in separated regions that have different rotational and radial velocities. Especially in the case of very narrow DACs and SACs, they cannot be photospheric; rather, they have a circumstellar or interstellar origin (Slettebak & Snow 1978). For example, Kondo, Morgan, and Modisette (1976) found that the shell absorption becomes stronger in intermediate to late B stars, and suggested that “it might be due to the rising temperature in the gaseous shell which converts Mg II to Mg III and to the weakening of the outward-driving mechanisms of the atmosphere”. In any case, the whole feature of the Mg II resonance lines is not the result of a uniform atmospheric region, but the components are created in different regions, which rotate and move radially with different velocities. As de Jager et al. (1979) proposed in their study of 33 stellar spectra of all the spectral types, variable mass loss in the late B supergiants occurs due to “occasional stellar ‘puffs’

superposed on a more or less regular wind”. They proposed that “there are concentrations of low-ionization species in the stellar wind as a result of the occurrence of significant density variations”. Also, in order to explain the complex profiles of the Mg II resonance lines, Cidale (1998) proposed that the Be stellar atmospheres are composed of a classical photosphere, an extending high-temperature chromosphere, and a cool envelope. There is a question about the contributions of different atmospheric layers, especially in the case of SAC and/or DAC phenomena, in constructing profiles of the Mg II resonance lines.

The aim of this work is to statistically investigate the presence of SACs and/or DACs in regions of Mg II resonance lines in Be stars and their kinematical characteristics. Also, we would like to search some conclusion about the limits of the rotational and radial velocities (V_{rot} , V_{rad}), as well as to check whether there exists a common physical structure for the atmospheric regions that create the SACs of the Mg II resonance lines in the spectra of all the Be stars. To do that, a statistical study of the UV Mg II resonance lines $\lambda\lambda$ 2795.523, 2802.698 Å in the spectra of 64 Be stars (all the spectral subtypes and luminosity classes) was performed. The study was based on a model proposed by Danezis et al. (2003) and Lyratzi and Danezis (2004).

We decided to study the Mg II resonance lines, because they are characteristic of the cool envelope in Be stellar atmospheres and very intense features in the spectra of Be stars and they mostly present a complex and peculiar structure. Besides, since they are resonance lines, they give us a possibility to test the validity of the proposed model. Because we have to

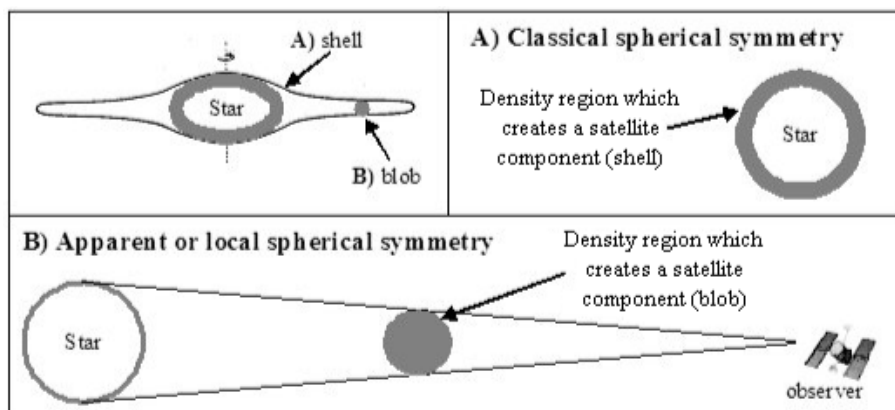


Fig. 1. Density regions that create the observed SACs or DACs in the stellar spectra.

adhere to all of the necessary physical criteria and techniques (Danezis et al. 2003). Our purpose here was to study spectral lines that are created in cool regions (Mg II) in Be stellar atmospheres. Danezis (1987), Sahade, Brandi, and Fontenla (1984), and Sahade and Brandi (1985) detected multistructures in the regions where Fe II lines (I.P.=7.870 eV) are created in the spectra of Be stars, which are characterized as iron stars. One of our purposes was to investigate whether the multistructure appears only in the Fe II spectral lines, or in also other spectral lines with a similar ionization potential (I.P.), as Mg II (I.P.=7.646 eV). This is another reason why we chose to study the Mg II resonance lines and not some other resonance lines of the cool envelope, as N II (I.P.=14.490 eV), C II (I.P.=11.260 eV), Si II (I.P.=8.110 eV), or Al II (I.P.=5.986 eV). The study of Mg II resonance lines provides us information not only about the cool envelope, but also about the multistructure of another ion that lies in the same region where the Fe II spectral lines are created.

In section 2, we describe the method of analysis, in section 3 the observational data, and in section 4 the results along with a discussion. In section 5 we give our conclusions.

2. Method of Spectral Line Analysis

Before describing the method used in our study, let us explain the differences between DACs and SACs. The DACs are components of a spectral line of a specific ion, shifted at different $\Delta\lambda$ from the transition wavelength of a line, because they are created in different density regions that rotate and move radially with different velocities (Lyrtzi & Danezis 2004). The DACs are discrete lines, easily observed, in the spectra of some Be stars of luminosity class III, in the case of the Mg II doublet. However, if the layers that give rise to such lines rotate with quite large velocities and move radially with small velocities, then the produced lines are quite broadened and slightly shifted. As a result, they are blended among themselves as well as with the main spectral component, and thus they do not appear as being discrete; consequently, they cannot be resolved. In such a case, the name Discrete Absorption Component is inappropriate. Besides, as Peton (1974) first pointed out, these components appear as “satellites” in the violet or in the red side of the main spectral

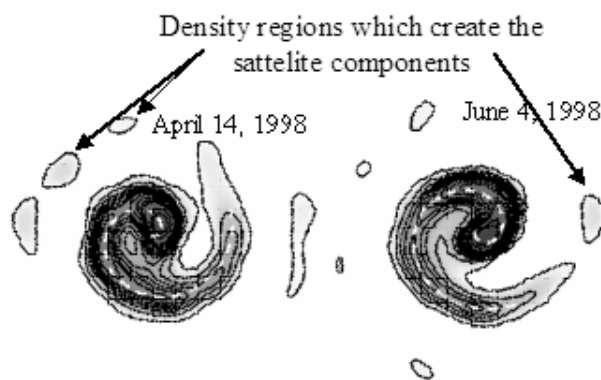


Fig. 2. Due to rotation of the star, the ejected matter forms spiral streams that produce blobs that create the observed SACs or DACs in the stellar spectra. This figure is taken from Tuthill, Monnier, and Danchi (1999).

line's component as a function of the time or the phase in the case of a binary system. For these two reasons, and in order to give a unique name to all of these lines that are components of the line profile whether they are discrete or not, it has been proposed (Lyrtzi & Danezis 2004) that they should be named Satellite Absorption Components (SACs) as a general expression, because the Discrete Absorption Components (DACs) are “Satellites” of a main spectral line, while the SACs are not always discrete, and cannot be easily resolved.

An additional peculiar phenomenon is that all of the lines of a specific ion have not DACs. The DAC phenomenon is not a general one, but is present in the case of some lines that have a low excitation potential. For example, while the Mg II resonance lines at 2795.523, 2802.698 Å (multiplet 1) have DACs in the spectra of some Be stars, their subordinate lines at 2790.768, 2797.989 Å (multiplet 3) do not present the same phenomenon. Therefore, we decided to study the Mg II resonance lines, since they are the only Mg II doublet having DACs.

In order to obtain a qualitative picture, we will use the spherical geometry. According to it, there are two possibilities (see figure 1).

- A) The region that creates the SACs or DACs may be an envelope around and near to a rapidly rotating star. In such a case, the spherical model could give only a rough approximation, but would allow us to obtain some qualitative results. We note that such an assumption is valid for some earlier models like, e.g., Doazan and Thomas (1982), which cannot explain the observed free-free emission or polarization, but we are interested here only in the kinematic characteristics. In this case, the calculated values of the radial velocity correspond to the component of the expansion or contraction velocity of the shell, which is projected to the observational axis.
- B) The region which creates the SACs or DACs may be an independent density region (blob), which is spherically symmetric around its own center. Such density regions have been observed around stars that eject mass. In figure 2, we can see this phenomenon in WR 104, observed by Tuthill, Monnier, and Danchi (1999). Such a region may be one that creates the Mg II resonance lines, and that lies in a cool envelope of the stellar atmosphere. Such a blob may have three different motions: a) it may rotate around the star, b) it may expand or contract, and c) it may move radially. This means that the calculated values of the radial velocity consist of three different components: a) the component of the rotational velocity of the blob around the star, projected to the observational axis, b) the component of the expansion or contraction velocity of the blob, projected to the observational axis, and c) the component of the velocity of the blob's radial motion, projected to the line of sight.

In principle, as known, the star ejects mass with a specific radial velocity. The stream of matter is twisted, forming density regions, such as the interaction of fast and slow wind components, corotating interaction regions (CIRs), and structures due to magnetic fields or spiral streams as a result of the stellar rotation (Underhill & Fahey 1984; Mullan 1984a, 1984b, 1986; Prinja & Howarth 1988; Cranmer & Owocki 1996; Kaper et al. 1996, 1997, 1999; Fullerton et al. 1997; Cranmer et al. 2000). Consequently, hydrodynamic and magnetic forces act as centripetal forces, causing the outward moving matter to twist and move around the star (see figure 2). This motion of the matter is responsible for the formation of high-density regions (shells, blobs, puffs, and spiral streams), that are either spherically symmetric with respect to the star or with respect to their own center (Danezis et al. 2003; Lyrtzi & Danezis 2004) (see figure 1).

In order to study the physical structure and the existence of SAC phenomena in the regions where these lines are created, we used a model proposed by Danezis et al. (2003) and Lyrtzi and Danezis (2004). This model allowed us to calculate the rotational (V_{rot}) and radial velocities (V_{rad}) of independent density layers of matter in these regions, as well as the optical depth (τ) and the column density (n). If the considered SACs or DACs originate from "puffs" or "blobs" created by stellar winds in a cool extended envelope, the real shape of the envelope is not crucial. If the considered features are created in the envelope's layers, we could also reach some qualitative

conclusions, since we are interested only in the kinematical properties here. Moreover, because there is no sophisticated or rough model of a Be star that could fit the observed profiles, considering their complex structure, there are no results of similar investigations for comparison.

Let us consider that the area of gas that creates a specific spectral line consists of i independent absorbing density regions, followed by j independent regions that both absorb and emit and by an outer absorbing region. Such a structure produces DACs or SACs in the observed spectra (Danezis et al. 2003). The final line function which can describe the complex line profiles of the observed spectral lines is (Danezis et al. 2003; Lyrtzi & Danezis 2004)

$$F_{\lambda} = [F_{\lambda 0} \prod_i e^{-L_i \xi_i} + \sum_j S_{\lambda e j} (1 - e^{-L_{e j} \xi_{e j}})] e^{-L_g \xi_g} \quad (1)$$

where F_{λ} is the observed flux, $F_{\lambda 0}$ the initial flux, $S_{\lambda e j}$ the source functions of each emitting density region, ξ the optical depth in the center of the line, and L_i , $L_{e j}$, L_g the distribution functions of the absorption coefficients ($k_{\lambda i}$, $k_{\lambda e j}$, $k_{\lambda g}$), respectively. Each L depends on the values of the rotational and the radial velocities of the density region, which forms each component of the spectral line (V_{rot} , V_{rad}) (Danezis et al. 2003; Lyrtzi & Danezis 2004). The product of L and ξ is the optical depth of each region.

This function does not depend on the geometry of the regions creating the observed feature. The considered geometry of the regions is taken into account in order to define the distribution function, L . This means that L may represent any distribution which decides a certain geometry (see the Appendix), without changing anything in F_{λ} .

Each component of the spectral line, which is formed by the i^{th} density region of matter, must be accurately reproduced by the function $e^{-L_i \xi_i}$ by applying appropriate values of $V_{rot i}$, $V_{rad i}$ and ξ_i . Using the best model fit for a complex spectral line, we can calculate the apparent radial and rotational velocities ($V_{rad i}$, $V_{rot i}$) and the optical depth (ξ_i) in the center of the line of the region where the main spectral line and its SACs are created.

In the case where we want to consider that some other physical parameters are responsible for the line broadening, and not the rotation of the region that produces the studied spectral lines, we may replace the exponential $e^{-L \xi}$ with another classical distribution.

In the case of emission lines, each emission component, which is formed by the j^{th} density region of matter, must be accurately reproduced by the function $S_{\lambda e j} (1 - e^{-L_{e j} \xi_{e j}})$, by applying the appropriate values of $V_{rot j}$, $V_{rad j}$, ξ_j , and S . Using the best model fit for a complex spectral line, we can calculate the apparent radial and rotational velocities ($V_{rad j}$, $V_{rot j}$), the optical depth (ξ_j) at the center of the line, and the source function, S , of the region where the emission component is created.

The proposed model is relatively simple, aiming to describe the regions where the spectral lines that present SACs are created. With this model we can study the regions of a specific ion that creates a specific spectral line.

This model presupposes that the main reason for the line broadening is rotation of the region that gives rise to the

Table 1. The list of Be stars.

Star	Spectral type	Camera	ref.	Star	Spectral type	Camera	ref.
HD 5394	B0 IV : evar	Lwr 07861	1	HD 25940	B3 V e	Lwr 05950	2
HD 53367*	B0 IV : e	Lwr 09286	1	HD 45725*	B3 V e	Lwp 10041	2
HD 203374 [†]	B0 IV pe	Lwp 07400	1	HD 183362	B3 V e	Lwp 11044	2
HD 206773	B0 V : pe	Lwr 14808	1	HD 208057	B3 V e	Lwp 29221	2
HD 200310	B1 V e	Lwr 09544	1	HD 205637	B3 V : p	Lwr 05947	4
HD 212571	B1 V e	Lwr 05948	2	HD 217543	B3 V pe	Lwp 13326	2
HD 44458*	B1 V pe	Lwp 30173	1	HD 217050 [†]	B4 III pe	Lwr 05933	2
HD 200120	B1.5 V nne	Lwr 11035	2	HD 89884	B5 III	Lwp 29529	6
HD 193237	B2 pe	Lwr 07990	2	HD 22192	B5 V e	Lwr 06898	2
HD 45910*	B2 III e	Lwr 12138	3	HD 23302	B6 III e	Lwr 09071	2
HD 37202	B2 IV p	Lwr 05888	4	HD 45542	B6 III e	Lwp 07631	2
HD 36576	B2 IV – V e	Lwp 14029	2	HD 109387	B6 III pe	Lwr 04132	2
HD 212076	B2 IV – V e	Lwr 03406	2	HD 23480	B6 IV e	Lwr 05219	2
HD 32991*	B2 V e	Lwr 11426	2	HD 217891	B6 V e	Lwr 09069	2
HD 58050	B2 V e	Lwr 14810	2	HD 138749	B6 V nne	Lwr 07858	2
HD 164284	B2 V e	Lwr 11038	2	HD 23630	B7 III	Lwr 09060	2
HD 41335	B2 V ne	Lwr 07384	2	HD 209409	B7 IV e	Lwp 15464	2
HD 52721	B2 V ne	Lwp 05462	5	HD 6811	B7 V e	Lwr 09070	7
HD 58343	B2 V ne	Lwr 07363	6	HD 192044*	B7 V e	Lwp 08135	8
HD 148184	B2 V ne	Lwr 06744	6	HD 210129	B7 V ne	Lwp 23173	7
HD 202904	B2 V e	Lwr 07343	2	HD 142983	B8 Ia/Iab	Lwr 07359	6
HD 65079	B2 V ne	Lwp 30119	5	HD 29866	B8 IV ne	Lwr 08745	2
HD 28497	B2 V ne	Lwr 07337	6	HD 47054	B8 V e	Lwp 13074	9
HD 45995*	B2 V nne	Lwr 08648	1	HD 183914*	B8 V e	Lwr 04609	9
HD 10516	B2 V pe	Lwr 07335	2	HD 50138	B8 V e	Lwr 09358	11
HD 187567*	B2.5 IV e	Lwp 14025	2	HD 58715	B8 V var	Lwp 10104	10
HD 191610	B2.5 V e	Lwr 07342	2	HD 23552 [†]	B8 V ne	Lwr 08744	7
HD 32343*	B2.5 V e	Lwr 05890	2	HD 185037	B8 V ne	Lwp 08136	9
HD 65875	B2.5 V e	Lwr 05616	2	HD 199218	B8 V nne	Lwp 09903	7
HD 60855 [†]	B2/B3 V	Lwp 15477	6	HD 91120	B8/B9 IV/V	Lwp 07475	6
HD 37490*	B3 III e	Lwr 07361	1	HD 142926	B9 pe	Lwr 05768	7
HD 50820	B3 IV e+...	Lwr 16776	2	HD 144	B9 III e	Lwr 08997	7

The list of Be stars with spectral type (columns 2, 6) and the type of the camera used during observations (columns 3, 7).

* Double system.

[†] Triple system.

References: (1) Morgan, Code, and Whitford (1955); (2) Lesh (1968); (3) Sahade, Brandi, and Fontenla (1984); (4) Herbig and Spalding (1955); (5) Guetter (1968); (6) Houk and Smith-Moore (1988); (7) Cowley (1972); (8) Osawa (1959); (9) Cowley et al. (1969); (10) Slettebak (1954); (11) Houziaux and Andriolat (1976).

spectral line (Doazan 1982). We can accept this assumption when we deal with the inner layers to the post coronal regions. Thus, for these atmospheric layers the model gives satisfactory results.

3. Observational Data and Fitting Procedure

The data that we used are the Mg II resonance lines of 64 Be stars taken from the International Ultraviolet Explorer (IUE) Archive Search database.¹ The stellar spectra were observed with the IUE satellite using the Long Wavelength range Prime and Redundant cameras (LWP, LWR) at high resolution (0.1 to 0.3 Å). In table 1, we give a list of stars, their spectral type, and the type of camera used during observations.

Our first step is to identify the spectral lines in the studied wavelength range, in order to determine which lines may be blended with the Mg II doublet, and thus may contribute to the observed features. The identification was made by using the NIST Atomic Spectra Database² as well as the catalogues of Moore (1968) and Kelly (1979). In this specific spectral range the adjacent features of the Mg II profiles are intense, but they are away from the Mg II spectral features, so that, in spite of their important influence on the wings, their much smaller influence in the central parts is not important for our discussion. Moreover, because we deal with resonance lines, we know that if one line of the doublet is well fitted, we should apply the same parameters to the other one, even if the fit is not very good. In this case, the unfitted regions correspond to blends.

¹ (<http://archive.stsci.edu/cgi-bin/iue>).

² (http://physics.nist.gov/cgi-bin/AtData/lines_form).

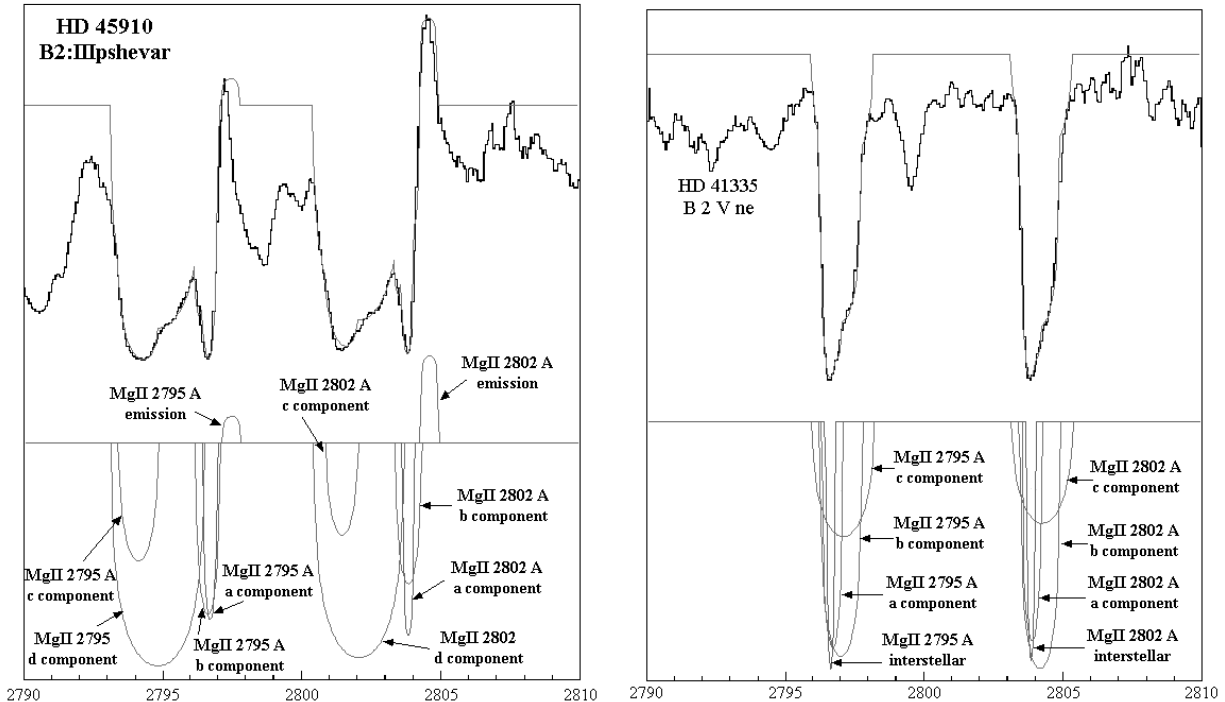


Fig. 3. Mg II resonance line profiles fitted with the model for HD 45910 and HD 41335. The thick lines present observations, and the thin lines present the best fit. The DACs (HD 45910) and SACs (HD 41335) are present below.

Also, the level of the continuum is calculated for the whole spectrum taken by IUE. This means that its suppression by the blends does not affect our calculations.

The procedure that we followed for decomposition of the lines is described in Danezis et al. (2003). The way, criteria, and discussion about the model that we used to fit the observed spectral lines are presented in Danezis et al. (2003). They are explained in more detail in Lyratzi and Danezis (2004) and an application of the method is given in Popović et al. (2004). This means that we tried to fit the observed profiles of the Mg II resonance lines with fewer possible components. We at first tried to fit the observed spectral feature with one component. If this was not possible, we added one more component and then another, until we accomplished the best fit with fewer possible components. This means that we fitted the observed Mg II features with one to four components, for different stars. Our results are given in tables 2 and 3.

In order to be certain that we accomplished the best fit, we performed an F-test, between the fit that we accepted as being the best, and a fit with one component less. We present the results of the F-test in table 4, where we give the values of the confidence with which the accepted fit is better than the fit with one component less. We did not perform an F-test between the best fit and a fit with one component more, because this last one fit presented extreme differences with the observed spectral line profiles, or because the values of the measured parameters go against the classical theory for resonance lines (Danezis et al. 2003; Lyratzi & Danezis 2004).

4. Results and Discussion

The DAC phenomenon is quite common in O- and early B-type stars. However, we found that the DAC phenomenon is also observed in late B-type stars (as in the case of HD 144). Moreover, many researchers (Underhill 1975; Morgan et al. 1977; Marlborough et al. 1978; de Jager et al. 1979; Doazan 1982; Sahade et al. 1984; Sahade & Brandi 1985; Hutsemékers 1985), even if they did not use the name DACs, observed the same phenomenon. We also point out that in Underhill (1970), Marlborough, Snow, and Slettebak (1978), Dachs (1980), Doazan (1982), Sahade, Brandi, and Fontenla (1984), Sahade and Brandi (1985), Hutsemékers (1985), Doazan et al. (1991), and Cidale (1998) only the known DAC phenomenon was investigated. However, in the present paper a similar phenomenon of SACs is introduced, and we investigate whether this phenomenon is able to explain the complex structure of the Mg II resonance lines in the stellar spectra of all the Be spectral subtypes. Our result is that the SAC phenomenon is able to explain this complex structure.

Using the model described above, we find the best fit for the Mg II resonance lines of 64 Be stars given in table 1. In figure 3, we give the best fit of the Mg II resonance lines for two stars (HD 45910 and HD 41335). The first one (HD 45910) presents DACs, where the decomposition of the three different components is easy, while the second one (HD 41335) presents SACs, where it is hard to decompose the three different components without a convenient model. One can thus see that the model conveniently describes the Mg II complex profiles and the complex structure of the regions where these lines are created. In the studied IUE spectra, the interstellar lines are

Table 2. The kinematical parameters for absorption regions for considered stars.

Star	Spectral type	V_{rot1}	V_{rad1}	V_{rot2}	V_{rad2}	V_{rot3}	V_{rad3}	V_{rot4}	V_{rad4}
HD 5394	B0 IV evar	25	8.8	50	12.3				
HD 53367	B0 IV e	24	-18.0	37	-12.0	71	-7.0		
HD 203374	B0 IV pe	24	4.5	36	3.5	60	2.0		
HD 206773	B0 V pe	28	15.5	46	18.5				
HD 200310	B1 V e	25	10.1						
HD 212571	B1 V e	22	-2.5	40	-11.0				
HD 44458	B1 V pe	22	-17.5	37	-19.5	83	-29.0		
HD 200120	B1.5 V nne	28	-0.4						
HD 193237	B2 pe	30	-18.6	45	-18.1	86 (DAC)	-200.6	115	(DAC) -200.1
HD 45910	B2 III e	24	13.0	42	11.0	60 (DAC)	-229.5	170	(DAC) -182.0
HD 37202	B2 IV p	29	-18.0	48	-21.0			125	-33.0
HD 36576	B2 IV-V e	29	-43.0			80	-21.0		
HD 212076	B2 IV-V e	20	-1.0	34	-1.5				
HD 32991	B2 V e	19	-15.4	38	-21.9				
HD 58050	B2 V e	25	-35.9	49	-28.4				
HD 164284	B2 V e	28	13.3			63	33.8		
HD 41335	B2 V ne	22	-9.5	38	-1.5	80	27.0	100	40.0
HD 52721	B2 V ne	18	12.3	34	11.3	65	31.3		
HD 58343	B2 V ne	21	-1.8	50	-5.2				
HD 148184	B2 V ne	17	19.9	30	20.9				
HD 202904	B2 V e	20	4.0	31	4.5				
HD 65079	B2 V ne	29	8.0			74	-12.5		
HD 28497	B2 V ne	8	-45.0	37	-34.5	60	-35.0		
HD 45995	B2 V nne	29	-17.0	45	-20.0	69	-24.0		
HD 10516	B2 V pe	22	-1.0	37	-2.3	50	-5.8		
HD 187567	B2.5 IV e	19	23.6	32	24.6	50	26.1		
HD 32343	B2.5 V e	20	8.4			78	17.9		
HD 65875	B2.5 V e	17	14.0	35	18.0				
HD 191610	B2.5 V e	20	-45.6	45	-53.6				
HD 60855	B2/B3 V			45	-14.6	71	22.9	139	-29.6
HD 37490	B3 III e	20	-5.3	35	-8.3	54	-18.8	98	-10.3
HD 50820	B3 IV e+...	24	-13.0	50	-9.5				
HD 25940	B3 V e	22	0.7	42	-2.3				
HD 45725	B3 V e	18	-9.5	34	-10.5	65	-13.0		
HD 183362	B3 V e	24	24.2	34	24.2	68	19.7		
HD 208057	B3 V e	23	12.3			75	9.8		
HD 205637	B3 V p	22	17.5	39	15.5			115	9.0
HD 217543	B3 V pe	26	16.5	51	15.5			130	23.5
HD 217050	B4 III pe	35	14.3	54	17.8	84	32.3		
HD 89884	B5 III			33	-9.5	60	1.5		
HD 22192	B5 V e	16	-2.0	32	-1.0	52	-7.0		
HD 23302	B6 III e	21	-9.9			86	-8.9		
HD 45542	B6 III e	15	-24.4	33	-24.9	58	-15.4		
HD 109387	B6 III pe	18	-11.4			66	-28.4		
HD 23480	B6 IV e	20	-7.7	32	0.3				
HD 217891	B6 V e	18	-0.8						
HD 138749	B6 V nne	27	22.5	47	14.5				
HD 23630	B7 III	20	-9.0	45	-9.0				
HD 209409	B7 IV e	21	-9.0	38	-9.0	83	-5.0		

Table 2. (Continued.)

Star	Spectral type	V_{rot1}	V_{rad1}	V_{rot2}	V_{rad2}	V_{rot3}	V_{rad3}	V_{rot4}	V_{rad4}
HD 6811	B7 V e	19	3.3	35	1.8			169	12.8
HD 192044	B7 V e	25	19.5	52	8.5				
HD 210129	B7 V ne	21	62.6	52	43.1				
HD 142983	B8 Ia/Iab	21	-7.0	39	8.0	60	11.5	95	16.5
HD 29866	B8 IV ne	26	-42.0			85	41.5		
HD 47054	B8 V e	24	-30.0	42	-31.5				
HD 183914	B8 V e	17	16.8	37	20.8				
HD 50138	B8 V e	27	-36.0						
HD 58715	B8 V var	22	-21.5	44	-9.0				
HD 23552	B8 V ne			33	24.7				
HD 185037	B8 V ne	26	12.0	45	18.0				
HD 199218	B8 V nne	17	4.7	35	4.2			95	7.7
HD 91120	B8/B9 IV/V	23	-13.5	39	-15.0				
HD 142926	B9 pe	18	-12.9	50	2.1	67	7.6	165	3.6
HD 144	B9 III e	28	-30.6	53	(DAC) -188.6	80	(DAC) -187.1	178	(DAC) -129.6

The rotational (V_{rot}) and the radial (V_{rad}) velocities in km s^{-1} .

systematically shifted to the red for $+99 \pm 16 \text{ km s}^{-1}$. We used the Hipparcos catalogues,³ and we applied the corrections for the systemic velocity of individual stars (Smith 2001) and for the orbital motion of the those stars that are members of binary systems. Our results, given in tables 2 and 3 as well as in figures 4–8, are correspondingly corrected.

We should note that in our sample, 15 binary and multiple systems are present (see table 1). Considering that the origin of DACs and SACs might in principle be different than in single stars, at the beginning we separately analyzed this kind of star (presented with open circles in figures 4–6). However, we found that there is no systematic difference between single and binary/multiple stars. Consequently, in a further analysis we will not treat binary/multiple systems in a different way.

From the fit we obtained the rotational (V_{rot_i}) and radial (V_{rad_i}) velocities for each Mg II resonance line originating within the region.

In tables 2 and 3, we present the kinematical parameters for the absorption Mg II resonance line forming regions (table 2), as well as for the emission ones (table 3). As one can see, not all of the studied stars have an emission component, but only those listed in table 3. One could assume that these emission components are the emission part of P Cygni profiles formed by scattering. In that case, their wavelength and width do not represent the radial and rotational velocities. This could explain the majority of positive radial velocities since, in such a case as outflowing wind, lines will be widened and red-shifted. However, two cases with large negative radial velocities indicate that the real picture may be more complicated. We know that disk models, in many cases, may produce theoretically only the shape of the line profiles, but they are not able to fit them. Thus, in such cases, we may consider that the observed profile results from a different mechanism. In table 2, we give a list of stars, their spectral subtype (columns 1 and 2, respectively) and the values of the rotational velocities (columns 3, 5, 7, and 9) and the radial velocities (columns 4, 6, 8, and 10) of the respective

Table 3. The same as in table 2, but for the emission component where it is present.

Star	Spectral type	$V_{rot,e}$	$V_{rad,e}$
HD 203374	B0 IV pe	20	72
HD 45910	B2 III e	34	81
HD 32991	B2 V e	57	13
HD 164284	B2 V e	120	-1
HD 148184	B2 V ne	50	33
HD 45995	B2 V nne	46	102
HD 65875	B2.5 V e	30	53
HD 50820	B3 IV e+...	59	-87
HD 217891	B6 V e	50	6
HD 192044	B7 V e	94	7
HD 210129	B7 V ne	97	-29
HD 47054	B8 V e	81	0
HD 50138	B8 V e	53	120
HD 199218	B8 V nne	131	15

components. Also, in table 3, we present the kinematical parameters of the emission component. In column 1 we present a list of stars, in column 2 their spectral subtype and in columns 3 and 4 values of the rotational and radial velocities, respectively. Let us point out, here, that the calculated values correspond to the regions that create the SACs or DACs. Especially, the obtained rotational velocities correspond to the rotation of the region around itself and not around the star.

In figures 4 and 5, we present, separately, the rotational velocities and the radial velocities, respectively, of all the SACs as a function of the spectral subtype. In figure 5, the radial velocity's values that correspond to the DACs are clearly shown. In figure 6, we present the radial velocities of all the SACs as a function of the respective rotational velocities. In figure 7, we present mean values of the rotational and radial velocities of the two resonance lines of the emission component as a function of the spectral subtype. Each point

³ (<http://vizier.u-strasbg.fr/viz-bin/VizieR-3>).

Table 4. Values of the confidence with which the accepted fit is better than the fit with the one less component.

Star	4–3 comps	3–2 comps	2–1 comps	Star	4–3 comps	3–2 comps	2–1 comps
HD 5394		0.9132		HD 25940		0.9972	
HD 53367	1.0000			HD 45725		1.0000	
HD 203374	0.9483			HD 183362	0.9807		
HD 206773		1.0000		HD 208057		1.0000	
HD 200310			0.9993	HD 205637	1.0000		
HD 212571		0.9826		HD 217543	1.0000		
HD 44458	0.9981			HD 217050	1.0000		
HD 200120			1.0000	HD 89884		1.0000	
HD 193237	1.0000			HD 22192		1.0000	
HD 45910	0.1609			HD 23302		1.0000	
HD 37202	1.0000			HD 45542		0.9998	
HD 36576		0.9931		HD 109387	0.9996		
HD 212076		1.0000		HD 23480		0.9998	
HD 32991		0.6737		HD 217891			
HD 58050		0.9978		HD 138749		0.9936	
HD 164284		0.7826		HD 23630		0.9986	
HD 41335	1.0000			HD 209409		0.9954	
HD 52721		0.9767		HD 6811	1.0000		
HD 58343		0.9928		HD 192044		0.8070	
HD 148184		0.9396		HD 210129		0.8927	
HD 202904		0.9475		HD 142983	1.0000		
HD 65079	1.0000			HD 29866		1.0000	
HD 28497	1.0000			HD 47054		0.9086	
HD 45995	0.1169			HD 183914		0.9975	
HD 10516	0.9981			HD 50138			0.6758
HD 187567		0.9747		HD 58715		0.9189	
HD 191610		0.9990		HD 23552			1.0000
HD 32343		0.7793		HD 185037		0.9500	
HD 65875		1.0000		HD 199218		0.9693	
HD 60855	0.9800			HD 91120		0.9778	
HD 37490	1.0000			HD 142926	1.0000		
HD 50820		0.6221		HD 144	1.0000		

refers to the mean value extracted for each spectral subtype. Finally, the radial velocities of the emission component as a function of the respective rotational velocities are shown in figure 8.

The values that we calculated lie within a small range, and we can obtain only the mean values of the radial and rotational velocities and their standard deviations. The points in the diagrams correspond to the mean values of the velocities for each spectral subtype, and the error bars that appear in some of the diagrams to the standard deviation. This standard deviation is not only a statistical error, but it also includes any possible variation of the inclination axis and the error of the spectral classification, since the spectral classification that was based in the optical range could not be appropriate for the UV range. This means that the error bars that appear in the diagrams include the statistical error as well as the dispersion of the values due to a different axis inclination.

The reproduction of the Mg II resonance lines $\lambda\lambda$ 2795.523, 2802.698 Å, using the model where SACs are present, suggests that the atmospherical regions where the Mg II doublet is created may be described in a unique way for all of the

studied Be stars. This result confirms the suggestion given by de Jager et al. (1979) that in Be stellar atmospheres there exists a concentration of low-ionization species in the stellar wind, which is due to the occurrence of significant density variations. This result is also in agreement with the results of Morgan, Kondo, and Modisette (1977), who proposed that there are “significant absorption features” on the left side of each resonance line, which are attributed to “additional absorption within the stellar extended atmosphere”. These “significant absorption features” can be the SACs that appear in the spectra of the early-type stars. Danezis et al. (2003) and Lyrtzi and Danezis (2004) suggested that the peculiar phenomena observed in the spectra of Oe and Be stars, such as the SACs, are due to independent density regions in the stellar environment. Such regions may be structures that cover all, or a significant part, of the stellar disk (shells, blobs, puffs, and bubbles) (Underhill 1975; de Jager et al. 1979; Lamers et al. 1980; Henrichs 1984; Underhill & Fahey 1984; Bates & Halliwell 1986; Grady et al. 1987; Waldron et al. 1992; Cranmer & Owocki 1996; Kaper et al. 1996, 1997, 1999; Rivinius et al. 1997; Markova 2000), interaction

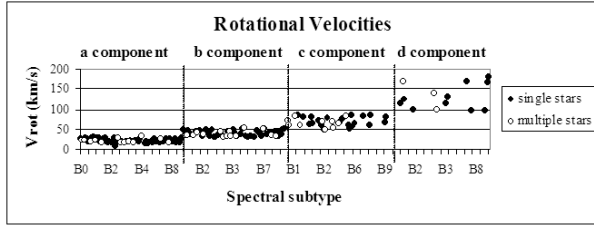


Fig. 4. Mean values for each spectral subtype of the rotational velocities of all the SACs as a function of the spectral subtype.

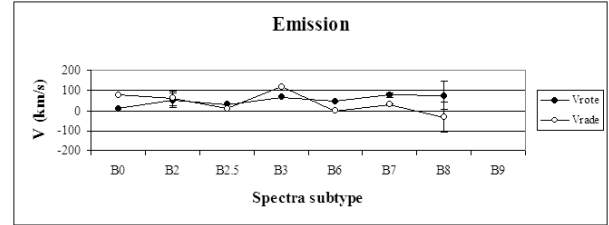


Fig. 7. Mean values for each spectral subtype of the rotational and radial velocities of the emission component as a function of the spectral subtype.

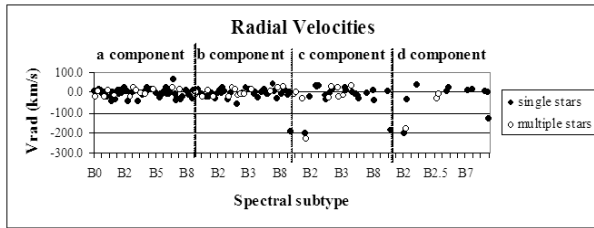


Fig. 5. Mean values for each spectral subtype of the radial velocities of all the SACs as a function of the spectral subtype.

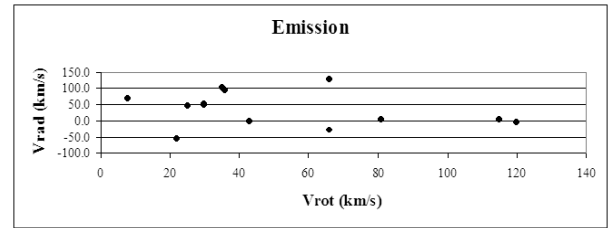


Fig. 8. Radial velocities of the emission component as a function of the respective rotational velocities.

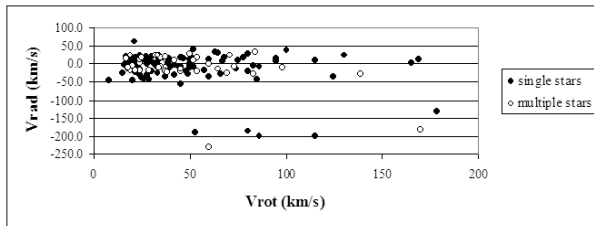


Fig. 6. Radial velocities of all the SACs as a function of the respective rotational velocities.

regions of fast and slow wind components, CIRs, structures due to magnetic fields or spiral streams as a result of the stellar rotation (Underhill & Fahey 1984; Mullan 1984a, 1984b, 1986; Prinja & Howarth 1988; Cranmer & Owocki 1996; Kaper et al. 1996, 1997, 1999; Fullerton et al. 1997; Cranmer et al. 2000). This is the common theory that explains the DAC phenomenon in early-type stars. We found DAC phenomena in early B-type stars (e.g., HD 45910), as well as in late B-type stars (e.g., HD 144).

As one can see from table 2, the SAC phenomenon appears to be a classical one for the Be stars. In figure 3 and in table 2 one can see that all of the studied stars present discernible (DACs) or indiscernible (SACs) components of the Mg II resonance lines. The indiscernible components appear in the spectra of all of the stars of luminosity classes IV and V, and most of the stars of luminosity class III. It is very interesting that the SACs are observed as discrete lines (DACs) in the spectra of the three stars, HD 193237 (B2 pe), HD 45910 (B2 III e), and HD 144 (B9 III e), because they present quite different radial shifts. This means that the regions that

create these lines move radially with relatively large velocities, producing lines shifted enough to be easily observed in the spectra. On the other hand, in the case of all of the other studied stars, the SACs of the Mg II resonance lines present similar radial velocities, resulting in the SACs being blended among themselves. In this case, we can distinguish these lines by systematic differentiations of the rotational velocities.

The decomposition of the observed profiles for the Mg II regions in Be stellar atmospheres confirms the existence of independent density regions, since by using such a structure, we were able to reproduce the resonance lines of Mg II in all of the studied stars. This decomposition is physically meaningful, since it enables us to detect kinematically different regions with different rotational and radial velocities, as well as the optical depth and the column density, for each of the Mg II independent density regions, which produce DACs or SACs.

Our analysis shows that regions where the considered Mg II resonance lines originate (“blobs” and “puffs” created by winds or cool extended envelopes) may consist of more independent density layers of matter with different kinematical properties (one to four in the analyzed cases). We identified them by the decomposition of observed Mg II lines in the number of components that best fit the observed profile. Namely, depending on particular stars, we obtained that SACs or DACs may be divided in several rotational velocity groups (average values for rotational velocity groups found to be present at 64 considered stars are $22 \pm 5 \text{ km s}^{-1}$, $41 \pm 7 \text{ km s}^{-1}$, $69 \pm 11 \text{ km s}^{-1}$, and $130 \pm 31 \text{ km s}^{-1}$). The corresponding radial velocities are near zero ($-3.3 \pm 20.3 \text{ km s}^{-1}$ for the first density region, $-3.6 \pm 20.6 \text{ km s}^{-1}$ for the second one, $-1.0 \pm 21.8 \text{ km s}^{-1}$ for the third one, and $+4.0 \pm 22.7 \text{ km s}^{-1}$ for the fourth one). In the spectra of the stars HD 193237 (B2 pe), HD 45910 (B2 III e), and HD 144 (B9 III e) the SACs appear as discrete components (DACs), and the radial velocities of the

third and the fourth density regions are $-205.7 \pm 21.7 \text{ km s}^{-1}$ and $-170.6 \pm 36.6 \text{ km s}^{-1}$, respectively. In the case of the star HD 144, the second component also appears as a discrete component. The radial velocity of the region that creates this component is -188.6 km s^{-1} (figures 4, 5, and 6). The observed velocity dispersion may be due to the different values of the rotational axis inclination of the regions where the SACs are created. The results presented above confirm that the Mg II doublet is more or less stable for a given spectral type as Gurzadyan (1975) suggested. We did not find any variation of the velocities in the Mg II regions with the luminosity class, except in the case of the peculiar stellar spectra, where the SACs appear as discrete lines (DACs), while Kondo, Morgan, and Modisette (1976) proposed that, apart from the difference among spectral subtypes, there is probably difference among luminosity classes too.

We assume that independent density regions corresponding to particular components of considered Mg II lines (one to four components corresponding to one to four regions in the case of 64 stars analyzed here) lie all in the cool stellar envelope. Depending on the temperature, different ions with different ionization potential are created in different regions at different distances from the star. This means that the spectral lines observed in the spectra of Be stars are derived from specific atmospherical regions, different among themselves. The ions that are created very close to the star lie in regions that present spherical symmetry around the star (case A in figure 1). On the other hand, the ions that are created at long distance from a star lie in regions that present spherical symmetry around their own center, and not around the star (case B in figure 1). As the ionization potential of the Mg II ions is $I.P.=7.646 \text{ eV}$, the Mg II ions can be created only at great distance from the center of the star, i.e., in the disk, where spherical symmetry around the star cannot be accepted. This means that the Mg II ions lie at regions which present topical or apparent spherical symmetry (case B in figure 1). As a result, the Mg II spectral lines and their SACs/DACs may be derived only from such regions (case B in figure 1), and not from classically spherical regions around the star (case A in figure 1). This kind of density regions (blobs) has been proposed by many researchers (Underhill 1975; de Jager et al. 1979; Lamers et al. 1980; Henrichs 1984; Underhill & Fahey 1984; Mullan 1984a, 1984b, 1986; Bates & Halliwell 1986; Grady et al. 1987; Prinja & Howarth 1988; Waldron et al. 1992; Cranmer & Owocki 1996; Kaper et al. 1996, 1997, 1999; Fullerton et al. 1997; Rivinius et al. 1997; Markova 2000; Cranmer et al. 2000) and are detected in many other cases, as in active stars (WR 104, see figure 2) and many quasars, as we observe DACs/SACs in their UV spectra (Danezis et al. 2006). This means that the density regions are a common phenomenon, observed at different levels. The fact that we found one to four components is accidental. In principle, there could be more or less. Although the number of components is different in different stars, we may conclude that the Mg II resonance lines forming regions present a complex structure.

Our proposition that the SAC phenomenon is responsible for the structure of Mg II lines means that we theoretically expect that the Mg II components have similar radial velocities, within the range of the statistical error ($\sim 10 \text{ km s}^{-1}$). The problem

was how to distinguish them. The common idea (Doazan 1982) is that the radial velocity of the kinematically independent regions is a function of the distance from the rapidly rotating Be star. Accordingly, our first thought was to distinguish these regions according to their rotational velocities, which was confirmed by our calculations. Namely, the regions that create the Mg II lines have similar radial velocities and different rotational velocities.

In our sample we could not detect high radial velocities, no matter what method we used (the proposed model or any other classical method). The radial velocities of all the SACs, in all the studied stars, are about 0 km s^{-1} , and only in the case of the stars HD 193237 (B2 pe), HD 45910 (B2 III e), and HD 144 (B9 III e), where we observed DACs, did we calculate radial velocities with values between -130 km s^{-1} and -230 km s^{-1} . We could detect the same phenomenon in the case of Si IV in a sample of 68 Be stars (values of radial velocities between -116 km s^{-1} and $+25 \text{ km s}^{-1}$) (Lyratzi et al. 2006), as well as in the case of H α in 120 Be stars (values of radial velocities around 0 km s^{-1}) (Lyratzi et al. 2005). These results indicate that in the atmospherical layers from the photosphere (very broad components of H α) to the cool envelope (Mg II resonance lines) we cannot detect very high radial velocities. However, as we expected, the presence of DACs in three stars of our sample indicated that from the regions near to the star toward the ones away from the star, the radial velocity increases, but it does not reach high values, as happens in the case of Oe stars. In the case of specific Be stars that present the DACs with high radial velocities in some of their spectra, e.g., 59 Cyg and γ Cas (Doazan et al. 1989; Telting & Kaper 1994), we should study each one of them as an exception of the classical rule. This proposition is based on the fact that the spectral classification was made in the optical range, and may not apply in the UV spectral range (Walborn 1971; Walborn & Panek 1984; Walborn & Nichols-Bohlin 1987) (see also the SIMBAD database⁴). This means that the spectral classifications in the optical and the UV ranges are not always in accord. As a result, some early Be stars could be late Oe stars, and we know that it is a common phenomenon to observe high radial velocities of SACs/DACs in Oe stars. However, in the case of Be stars, we have not observed the same phenomenon. This difference in the behavior of density regions in Oe and Be stars is very interesting and requires further investigation. Finally, we should pay attention to the way that the radial velocities are calculated. The classical method considered that the whole observed feature corresponds to only one spectral line, meaning that the radial velocity was calculated by the displacement of the deeper point of the observed feature. Considering the SAC idea, the observed feature consists of a number of spectral line components. As a result, the deeper point of the observed feature is only the result of the synthesis of all the SACs. In this case we should calculate the radial velocity of every one of these components.

An emission component is present in the spectra of B0, B2, B2.5, B3, B6, B7, B8, and B9 type stars (figure 7). This means that emission does not appear in the spectra of the middle spectral subtypes of Be stars (Kondo et al. 1975). The radial

⁴ (<http://simbad.u-strasbg.fr/sim-fid.pl>).

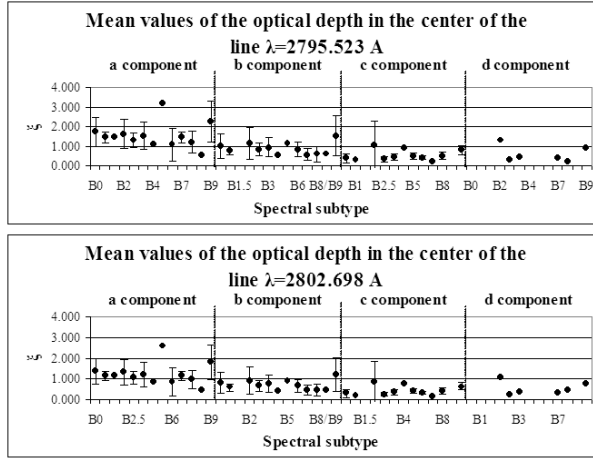


Fig. 9. Mean values of the optical depth, ξ , in the center of the line for all kinematically separated components of each resonance line, as a function of the spectral subtype.

velocity of the emission component decreases as the rotational velocity increases. The emission component presents positive or negative radial velocity. If one takes into account that negative radial velocities exist, which is not in agreement with the assumption that all emission components are the emission part of P Cygni profiles formed by scattering, one can assume the following. The obtained velocities correspond to the regions where the emission component is created as, e.g., strings, blobs, puffs, bubbles. This means that the emission region may approach, or move away from, the observer, and its different position and motion around the star is responsible for whether this value is positive or negative. In figures 7 and 8, one can see that as the rotational velocity increases the radial velocity decreases, in contrast to the relation of the two velocities of the absorption components. A problem with the emission component is that it is blended with the absorption lines of other ions, and thus it is difficult to evaluate the rotational and radial velocities. As a result, the calculated values present greater statistical error than in the case of the absorption components.

According to the criteria described in Danezis et al. (2003), the same components of the two resonance lines should have the same values of rotational and radial velocities and the ratio of the optical depth (ξ) should be the same as the respective ratio of the relative intensities. In figure 9, we present the mean values of the optical depth (ξ) in the center of the line for all kinematically separated components of each resonance line, as a function of the spectral subtype. As one can see, the value of ξ of the first kinematical region is obviously higher than in the other three. It tends to decrease from the first kinematical region to the fourth. That, also, may indicate physically separated regions.

5. Conclusions

We applied a method developed in Danezis et al. (2003) and Lyrtzi and Danezis (2004) to the Mg II resonance line of 64 Be stars in order to investigate the kinematical

properties of the Mg II resonance line forming region. We obtained the rotational and radial velocities, which allowed us to extract some general physical properties concerning the Mg II regions of Be stars. Some interesting results inferred from the investigations are the following: (i) The proposed rotation model gives satisfactory results for the region of the Mg II $\lambda\lambda$ 2795.523, 2802.698 Å resonance lines. (ii) The atmospherical absorption region where the Mg II resonance lines are created presents a complex structure. It tends to be composed by more than one kinematically independent region (only four stars present a simple structure). We found that the kinematically independent regions rotate with different velocities: 22 km s⁻¹, 41 km s⁻¹, 69 km s⁻¹, and 130 km s⁻¹. The respective radial velocities are near to zero for all of these regions. These calculated values lead us to accept that the Mg II resonance lines of the Be stellar spectra present Satellite Absorption Components (SACs). (iii) The rotational velocities of the found independent regions present a uniform fluctuation with the spectral subtype. (iv) The emission lines were detected for the earliest and latest spectral subtypes with positive radial velocities with several exceptions; i.e., they have negative radial velocities ranging from 0 to -87 km s⁻¹. If lines are formed by scattering, the positive values are not radial velocities.

This research project is progressing at the University of Athens, Department of Astrophysics, Astronomy and Mechanics, under the financial support of the Special Account for Research Grants, for which we give much thanks. This work was also supported by the Ministry of Science and Environment Protection of Serbia, through the projects, Influence of collisional processes on astrophysical plasma line shapes and Astrophysical spectroscopy of extragalactic objects. Finally, we thank an anonymous referee for his/her very useful comments.

Appendix. Calculation of the Distribution Function L

As we know, the distribution function (L) of the absorption coefficient (k_λ) has the same form as the distribution function of each component of the spectral line. This means that we can replace the distribution function of the absorption coefficient, L_i , with another expression for the distribution function of each component.

It is also known that Be and Oe stars are rapid rotators. This means that we accept that the main reason for the line broadening is rotation of the regions that produce each satellite component of the whole observed spectral feature. These rapidly rotating density regions may also present radial motion. For these two reasons, we seek another expression for the distribution function of the spectral line's components that has as parameters the rotational and radial velocities of the spherical density regions.

For a spherical density region, we assume the following hypotheses: i) the natural broadening of the spectral lines follows the Lorentz distribution; ii) Lambert's sinus law stands for each point of the spherical region; iii) the angular velocity of rotation is constant.

In order to calculate the total radiation, we divide the

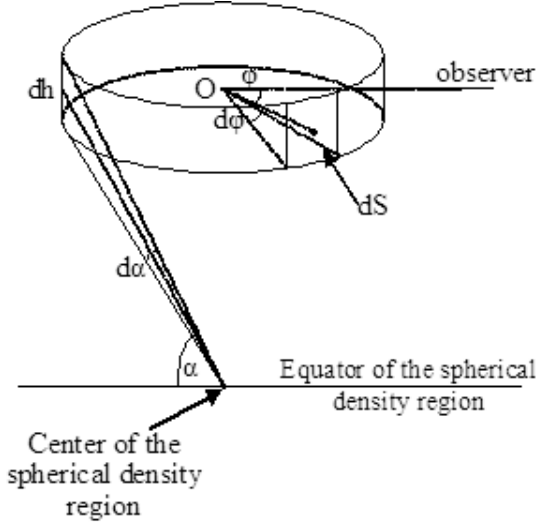


Fig. 10. Elementary ring of the spherical density region.

spherical layer in very thin cylindrical surfaces that are perpendicular to the rotational axis. Lambert's law allows us to consider that the luminosity from each point on the sphere is the same.

On the above cylindrical surface we also consider the surface dS . According to Lambert's law, when this surface rotates with an angular velocity ω , its radiation intensity is

$$dI(\omega) = Q(\omega)dS \cos \theta, \quad (\text{A1})$$

where θ is the angle between the vertical on dS and the line of sight and

$$Q(\omega) = C_1 \frac{\gamma}{(\omega - \omega_k)^2 + \left(\frac{\gamma}{2}\right)^2}. \quad (\text{A2})$$

C_1 is a constant and γ is the Lorentzian full width at half maximum, which in the case of natural broadening has a value of $\gamma \cong 10^8$ Hz.

When the surface dS does not rotate, the center of the formed spectral line has the observed wavelength, λ_0 , which corresponds to a frequency, ν_0 . Thus,

$$\omega_0 = 2\pi\nu_0 = 2\pi \frac{c}{\lambda_0}. \quad (\text{A3})$$

When the surface dS rotates with a rotational velocity V_{rot} , the center of the formed line has the wavelength λ_k , and in this case $\omega_k = \omega_0(1 - z \sin \varphi)$, where $z = V_{\text{rot}}/c$.

We also have $\cos \theta \cong \cos \alpha \cos \varphi$. The angles α and φ are shown in figure 10.

The surface dS can be written as $dS = rdh d\varphi$, where r is the radius of the cylinder, $d\varphi$ the angle under which the observer sees dS , and dh the height of dS .

Making the above substitutions in equation (A1), we have

$$dI(\omega) = \frac{C_1 r dh \gamma \cos \alpha \cos \varphi d\varphi}{[\omega - \omega_0(1 - z \sin \varphi)]^2 + \left(\frac{\gamma}{2}\right)^2}. \quad (\text{A4})$$

Thus, the radiation intensity from the semicylinder is

$$I(\omega) = \int_{-\pi/2}^{\pi/2} \frac{C_1 r dh \gamma \cos \alpha \cos \varphi d\varphi}{[\omega - \omega_0(1 - z \sin \varphi)]^2 + \left(\frac{\gamma}{2}\right)^2} \quad (\text{A5})$$

or

$$I(\omega) = \frac{4C_1 r dh}{\gamma} \times \int_{-\pi/2}^{\pi/2} \frac{\cos \alpha d(\sin \varphi)}{\{[\omega/(\gamma/2)] - [\omega_0/(\gamma/2)](1 - z \sin \varphi)\}^2 + 1}. \quad (\text{A6})$$

If we take that $\tilde{\omega} = \omega/(\gamma/2)$, $\tilde{\omega}_0 = \omega_0/(\gamma/2)$, $x = \sin \varphi$, we have

$$I(\tilde{\omega}) = \frac{4C_1 r \cos \alpha dh}{\gamma} \int_{-1}^1 \frac{dx}{[\tilde{\omega} - \tilde{\omega}_0(1 - zx)]^2 + 1}. \quad (\text{A7})$$

Taking that $y = \tilde{\omega} - \tilde{\omega}_0(1 - zx)$, the above integral becomes

$$I(\tilde{\omega}) = \frac{4C_1 r \cos \alpha dh}{\gamma \tilde{\omega}_0 z} \int_{\tilde{\omega} - \tilde{\omega}_0(1+z)}^{\tilde{\omega} - \tilde{\omega}_0(1-z)} \frac{dy}{y^2 + 1}. \quad (\text{A8})$$

Finally, we have

$$I(\tilde{\omega}) = \left(\frac{4C_1 r \cos \alpha dh}{\gamma} \right) \times \left(\frac{\arctan[\tilde{\omega} - \tilde{\omega}_0(1 - z)] - \arctan[\tilde{\omega} - \tilde{\omega}_0(1 + z)]}{\tilde{\omega}_0 z} \right). \quad (\text{A9})$$

The above function describes the radiation intensity from a visual semicylinder with radius r and height dh .

Under the angle $d\alpha$ is seen dh from the center of the spherical region. This cylinder rotates with a rotational velocity, $z = V_{\text{rot}}/c$, and a constant angular velocity, $\tilde{\omega}$.

We consider the function

$$P(\tilde{\omega}, z) = \frac{\arctan[\tilde{\omega} - \tilde{\omega}_0(1 - z)] - \arctan[\tilde{\omega} - \tilde{\omega}_0(1 + z)]}{\tilde{\omega}_0 z}. \quad (\text{A10})$$

We study the limit of this function in the case that the density layer does not rotate, i.e., when $z \rightarrow 0$. In such a case,

$$\lim_{z \rightarrow 0} P(\tilde{\omega}, z) = \lim_{z \rightarrow 0} \frac{\arctan[\tilde{\omega} - \tilde{\omega}_0(1 - z)] - \arctan[\tilde{\omega} - \tilde{\omega}_0(1 + z)]}{\tilde{\omega}_0 z}. \quad (\text{A11})$$

We apply L' Hospital's theorem and we obtain

$$\lim_{z \rightarrow 0} P(\tilde{\omega}, z) = \lim_{z \rightarrow 0} \frac{\frac{d}{dz} \{\arctan[\tilde{\omega} - \tilde{\omega}_0(1 - z)]\} - \frac{d}{dz} \{\arctan[\tilde{\omega} - \tilde{\omega}_0(1 + z)]\}}{\frac{d}{dz} (\tilde{\omega}_0 z)}, \quad (\text{A12})$$

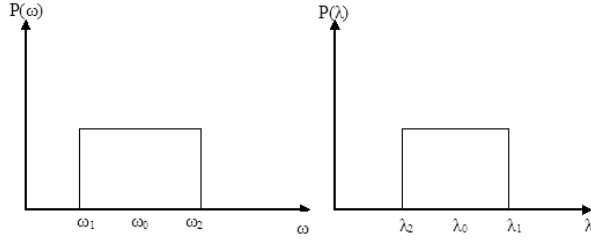


Fig. 11. Quadratic pulsation.

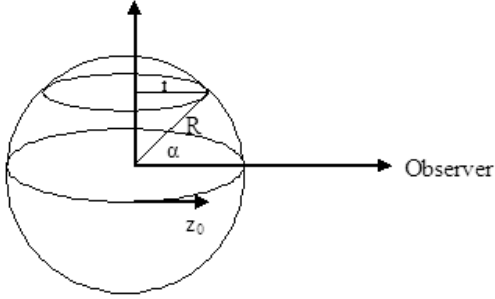


Fig. 12. Rotating spherical density region that produces SACs or DACs.

$$\begin{aligned} \lim_{z \rightarrow 0} P(\tilde{\omega}, z) &= \lim_{z \rightarrow 0} \left[\frac{1}{1 + [\tilde{\omega} - \tilde{\omega}_0(1 - z)]^2} + \frac{1}{1 + [\tilde{\omega} - \tilde{\omega}_0(1 + z)]^2} \right] \\ &= \frac{2}{(\tilde{\omega} - \tilde{\omega}_0)^2 + 1}. \end{aligned} \quad (\text{A13})$$

It is obvious that in the nonrotating case this form corresponds to the Lorentz's distribution for the naturally broadened spectral lines.

In the case where the rotation broadening, $|\lambda_1 - \lambda_2|$ (or $|\omega_1 - \omega_2|$), is much larger than the natural broadening (the natural broadening of a spectral line is of an order of 10^{-3} – 10^{-4} Å), the above function, $P(\tilde{\omega}, z)$, presents the form of one quadratic pulsation (see figure 11)

For each ω with $\omega_1 < \omega < \omega_2$, the relative shift is $z = |\Delta\omega|/\omega_0$. For a point ω_1 we have $(\omega_0 - \omega_1)/\omega_0 = z$, so that $\omega_1 = \omega_0(1 - z)$. Likewise, for a point ω_2 we have $\omega_2 = \omega_0(1 + z)$. But, $\omega = 2\pi\nu = 2\pi c/\lambda$. Thus, $\lambda_1 = \lambda_0/(1 - z)$ and $\lambda_2 = \lambda_0/(1 + z)$ with $\lambda_1 > \lambda_2$.

This means that $\Delta\lambda_{\text{total}} \equiv \lambda_1 - \lambda_2 = 2\lambda_0 z/(1 - z^2)$ and so $\lambda_{\text{min}} \equiv \lambda_2 = \lambda_0 - \Delta\lambda_{\text{total}}/2 = \lambda_0 - \lambda_0 z/(1 - z^2)$ and $\lambda_{\text{max}} \equiv \lambda_1 = \lambda_0 + \Delta\lambda_{\text{total}}/2 = \lambda_0 + \lambda_0 z/(1 - z^2)$.

We set $\rho = \lambda_0 z/(1 - z^2)$ and normalize to 1. In this way, the function $P(\tilde{\omega}, z)$ could be approximated by the function $f(\lambda)$ where:

$$f(\lambda) = \begin{cases} 1 & |\lambda - \lambda_0| < \rho \\ 0 & \text{otherwise} \end{cases}. \quad (\text{A14})$$

We now assume that the spherical density region rotates with equatorial velocity $z_0 = V_0/c$ (figure 12).

The points of the circle with radius r rotate with a velocity V_{rot} and for $r = R \cos \alpha$ we take $V_{\text{rot}} = \omega r = \omega R \cos \alpha$.

We set $V_0 = \omega R$. Also, $\omega = \text{const}$. Thus, $V_{\text{rot}} = (V_0/R) R \cos \alpha = V_0 \cos \alpha$ and $z = z_0 \cos \alpha$. We also have $dh = R d\alpha$ and equation (A1) becomes

$$\begin{aligned} dI(\tilde{\omega}) &= \frac{4C_1 R}{\gamma} \\ &\times \frac{\arctan[\tilde{\omega} - \tilde{\omega}_0(1 - z_0 \cos \alpha)] - \arctan[\tilde{\omega} - \tilde{\omega}_0(1 + z_0 \cos \alpha)]}{\tilde{\omega}_0 z_0 \cos \alpha} \\ &\times \cos \alpha d\alpha. \end{aligned} \quad (\text{A15})$$

The integral of this equation is

$$\begin{aligned} I(\tilde{\omega}) &= \frac{4C_1 R}{\gamma} \\ &\times \int_{-\pi/2}^{\pi/2} \frac{\arctan[\tilde{\omega} - \tilde{\omega}_0(1 - z_0 \cos \alpha)] - \arctan[\tilde{\omega} - \tilde{\omega}_0(1 + z_0 \cos \alpha)]}{\tilde{\omega}_0 z_0 \cos \alpha} \\ &\times \cos \alpha d\alpha. \end{aligned} \quad (\text{A16})$$

When we take into account the function $P(\tilde{\omega}, z)$, the above function becomes

$$I(\tilde{\omega}) = \frac{4C_1 R}{\gamma} \int_{-\pi/2}^{\pi/2} P(\tilde{\omega}, z_0 \cos \alpha) \cos \alpha d\alpha. \quad (\text{A17})$$

We approximate $P(\tilde{\omega}, z_0 \cos \alpha)$ at $f(\lambda)$ and take the integral for the observation angle $\theta \in [-\theta_0, \theta_0]$ from the equatorial plane.

We have

$$I(\tilde{\omega}) \cong I_1 = \frac{4C_1 R}{\gamma} \int_{-\theta_0}^{\theta_0} 1 \cdot \cos \theta d\theta, \quad (\text{A18})$$

$$I_1 = \frac{4C_1 R}{\gamma} \int_{-\theta_0}^{\theta_0} \cos \theta d\theta = \frac{4C_1 R}{\gamma} [\sin \theta]_{-\theta_0}^{\theta_0} = \frac{8C_1 R}{\gamma} \sin \theta_0. \quad (\text{A19})$$

If we normalize the constant, we have

$$I_1 = \sin \theta_0 = \sqrt{1 - \cos^2 \theta_0}. \quad (\text{A20})$$

For angle θ_0 we have

$$|\lambda - \lambda_0| \leq \rho = \frac{\lambda_0 z_0 \cos \theta_0}{1 - z_0^2 \cos^2 \theta_0}. \quad (\text{A21})$$

For a wavelength λ or for a shift of $\Delta\lambda = |\lambda - \lambda_0|$ from the center of the spectral line, the absorbing (or emitting) regions are those with angular distance θ from the equatorial plane, with $|\theta| \leq \theta_0$.

For the equatorial plane we have

$$\Delta\lambda = \frac{\lambda_0 z_0 \cos \theta_0}{1 - z_0^2 \cos^2 \theta_0}. \quad (\text{A22})$$

From this equation we can calculate the angle θ_0 as

$$\cos \theta_0 = \frac{-\lambda_0 \pm \sqrt{\lambda_0^2 + 4\Delta\lambda^2}}{2\Delta\lambda z_0}. \quad (\text{A23})$$

Since θ_0 is between $-\pi/2$ and $\pi/2$, we have $\cos \theta_0 \geq 0$, and so

$$\cos \theta_0 = \frac{-\lambda_0 + \sqrt{\lambda_0^2 + 4\Delta\lambda^2}}{2\Delta\lambda z_0}. \quad (\text{A24})$$

Thus, the distribution function I_1 takes its final form:

$$I_1 = \sqrt{1 - \cos^2 \theta_0} \quad \text{if} \quad \cos \theta_0 = \frac{-\lambda_0 + \sqrt{\lambda_0^2 + 4\Delta\lambda^2}}{2\Delta\lambda z_0} < 1 \quad (\text{A25})$$

and

$$I_1 = 0 \quad \text{otherwise.} \quad (\text{A26})$$

It is obvious that the distribution function I_1 is a function of the wavelength (λ). This means that $I_1 = I_1(\lambda)$. This distribution function has the same form as the distribution function of the absorption coefficient, L , and may replace it (in $e^{-L\xi}$), when the main reason of the line broadening is rotation. We name it the rotation distribution function.

The spectral line profile, which is formed by a spherical density region, is reproduced by the function $e^{-L\xi}$ by applying an appropriate value of the rotational velocity, V_{rot} (from z_0), the radial velocity, V_{rad} [from $V_{\text{rad}}/c = (\lambda_0 - \lambda_{\text{lab}})/\lambda_{\text{lab}}$], and the optical depth, ξ , in the center of the line.

References

- Bates, B., & Halliwell, D. R. 1986, MNRAS, 223, 673
 Cidale, L. S. 1998, ApJ, 502, 824
 Cowley, A. 1972, AJ, 77, 750
 Cowley, A., Cowley, C., Jaschek, M., & Jaschek, C. 1969, AJ, 74, 375
 Cranmer, S. R., & Owocki, S. P. 1996, ApJ, 462, 469
 Cranmer, S. R., Smith, M. A., & Robinson, R. D. 2000, ApJ, 537, 433
 Dachs, J. 1980, Second European IUE Conf. (ESA SP-157), (Paris: ESA), 139
 Danezis, E. 1983, PhD Thesis, University of Athens
 Danezis, E. 1987, in Physics of Be Stars, ed. A. Slettebak & T. P. Snow (Cambridge: Cambridge University Press), 445
 Danezis, E., et al. 2003, Ap&SS, 284, 1119
 Danezis, E., Popović, L. Č., Lyrtzi, E., & Dimitrijević, M. S. 2006, in The Physics of Ionized Gases, ed. L. Hadzievski, B. Marinkovic, & N. Simonovic (AIP), 373
 Danezis, E., Theodossiou, E., & Laskarides, P. G. 1991, Ap&SS, 179, 111
 de Jager, C., Kondo, Y., Hoekstra, R., van der Hucht, K. A., Kamperman, T. M., Lamers, H. J. G. L. M., Modisette, J. L., & Morgan, T. H. 1979, ApJ, 230, 534
 Doazan, V. 1982, in B Stars With and Without Emission Lines, ed. A. Underhill & V. Doazan (Washington, D. C. : NASA), 279
 Doazan, V., Barylak, M., Rusconi, L., Sedmak, G., Thomas, R. N., & Bourdonneau, B. 1989, A&A, 210, 249
 Doazan, V., Sedmak, G., Barylak, M., & Rusconi, L. 1991, A Be Star Atlas of Far UV and Optical High-Resolution Spectra (ESA SP-1147), (Noordwijk: ESA Publications Division)
 Doazan, V., & Thomas, R. N. 1982, in B Stars With and Without Emission Lines, ed. A. Underhill & V. Doazan (Washington, D. C. : NASA), 409
 Fullerton, A. W., Massa, D. L., Prinja, R. K., Owocki, S. P., & Cranmer, S. R. 1997, A&A, 327, 699
 Grady, C. A., Sonneborn, G., Wu, C.-C., & Henrichs, H. F. 1987, ApJS, 65, 673
 Guetter, H. H. 1968, PASP, 80, 197
 Gurzadyan, G. A. 1975, PASP, 87, 289
 Henrichs, H. F. 1984, Fourth European IUE Conf. (ESA SP-218), (Noordwijk: ESA), 43
 Herbig, G. H., & Spalding, J. F., JR. 1955, ApJ, 121, 118
 Houk, N., & Smith-Moore, M. 1988, Michigan Catalogue of Two-Dimensional Spectral Types for HD Stars, vol.4
 Houziaux, L., & Andriolat, Y. 1976, IAU Symp., 70, 87
 Hutsemekers, D. 1985, A&AS, 60, 373
 Kaper, L., et al. 1997, A&A, 327, 281
 Kaper, L., Henrichs, H. F., Nichols, J. S., Snoek L. C., Volten, H., & Zwarthoed G. A. A. 1996, A&AS, 116, 257
 Kaper, L., Henrichs, H. F., Nichols, J. S., & Telting, J. H. 1999, A&A, 344, 231
 Kelly, R. L. 1979, Atomic Emission Lines in the Near Ultraviolet (NASA TM 80268), (Washington, D. C. : NASA)
 Kondo, Y., Modisette, J. L., & Wolf, G. W. 1975, ApJ, 199, 110
 Kondo, Y., Morgan, T. H., & Modisette, J. L. 1976, ApJ, 209, 489
 Lamers, H. J. G. L. M., Faraggiana, R., & Burger, M. 1980, A&A, 82, 48
 Laskarides, P. G., Theodossiou, E., & Danezis, E. 1992, Ap&SS, 179, 13
 Lesh, J. R. 1968, ApJS, 17, 371
 Lyrtzi, E., & Danezis, E. 2004, AIP Conf. Proc., 740, 458
 Lyrtzi, E., Danezis, E., Antoniou, A., Nikolaidis, D., Popović, L. Č., & Dimitrijević, M. S. 2006, IAU Joint Discussion 4
 Lyrtzi, E., Danezis, E., Nikolaidis, D., Popović, L. Č., Dimitrijević, M. S., Theodossiou, E., & Antoniou, A. 2005, Mem. Soc. Astron. Ital. Suppl., 7, 114
 Lyrtzi, E., Danezis, E., Stathopoulou, M., Theodossiou, E., Nikolaidis, D., Drakopoulos, C., & Soulikias, A. 2003, Publ. Astron. Obs. Belgrade, 76, 27
 Markova, N. 2000, A&AS, 144, 391
 Marlborough, J. M., Snow, T. P., JR., & Slettebak, A. 1978, ApJ, 224, 157
 Moore, C. E. 1968, National Bureau of Standard Circ., 488
 Morgan, T. H., Kondo, Y., & Modisette, J. L. 1977, ApJ, 216, 457
 Morgan, W. W., Code, A. D., & Whitford, A. E. 1955, ApJS, 2, 41
 Mullan, D. J. 1984a, ApJ, 283, 303
 Mullan, D. J. 1984b, ApJ, 284, 769
 Mullan, D. J. 1986, A&A, 165, 157
 Osawa, K. 1959, ApJ, 130, 159
 Peton, A. 1974, Space Sci. Rev., 30, 481
 Popović, L. Č., et al. 2004, AIP Conf. Proc., 740, 497
 Prinja, R. K., & Howarth, I. D. 1988, MNRAS, 233, 123
 Rivinius, T., et al. 1997, A&A, 318, 819
 Sahade, J., & Brandi, E. 1985, Rev. Mex. Astron. Astrofis., 10, 229
 Sahade, J., Brandi, E., & Fontenla, J. M. 1984, A&AS, 56, 17
 Slettebak, A. 1954, ApJ, 119, 146
 Slettebak, A., & Snow, T. P., JR. 1978, ApJ, 224, L127
 Smith, M. A. 2001, PASP, 113, 882
 Telting, J. H., & Kaper, L. 1994, A&A, 284, 515
 Tuthill, P. G., Monnier, J. D., & Danchi, W. C. 1999, Nature, 398, 487

- Underhill, A. B. 1970, in Spectrum Formation in Stars With Steady-State Extended Atmospheres, ed. H. G. Groth & P. Wellman (Washington, D. C. : National Bureau of Standards), 3
- Underhill, A. B. 1975, ApJ, 199, 691
- Underhill, A. B., & Fahey, R. P. 1984, ApJ, 280, 712
- Walborn, N. R. 1971, ApJS, 23, 257
- Walborn, N. R., & Nichols-Bohlin, J. 1987, PASP, 99, 40
- Walborn, N. R., & Panek, R. J. 1984, ApJ, 280, L27
- Waldron, W. L., Klein, L., & Altner, B. 1992, ASP Conf. Ser., 22, 181

The Peculiar Absorption And Emission Phenomena From Stars To Quasars

E. Danezis¹, L. Č. Popović², E. Lyratzi¹, M. S. Dimitrijević²

1. University of Athens, Faculty of Physics, Department of Astrophysics, Astronomy and Mechanics,
Panepistimioupoli, Zographou 157 84, Athnes – Greece

2. Astronomical Observatory, Volgina 7, 11160 Belgrade, Serbia

Abstract. The spectra of Hot Emission Stars and AGNs present peculiar profiles that result from dynamical processes such as accretion and/or ejection of matter from these objects. In this paper we analyze DACs and SACs phenomena, which indicate the existence of layers of matter with different physical conditions and we propose that these phenomena can explain the spectral lines peculiarity in Hot Emission Stars and AGNs. We also propose a new model with which we can study the density regions in the plasma surrounding the studied objects, where DACs and SACs of a spectral line are created producing the observed peculiar profiles. Finally, we present some tests to justify the proposed model.

Keywords: Hot Emission Stars, AGNs, DACs, SACs.

PACS: 97.10.Ex, 97.10.Fy, 97.20.Ec, 97.30.Eh, 98.54.Aj

THE SPECTRAL LINES IN ASTROPHYSICAL OBJECTS

It is well known that the absorption spectral lines that we can detect in the spectra of normal stars are an important factor to study physical parameters stellar atmospheres.

In the classical stellar spectra we observe “normal” absorption lines (Fig. 1). However, in the spectra of hot emission stars (Oe and Be stars) we observe spectral lines with complex and peculiar profiles (combination of absorption and emission spectral lines, e.g. P Cygni profiles etc., Fig. 2). The same phenomena also occur in the case of galactic spectra. This means that “normal” galaxies present spectra without emission lines, which are composed spectra of stars from the galaxy. In contrary Active Galactic Nuclei (AGNs) present emission lines ($H\alpha$, $H\beta$) like active Oe and Be stars (Fig. 3). The peculiar lines are always characteristic of the objects with very dynamical processes (accretion, jets, winds etc.). For example, in the case of stars, the peculiar spectral profiles are created in density regions of matter that we can detect quite away from the stellar object (Fig. 4), while in the case of AGNs, accretion, wind (jets, ejection of matter etc.), Broad Line Regions (BLR) and Narrow Line Regions (NLR) are responsible for the construction of the observed peculiar profiles of the spectral lines (Fig. 5).

The spectral lines of hot emission stars and AGNs may be very broad and satellite lines may appear (Fig. 6). An answer for the origin of satellite lines is the matter that exists between the observer and an object (Fig. 7).

Main Sequence B5 – A5

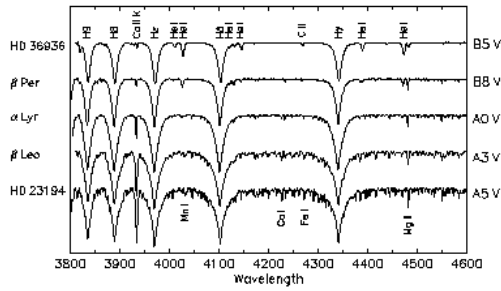


FIGURE 1. Classical Stellar Spectra for different spectral subtype.

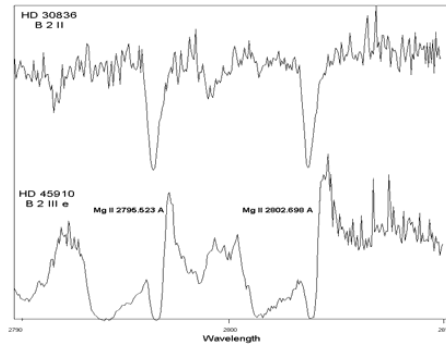


FIGURE 2. Comparison of Mg II resonance lines between the spectrum of a “normal” B star and the spectrum of an active Be star that presents complex and peculiar spectral lines. The combination of an emission and some absorption components construct the P Cygni profile.

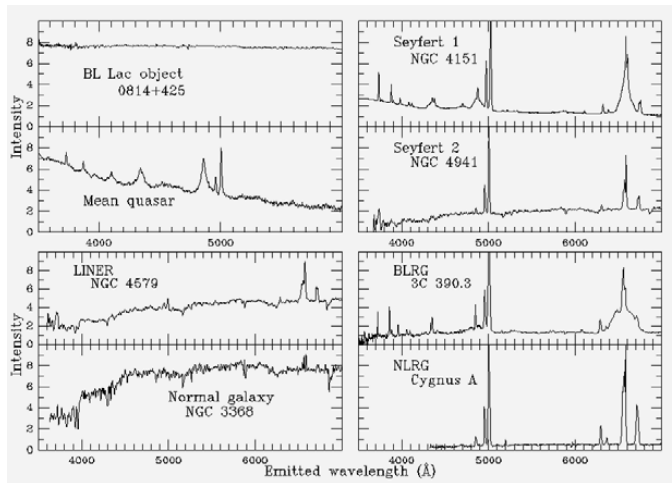


FIGURE 3. Spectra of different types of AGNs.

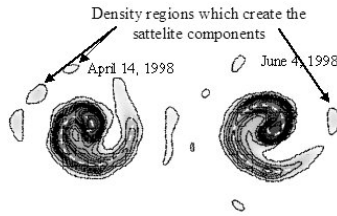


FIGURE 4. Around a Wolf-Rayet star (WR 104) we can detect density regions of matter quite away from the stellar object, able to produce peculiar profiles. (This figure is taken by Tuthill, Monnier & Danchi [1] with Keck Telescope.).

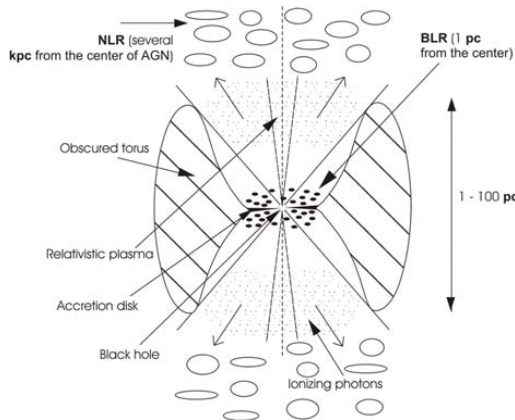


FIGURE 5. In the case of AGNs, accretion, wind (jets, ejection of matter etc.), BLR (Broad Line Regions) and NLR (Narrow Line Regions) are the density regions that construct peculiar profiles of the spectral lines.

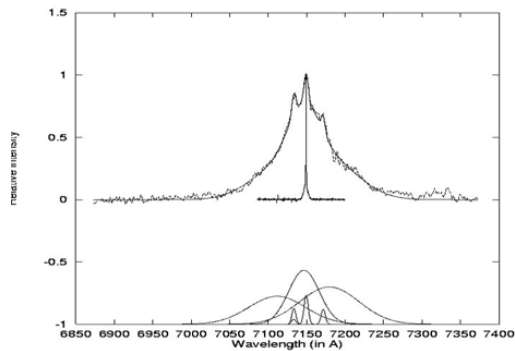


FIGURE 6. Comparison between the observed H α line of an AGN (III Zw2) with the same line obtained from laboratory plasma. This spectral line is blended with two [NII] satellite lines. The line broadening is a kinematical effect (radial, rotational and random velocities) that arises from the geometry of the emitting region.

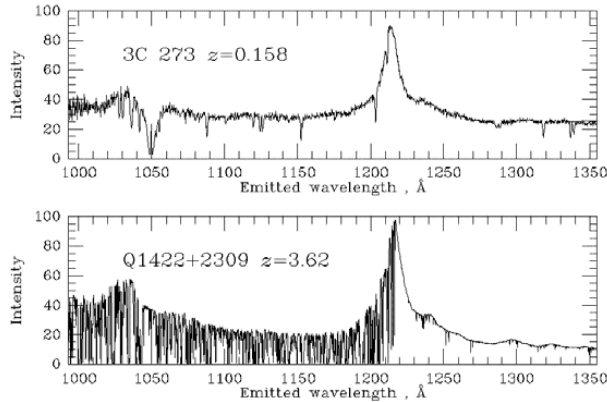


FIGURE 7. Difference between absorption lines in quasar spectra: The absorption lines which are created in the heart of a quasar (up) in comparison with the absorption that can be constructed by matter located between an observer and the quasar.

A MODEL FOR THE REPRODUCTION OF PECULIAR SPECTRAL LINE PROFILES

There are some models to reproduce the observed peculiar profiles in hot emission stars and AGNs. These are several Non-LTE models, which give bad reproduction and several Non-LTE specialized models (e.g. PHOENIX), having very complicated codes that may reproduce the peculiar profiles, but only in some cases.

In order to explain the peculiar profile that we observe in the spectra of hot emission stars and AGNs, Danezis et al. [2, 3] proposed a simple model that is able to explain the structure of the regions that produce these spectral lines. We point out that with this model we can study and reproduce specific spectral lines. This means that we can study specific density regions in the plasma surrounding the studied objects. In order to construct a general model we need to study a number of density regions which produce spectral lines of different ionization potential, meaning different temperature and thus different distance from the studied object.

In order to explain simply our model, we need to explain two similar phenomena, the DACs and SACs phenomena, able to construct peculiar spectral line profiles in some Hot Emission Stars and AGNs.

The DACs Phenomenon

In a stellar atmosphere or disc that we can detect around hot emission stars, an absorption line can be produced in several regions that present the same temperature. From each one of these regions an absorption line arises.

The line profile of each one of these absorption components is a function of a group of physical parameters, as the radial, the rotational, the random velocities and the optical depth of the region that produces the specific components of the spectral line. These spectral lines were named Discrete Absorption Components (DACs) [4].

DACs are discrete but not unknown absorption spectral lines. They are spectral lines of the same ion and the same wavelength as a main spectral line, shifted at different $\Delta\lambda$, as they are created in different density regions which rotate and move radially with different velocities [2]. DACs are lines, easily observed, in the spectra of some Be stars, because the regions that give rise to such lines, rotate with low velocities and move radially with high velocities (Fig. 8).

It is very important to point out that we can detect the same phenomenon in the spectra of AGNs, so called Broad Absorption Line Quasars (BAL QSOs). In Fig. 9 one can see the C IV UV doublet of the BAL QSO PG 0946+301.

From the values of radial displacements and the ratio of the line intensities we can detect that the two observed C IV shapes indicate the presence of a DACs phenomenon similar to the DACs phenomenon that we can detect in the spectra of hot emission stars.

The SACs Phenomenon

However, if the regions that give rise to such lines rotate with large velocities and move radially with small velocities, the produced lines have large widths and small shifts. As a result they are blended among themselves as well as with the main spectral line and thus they are not discrete. In such a case the name Discrete Absorption Component is inappropriate and we use only the name Satellite Absorption Components (SACs) [3].

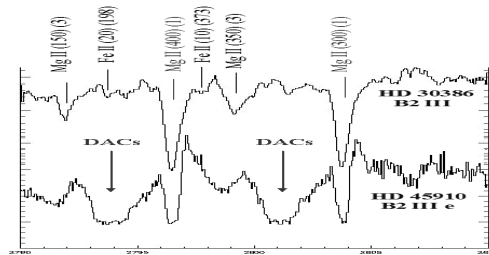


FIGURE 8 Mg II doublet in the UV spectrum of AX Mon, compared with the Mg II lines of the classic B2 star HD30386. In these line profiles we can see the main spectral line and in the left of each one of them a group of DACs.

FIGURE 9. C IV UV doublet of the quasar PG 0946+301. We can detect that the two observed C IV shapes indicate the presence of a DACs phenomenon similar to the DACs phenomenon that we can detect in the spectra of hot emission star.

Calculation Of The Peculiar Line Shapes

In the case of SACs phenomenon we need to calculate the line function of the complex line profile.

Recently Danezis et al. [2, 3] proposed a model in order to explain the complex structure of the density regions of hot emission stars and some AGNs, where the spectral lines that present SACs or DACs are created.

The main hypothesis of this model is that the stellar envelope is composed of a number of successive independent absorbing density layers of matter, a number of emission regions and an external general absorption region. By solving the radiation transfer equations through a complex structure, (in more details see [2, 3]) we obtained a function for the line profile, able to give the best fit for the main spectral line and its Satellite Components at the same time:

$$I_{\lambda} = \left[I_{\lambda 0} \prod_i e^{-\tau_{ai}} + \sum_j S_{\lambda ej} (1 - e^{-\tau_{ej}}) \right] e^{-\tau_g} \quad (1)$$

where: $I_{\lambda 0}$: is the initial radiation intensity, $S_{\lambda ej}$ is the source function, which, at the moment when the spectrum is taken, is constant and τ is the optical depth in the center of the considered component.

In Eq. (1), the functions $e^{-\tau_{ai}}$, $S_{\lambda ej} (1 - e^{-\tau_{ej}})$ and $e^{-\tau_g}$ are the distribution functions of each satellite component and we can replace them with a known distribution function (Gauss, Lorentz, Voigt).

An important fact is that in the calculation of I_{λ} we can include different geometries (in the calculation of τ) of the absorbing or emitting independent density layers of matter.

The decision on the geometry is essential for the calculation of the distribution function that we use for each component. This means that for different geometries we have different line shapes, presenting the considered SACs.

In the case of rapidly rotating hot emission stars, it is very important to insert in the line function (Eq. 1) the rotational, radial and random velocities of the regions which produce the satellite components. In this case we have to assume the geometry for the corresponding regions.

The Spherical Symmetry Hypothesis

In order to assume the appropriate geometry we took into account the following important facts:

The spectral line profile was reproduced in the best way when one assumes spherical symmetry for the independent density regions. Such symmetry has been proposed by many researchers [5-11].

However, the independent layers of matter, where a spectral line and its SACs are born, could lie either close to the star, as in the case of the photospheric components of the H α line in Be stars [12, 13], when spherical symmetry is justified, or at a larger distance from the star, where the spherical symmetry can not be justified.

These lead us to conclude that:

1. In the case of independent density layers of matter which lie close to the star we could suppose the existence of a classical spherical symmetry around the star [5-11].
2. In the case of independent density layers of matter which lie at a larger distance from the photosphere, we could suppose the existence of independent density regions such as blobs, which could cover a substantial fraction of the stellar disk and are outwards moving inhomogeneities, spiral streams or CIRs (Corotating Interaction Regions), which may result from non-radial pulsations, magnetic fields or the stellar rotation and are able to make structures that cover a substantial part of the stellar disk [9, 11, 14-23]. These regions, though they do not present spherical symmetry around the star, they form spectral line profiles which are identical with those deriving from a spherically symmetric structure. In such a case, though the density regions are not spherically symmetric, through their effects on the line profiles, they appear as spherically symmetric structures to the observer.

The above mentioned ideas led us to suppose spherical symmetry (or apparent spherical symmetry) around the center of the density regions of matter, where the main spectral line as well as its SACs are born.

So, in the case of spherical symmetry, Eq. 1 takes the following form:

$$I_{\lambda} = \left[I_{\lambda 0} \prod_i e^{-L_i \xi_i} + \sum_j S_{\lambda_{ej}} \left(1 - e^{-L_{ej} \xi_{ej}} \right) \right] e^{-L_g \xi_g} \quad (2)$$

where: $I_{\lambda 0}$: is the initial radiation intensity, L_i , L_{ej} , L_g : are the distribution functions of the absorption coefficients k_{λ_i} , $k_{\lambda_{ej}}$, k_{λ_g} , ξ is the optical depth in the centre of the spectral line, $S_{\lambda_{ej}}$: is the source function, that is constant during one observation.

Calculation Of The Distribution Functions L

It is known that Be and Oe stars are rapid rotators. This means that we accept that a reason of the line broadening is the rotation of the regions that produce each satellite component. These rapidly rotating density regions may also present radial and random motions. For this reason we search an expression for the distribution function (L) of the spectral line components that has as parameters the rotational, the random and the radial velocities of the spherical region.

The distribution function (L) has the form:

$$L_{\text{final}}(\lambda) = \frac{1}{2\lambda_0 z} \int_{-\frac{\pi}{2}}^{\frac{\pi}{2}} \left[\operatorname{erf} \left(\frac{\lambda - \lambda_0}{\sqrt{2}\sigma} + \frac{\lambda_0 z}{\sqrt{2}\sigma} \cos \theta \right) - \operatorname{erf} \left(\frac{\lambda - \lambda_0}{\sqrt{2}\sigma} - \frac{\lambda_0 z}{\sqrt{2}\sigma} \cos \theta \right) \right] \cos \theta d\theta \quad (3)$$

where λ_0 is the observed wavelength of the center of the spectral line and $\lambda_0 = \lambda_{lab} + \Delta\lambda_{rad}$ where λ_{lab} is the laboratory wavelength and $\Delta\lambda_{rad}$ is the radial displacement, where

$z = \frac{V_{rot}}{c}$ and V_{rot} is the rotational velocity of the region which creates the spectral line.

We use this distribution function $L_{final}(\lambda)$ in the line function $e^{-L\xi}$, when the line broadening is an effect of both the rotational velocity of the density region as well as the random velocities of the ions. This means that now we have a new distribution function to fit every satellite component of a complex line profile that present DACs or SACs. We name this function Gauss-Rotation distribution function (GR distribution function).

In Figs. 10-12 we present the fittings of some hot emission stars and AGNs with the proposed model. The thick line presents the observed spectral line profiles and the thin one the best fits. The differences between the observed spectrum and its fit are some times hard to see, as we have accomplished the best fit.

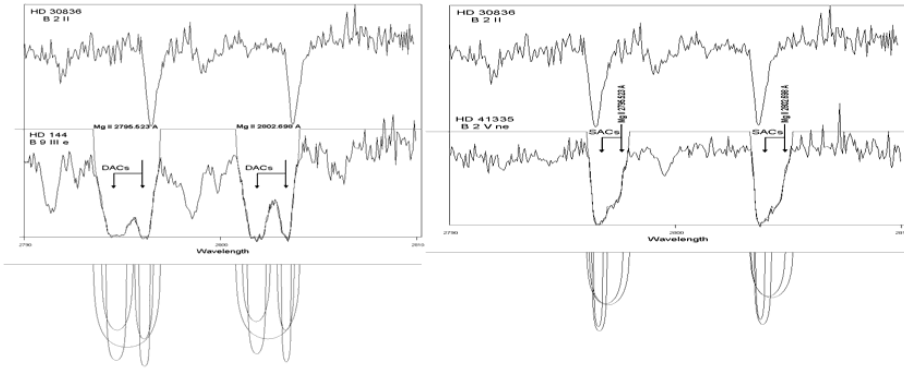


FIGURE 10. Fitting with the proposed model of the Mg II spectral lines of two Be stars that present DACs and SACs, respectively. We point out that we cannot explain and fit these spectral lines with another method. The thick line presents the observed spectral line's profile and the thin one the model fit.

DISCUSSION OF THE PROPOSED MODEL

In order to accept a fit of the complex spectral line as the best, we should apply all the physical criteria and techniques, such as the following:

1. It is necessary to check practically and theoretically the presence of blended lines that can deform the line shape as well as the existence of SACs.
2. The resonance lines as well as all the lines originating in a particular region should have the same number of SACs, depending on the structure of this region, without influence of ionization stage or ionization potential of emitters/absorbers. As a consequence, the respective SACs should have similar or same values of the radial and rotational velocities.
3. The ratio of the optical depths in the centre of two resonance lines has to be the same as the ratio of the respective relative intensities.

4. The proposed line function (Eq. 2) can be used in the case that $i=1$ and $j=1$, meaning when we deal with simple, classical spectral lines. This means that we can calculate all the important physical parameters, such as the rotational, the radial and the random velocities, the optical depth and the column density, for all the simple and classic spectral lines in all the spectral ranges.
5. We check the correct number of satellite components that construct the whole line profile. At first we fit using the number of the components that give the best difference graph between the fit and the observed spectral line. Then we fit using one component less than in the previous fit. The F-test between them allows us to take the correct number of satellite components that construct in the best way the whole line profile

FIGURE 11. Fitting of the C IV UV resonance lines of the BAL QSO PG 0946+301, that present DACs, with the proposed model. We point out that we cannot perfectly fit these spectral lines with another model. The thick line presents the observed spectral line profile and the thin one the model fit.

FIGURE 12. Fitting of the Si IV and C IV resonance lines of the BAL QSO H 1413+1143, that present SACs with the proposed model. The SACs phenomenon is able to explain the observed shape. We point out that we cannot perfectly fit these spectral lines with another model. The thick line presents the observed spectral line profile and the thin one the model fit.

TESTING THE MODEL

In order to check the spectral line function (Eq. 2), we calculated the rotational velocity of the He I absorption line at λ 4387.928 Å for five Be stars, using two methods, the classical Fourier analysis and our model. The rotational velocities that we calculate with both methods are almost the same.

We point out that with our model, apart from the rotational velocities, we can also calculate some other parameters as the standard Gaussian deviation (σ), the velocity of random motions of the ions, the radial velocities of the regions producing the studied spectral lines, the full width at half maximum (FWHM), the optical depth, the column density and the absorbed or emitted energy.

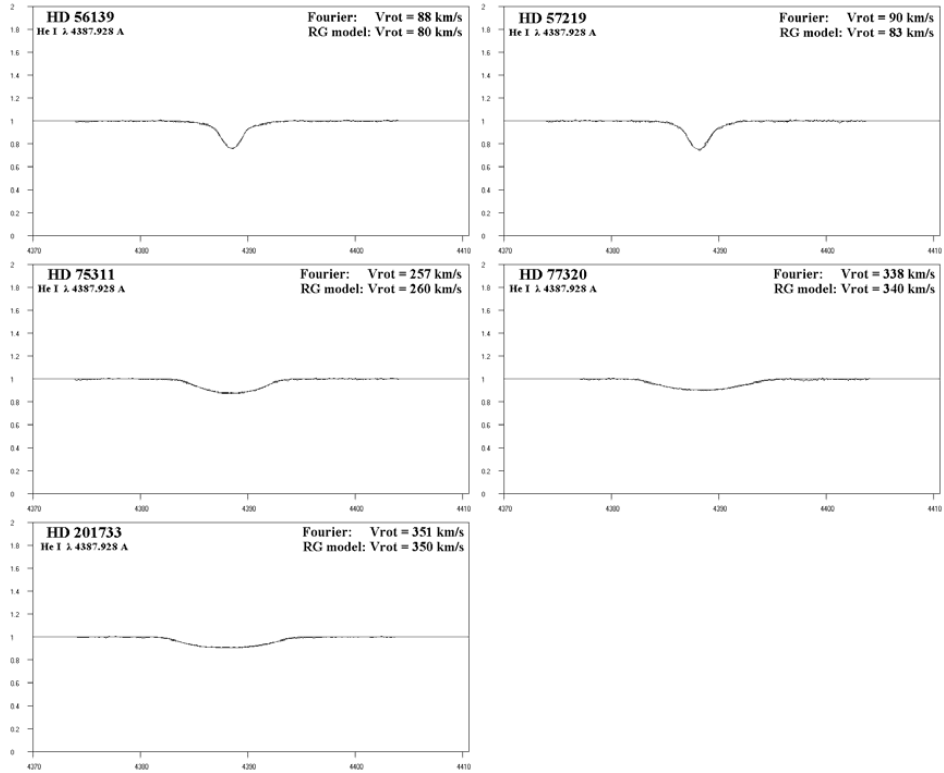


FIGURE 17. The five He I λ 4387.928 Å fittings for the studied Be stars and the measured rotational velocities with both methods. The results are favorable for our model. The thick line presents the observed spectral line profile and the thin one the model fit.

A second test of our model is to calculate the random velocities of the layers that produce the C IV satellite components of 20 Oe stars with different rotational velocities. The values of the random velocities do not depend on the inclination of the rotational axis. As the ionization potential of the regions that create the satellite

components for all the studied stars is the same, we expect similar average values of the random velocities for each component for all the studied stars.

We apply the model on the C IV line profiles of 20 Oe stellar spectra taken with the IUE –satellite (IUE Database <http://archive.stsci.edu/iue>).

We examine the complex structure of the C IV resonance lines (λ 1548.155 Å, 1550.774 Å). Our sample includes the subtypes O4 (one star), O6 (four stars), O7 (five stars), O8 (three stars) and O9 (seven stars). The values of the photospheric rotational velocities are taken from the catalogue of Wilson [24].

After the study of the C IV spectral lines we detect two components in 9 stars, three in 7 stars, four in 3 stars and five in one star. The results that we present in these figures are favourable for our model. The differences between the average values of the random velocities of the satellite components arise from the small variations of the temperature that exist in each one of the regions that produce the satellite components.

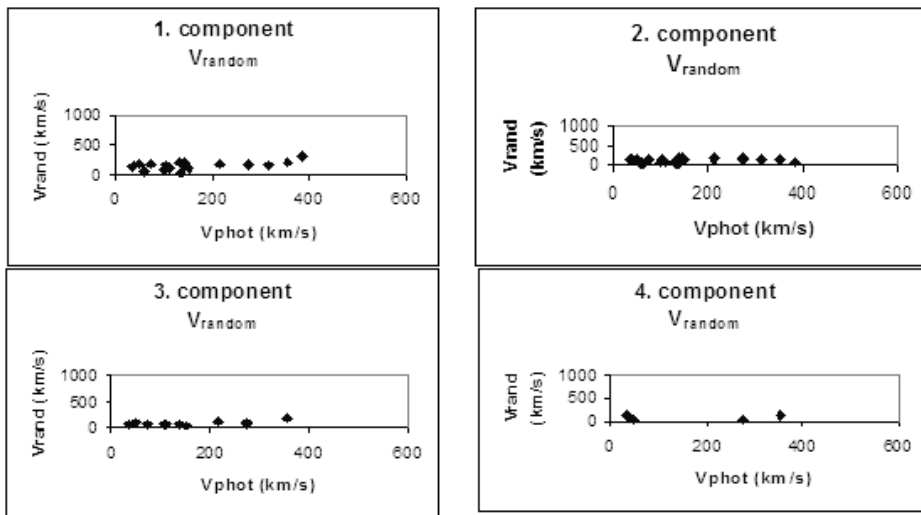


FIGURE 18. Relation between the random velocities and the photospheric rotational velocities of the studied stars.

CONCLUSIONS

We presented an overview of peculiar line profiles from stars to AGNs and a model that can describe peculiar lines.

Here we give some of our conclusions:

1. The peculiar spectral lines in Hot Emission Stars and AGNs are caused mainly by accretion and/or ejection of matter from these objects.
2. Some of the spectral lines peculiarity could be explained by DACs and SACs phenomena, indicating the existence of layers of matter with different physical conditions.
3. The results obtained confirm the assumptions of the proposed model.

ACKNOWLEDGMENTS

This research project is progressing at the University of Athens, Department of Astrophysics, Astronomy and Mechanics, under the financial support of the Special Account for Research Grants, which we thank very much. This work also was supported by Ministry of Science and Environment Protection of Serbia, through the projects “Influence of collisional processes on astrophysical plasma line shapes” and “Astrophysical spectroscopy of extragalactic objects”.

REFERENCES

1. P. Tuthill, J. Monnier and W. Danchi, *Nature*, **398**, 487 (1999).
2. E. Danezis, D. Nikolaidis, V. Lyratzi, M. Stathopoulou, E. Theodossiou, A. Kosionidis, C. Drakopoulos, G. Christou and P. Koutsouris, *Ap&SS*, **284**, 1119 (2003).
3. E. Danezis, D. Nikolaidis, E. Lyratzi, L. Č. Popović, M. S. Dimitrijević, E. Theodossiou and A. Antoniou, *Mem. S.A.It.Suppl.*, **7**, 107-113 (2005).
4. B. Bates and D. R. Halliwell, *Mon. Not. R. Astr. Soc.* **223**, 673-681 (1986).
5. H. J. G. L. M. Lamers, R. Gathier and T. P. Snow, *Ap. J.*, **258**, 186 (1982).
6. B. Bates and S. Gilheany, *Mon. Not. R. Astr. Soc.*, **243**, 320 (1990).
7. S. Gilheany, B. Bates, M. G. Catney and P. L. Dufton, *Ap&SS*, **169**, 85 (1990).
8. W. L. Waldron, L. Klein and B. Altner, *ivos.work*, 181(1992).
9. Th. Rivinius, O. Stahl, B. Wolf, A. Kaufer, Th. Gäng, C. A. Gummersbach, I. Jankovics, J. Kovács, H. Mandel, J. Peitz, Th. Szeifert and H. J. G. L. M. Lamers, *A&A*, **318**, 819 (1997).
10. L. S. Cidale, *Ap. J.*, 502, 824 (1998).
11. Markova, N.: 2000, *A&A, Supl. Ser.*, 144, 391.
12. Y. Andriillat and Ch. Fehrenbach, *A&A Supl. Ser.*, **48**, 93-136 (1982).
13. Y. Andriillat, *A&A, Supl. Ser.*, **53**, 319-338 (1983).
14. S. R. Cranmer and S. P. Owocki, *Ap. J.*, **462**, 469 (1996).
15. A. W. Fullerton, D. L. Massa, R. K. Prinja, S. P. Owocki and S. R. Cranmer, *A&A*, **327**, 699 (1997).
16. S. R. Cranmer, M. A. Smith and R. D. Robinson, *Ap. J.*, **537**, 433 (2000).
17. D. J. Mulan, *Ap. J.*, **283**, 303 (1984a).
18. D. J. Mulan, *Ap. J.*, **284**, 769 (1984b).
19. D. J. Mulan, *A&A*, **165**, 157 (1986).
20. R. K. Prinja and I. D. Howarth, *Mon. Not. R. Astr. Soc.*, **233**, 123 (1988).
21. L. Kaper, H. F. Henrichs, J. S. Nichols, L. C. Snoek, H. Volten and G. A. A. Zwarthoed, *A&A Supl. Ser.*, **116**, 257 (1996).
22. L. Kaper, H. G. Henrichs, A. W. Fullerton, H. Ando, K. S. Bjorkman, D. R. Gies, R. Hirata, E. Dambe, D. McDavid and J. S. Nichols, *A&A*, **327**, 281 (1997).
23. L. Kaper, H. F. Henrichs, J. S. Nichols and J. H. Telting, *A. & Ap.*, **344**, 231 (1999).
24. R. E. Wilson, *General Catalogue Of Stellar Radial Velocities*, Washington, Carnegie Institution of Washington Publication 601, (1963).

Long Term Variability of the Coronal and Post-Coronal Regions of the Oe Star HD 149757 (zeta Oph)

Antonis Antoniou^{*}, Emmanouel Danezis^{*}, Evaggelia Lyratzi^{*,†},
Dimitris Nikolaidis^{*}, Luka Č. Popović^{**} and Milan S. Dimitrijević^{**}

^{*}*University of Athens, Faculty of Physics, Department of Astrophysics, Astronomy and Mechanics,
Panepistimioupoli, Zographou 157 84, Athens – Greece*

[†]*Eugenides Foundation, 387 Sygrou Av., 17564, Athens, Greece*

^{**}*Astronomical Observatory, Volgina 7, 11160 Belgrade, Serbia*

Abstract. In the spectra of Oe and Be stars, many spectral lines present peculiar and complex profiles due to the fact that the observed absorption features are composed of two or more absorption components (Discrete or Satellite Absorption Components - DACs/SACs). Here we detected the presence the SACs phenomenon in the C IV, N IV and N V spectral lines in 11 spectra of the Oe star HD 149757 (zeta Oph), taken with IUE during a period of 13 years.

Keywords: stars: Oe, HD 149757; stars: line profiles – absorption components

PACS: 97.10.Ex; 97.10.Fy; 97.20.Ec; 97.30.Eh

INTRODUCTION

HD 149757 (ζ Oph) is a bright O9V(e) star [1], rapidly rotating and a strong non radial pulsator [2, 3] that, on occasion, shows the distinct H α emission [4].

Hoogerwerf et al. [5] consider it as runaway star from Sco OB2 association. (Binary Supernova Scenario, BSC).

In this paper, applying the Gauss-Rotation (GR) model [6, 7] to the star HD 149757, we study the C IV, N IV and N V regions through the variation of kinematical parameters, such as the apparent rotational and radial velocities, as well as the random velocities of the thermal motions of the ions.

THE STUDY OF THE CORONAL AND POST-CORONAL REGIONS OF THE MOVING ATMOSPHERE OF THE Oe STAR HD 149757

In Fig. 1a,b,c we present a spectral line from each of C IV, N IV and N V regions and their best fit. In the graph below each profile, we present the difference between the fit and the observed spectral line. Below the fit, is the decomposition of the observed profile to its SACs.

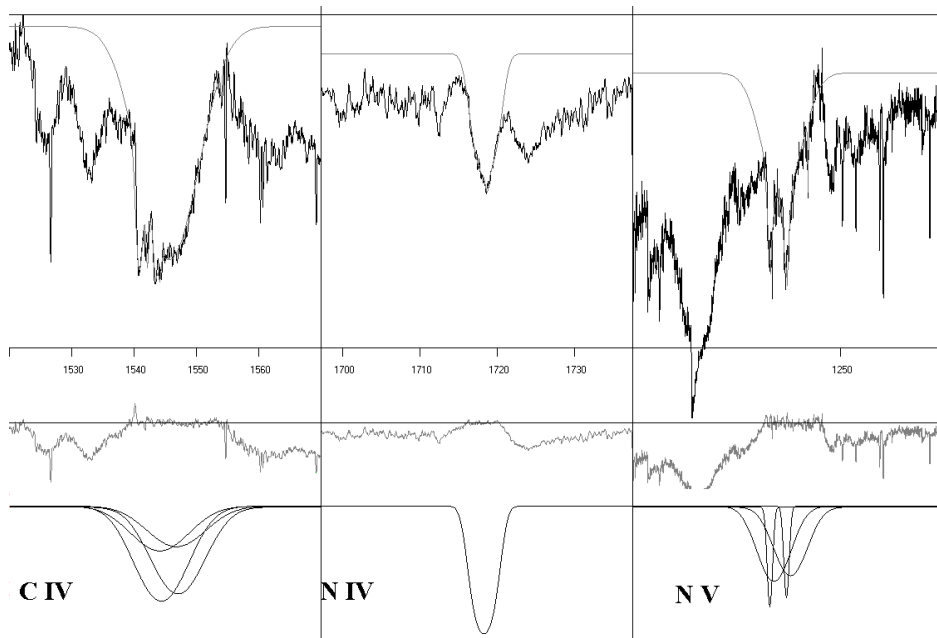


FIGURE 1a, b, c. The best fit of the C IV, N IV and N V resonance lines with two components in the spectrum of the star HD 149757. The graph below the fit indicates the differences between the observed spectrum and the fit. Below, one can see the decomposition of the observed profile to its SACs.

The Study of the C IV Density Regions

In Fig. 2a,b we present the time-scale change of the apparent rotational and radial velocities of the independent density regions of matter, which create the 2 satellite components of the C IV resonance lines ($\lambda\lambda$ 1548.155, 1550.774 Å).

In the case of the rotational velocities (Fig. 2a) and in the years 1980, 1981, 1990, 1991, relatively low values of about 300 km/s correspond to the spectra that we fit with the Gaussian way. This means that for these spectra the main reason for the line broadening is the random ion motions. All the rest spectra were fitted with the Rotational method, i.e. the main reason for the line broadening is the rotation of the region which creates the respective component. Apart from these values, we see a constant behavior of the apparent rotational velocities with values of about 1400 km/s for the first component and about 950 km/s for the second one. The marks x and + correspond to the spectra in which the best fit has been obtained with the Gaussian method. In the case of the radial velocities (Fig. 2b) we detect also a constant behavior with values of about -800 km/s for the first component and of about -700 km/s for the second component.

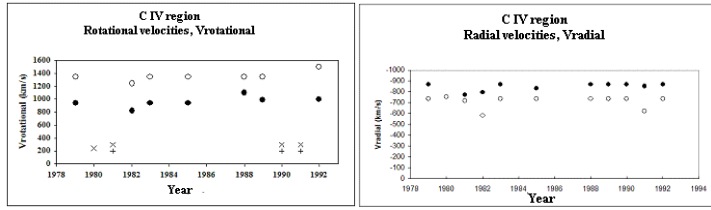


FIGURE 2a,b. Timescale variations of the apparent rotational velocities V_{rot} (km/s) (left) and radial velocities V_{rad} (km/s) (right) of the two C IV line components between the years 1979 and 1992.

The Study of the N IV Density Region

In Fig. 3a,b we present the timescale changes of the apparent radial velocities V_{rad} (km/s) and the random velocities V_{rand} (km/s) of the density region where the N IV (λ 1718.8 Å) spectral line is created.

In the case of the radial velocities (Fig. 3a) we detect a constant behavior with values lower than -50 km/s.

In the case of the random velocities (Fig. 3b), the values of about 100 km/s correspond to the spectra fitted with the Rotational method. This means that in these spectra the random ion velocities are not dominant. The values between 350 and 400 km/s (points \times) correspond to the spectra fitted with the Gaussian method.

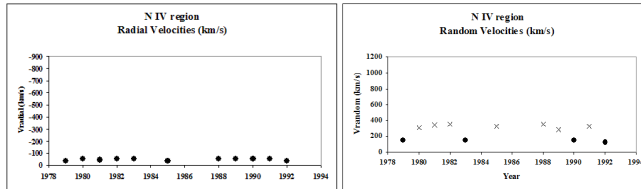


FIGURE 3a,b. Timescale variations of the apparent radial velocities V_{rad} (km/s) (left) and the random velocities V_{rand} (km/s) (right) of the density region where the N IV λ 1718.8 Å spectral line is created.

The Study of the N V Density Regions

In Figs. 4a,b we present the timescale variations of the values of the apparent radial velocity V_{rad} (km/s) and the random velocities V_{rand} (km/s) of the ions, in the density regions which create the two or three absorption components of the N V resonance lines at $\lambda\lambda$ 1238.821, 1242.804 Å.

For the radial velocities (Fig. 4a) we detect a constant behavior with values of about -1160 km/s for the first component (points o), of about -1400 km/s for the second (points \bullet) and about -1450 km/s for the third one (points Δ).

For the random velocities (Fig. 4b) we calculate values of about 1000 km/s for one satellite component and values of about 200 km/s for the others (points \times). The points \bullet correspond to the spectral lines which are best fitted with the Rotational method.

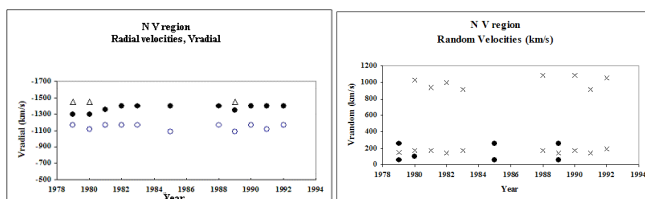


FIGURE 4a,b. Timescale variations of the values of the apparent radial velocity V_{rad} (km/s) (left) and the random velocities V_{rand} (km/s) (right) for the independent density regions of matter which create the 2 or 3 satellite components of the N V resonance lines at $\lambda\lambda$ 1238.821, 1242.804 Å.

CONCLUSIONS

The detected timescale variation of the parameter values in the C IV, N IV and N V density regions in the UV spectrum of the Oe star HD 149757 indicate that the radial, rotational and random velocities present only small variations. This fact lead us to accept that the matter which creates DACs/SACs remains, practically, stable during the studied period of 13 years. Another explanation of this phenomenon is that in the area where we can detect high density regions, matter flows and only the physical properties (conditions), which lead to the high density, remain stable (e.g. magnetic fields, shocks from a companion in the case of a binary system)

ACKNOWLEDGMENTS

This research project is progressing at the University of Athens, Department of Astrophysics - Astronomy and Mechanics, under the financial support of the Special Account for Research Grants, which we thank very much. The project is co-financed within Op. Education by the ESF (European Social Fund) and National Resources, under the “Pythagoras II” project. This work also was supported by Ministry of Science of Serbia, through the projects: Influence of collisional processes on astrophysical plasma line shapes - P146001 and Astrophysical spectroscopy of extragalactic objects - P146002.

REFERENCES

1. P. S. Conti, *ApJ* **179**, 181 (1973).
2. E. Kambe, H. Ando, R. Hirata, *Ap&SS* **210**, 219 (1993).
3. A. H. N. Reid, C. T. Bolton, R. A. Crowe, M. S. Fieldus, A. W. Fullerton, D. R. Gies, I. D. Howarth, D. McDavid, R. K. Prinja, K. C. Smith, *ApJ* **417** 320 (1993).
4. P. K. Barker, T. Brown, *ApJ* **192**, 11 (1974).
5. R. Hoogerwerf, J. H. J. Bruijne, R. T. De Zeeuw, *ApJ* **544**, 133 (2001).
6. E. Danezis, D. Nikolaidis, E. Lyratzi, A. Antoniou, L. Č Popović, M. S. Dimitrijević, *Mem. Soc. It. Suppl.* **7**, 107 (2005).
7. E. Danezis, D. Nikolaidis, E. Lyratzi, L. Č. Popović, M. S. Dimitrijević, A. Antoniou, E. Theodosiou, *PASJ* **59**, in press (2007).